이학박사학위논문

Ecology of the azaspiracid producer dinoflagellate *Azadinium poporum* from Shiwha bay, Korea:

- taxonomy, population dynamics, azaspiracid content, predation, and growth

한국 시화호 해역의 azaspiracid 생산자인 *Azadinium poporum* 의 생태 연구: 분류, 개체군 동태, azaspiracid, 포식 및 성장

2014년 8월

서울대학교 대학원

지구환경과학부 해양학전공

Éric Potvin

Ecology of the azaspiracid producer dinoflagellate *Azadinium poporum* from Shiwha bay, Korea:

- taxonomy, population dynamics, azaspiracid content, predation, and growth -

지도 교수 정 해 진
이 논문을 이학박사 학위논문으로 제출함
2014 년 08 월
서울대학교 대학원
지구환경과학부 해양학 전공
Éric Potvin

Éric Potvin의 박사 학위논문을 인준함
2014 년 08 월

위 원 장 _____ (인)

부위원장 _____ (인)

위 원 _____ (인)

위 원 _____ (인)

위 원 _____ (인)

To my family and friends who were far away,
To those who are gone,
To the one who came before,
To those of the future

List of abbreviations

Abbreviation	Definition
ASP	Amnesic shellfish poisoning
AT	Annealing temperature
ATP	Adenosine triphosphate
AZA	Azaspiracid
AZP	Azaspiracid poisoning
BTX	Brevetoxin-b
CAD	Collisionally activated dissociation
CE	Collision energy
Chl-a	Chlorophyll a
CID	Collision-induced dissociation
COI	Mitochondrial cytochrome oxidase I
CT	Cycle threshold
CTX	Ciguatoxin-P
DA	Domoic acid
DNA	Deoxyribonucleic acid
dNTP	Deoxyribonucleotide triphosphate
DO	Dissolved oxygen
DSP	Diarrhetic shellfish poisoning
DTX	Dinophysistoxin
EPI	Enhanced product ion
ESD	Equivalent spherical diameter
FE-SEM	Field emission-scanning electron microscopy
FISH	Fluorescence *in situ* hybridization
FTICR-MS	Fourier transform ion cyclotron resonance-mass spectrometry
GGE	Gross growth efficiency
GYM	Gymnodimine
HPLC	High performance liquid chromatography

HTD	Heterotrophic dinoflagellate
ITS rDNA	Internal transcribed spacer ribosomal DNA
LC	Liquid chromatography
LCMS	Liquid chromatography mass spectrometry
LSU rDNA	Large subunit ribosomal RNA gene
ML	Maximum likelihood
MP	Maximum parsimony
MRM	Multiple reaction monitoring
MS	Mass spectrometry
MS/MS	Tandem mass spectrometry
m/z	Mass to charge ratio
NH_4^+	Ammonium
NJ	Neighbor joining
NMR	Nuclear magnetic resonance
NO_2^-	Nitrite
NO_3^-	Nitrate
NSP	Neurotoxic shellfish poisoning
OA	Okadaic acid
PC	Polycarbonate
PCL	Prorocentrolide
PCR	Polymerase chain reaction
PLTX	Palytoxin
PnTX	Pinnatoxin
PO_4^{3-}	Phosphate
PSP	Paralytic shellfish poisoning
PTX	Pectenotoxin-2
qPCR	Quantitative polymerase chain reaction
RDA	Retro-Diels-Alder reaction
rDNA	Ribosomal DNA
RMGI	μ_m to I_{max} ratio
RNA	Ribonucleic acid

SD	Secchi depth
SEM	Scanning electron microscopy
SiO_3^{2-}	Silicate
SPX	Spirolide
SRC	Sedgwick-Rafter chamber
SSU rDNA	Small subunit ribosomal RNA gene
STX	Saxitoxin
Taq	*Thermus aquaticus*
TMSDM	Trimethylsilyl diazomethane
UV	Ultraviolet
v/v	Volume to volume ratio
w/v	Weight to volume ratio
YTX	Yessotoxin

Abstract

Ecology of the azaspiracid producer dinoflagellate *Azadinium poporum* from Shiwha bay, Korea:

- taxonomy, population dynamics, azaspiracid content, predation, and growth -

Éric Potvin
Oceanography
School of Earth and Environmental Sciences
College of Natural Sciences
Seoul National University

The azaspiracids (AZAs) are the most recently discovered group of lipophilic marine biotoxins of microalgal origin associated with cases of shellfish poisoning in humans. Since the discovery of *Azadinium spinosum* as a primary producer of AZA, there has been an urgent need to know more about closely related species and their distribution, the variety of AZA analogues they are producing, their population dynamics in the field, their ecophysiology, and their ecological niche within the planktonic food web.

At the initiation of that work, species of the genus *Azadinium* were only

known from northern European waters. Following the isolation of another strain of the genus *Azadinium* in 2010 from Shiwha bay, a highly eutrophic area from Korea, works were undertaken in order to explore the taxonomic identity, content of AZA, population dynamics in the field, variety of grazers, and physiology of the new isolate.

The morphology based on optical and scanning electron microscopy as well as the ITS rDNA region and LSU rRNA gene phylogenies demonstrated that the strain was closely related to *Azadinium poporum*, but minor morphological dissimilarities and an instable phylogenetic position led us to designate it as *Azadinium* cf. *poporum* at the time. Later work revealed that the strain was conspecific with *Azadinium poporum*. This work extended the known distribution of the genus *Azadinium* further south.

The strain isolated from Shiwha bay preliminarily showed not to contain any known AZA. However, further analyses of the Korean strain by triple quadrupole mass spectrometry on the precursor and product ion mode revealed a new compound, or analogue, with high similarity to AZAs. The structure of the new compound was proposed by interpretation of fragmentation patterns and high resolution mass measurements using Fourier transform ion cyclotron resonance-mass spectrometry. This work increased the known molecular diversity of AZA produced by species in the genus *Azadinium*.

The long term temporal dynamics of species of the genus *Azadinium* in the field was completely unknown. Therefore, the population dynamics of *A. poporum* from Shiwha bay was investigated by qPCR (quantitative polymerase chain

reaction). *A. poporum* revealed to occur always in relatively low concentration from 2009 to 2011 in comparison to common species found in Shiwha bay.

The reduced knowledge on interactions implicating *Azadinium* within the planktonic food web, the relevance of the Korean isolate of *A. poporum* as an AZA producer, and the possible role of predation in its field dynamics led us to determine its protistan and metazoan grazers. Furthermore, grazing and growth rates as well as gross growth efficiencies were established for some grazers. Many protistan grazers and copepods were able to feed on *A. poporum*. However, only two species, the heterotrophic dinoflagellate *Oxyrrhis marina* and the ciliate *Strobilidium* sp., were able to achieve sustained growth on *A. poporum* as the sole prey. Furthermore, for these predators, the maximum ingestion rates and maximum growth rates were the highest and lowest when compared with other prey species, respectively. This suggests that *A. poporum* was a low quality prey. In addition, the field concentrations of *A. poporum* assessed by qPCR were generally too low to affect the dynamics of the predators found in this study. Therefore, predation reveals unlikely to be a driving force in the dynamics of *A. poporum* in the field.

In order to further determine the causes explaining the dynamics of *A. poporum* in Shiwha bay, we assessed the tendency and seasonality of some environmental parameters through time such as the temperature, the salinity, the pH, the dissolved oxygen, the Secchi depth, the concentration of nutrients, and the concentration of chlorophyll a. We also determined if the previous parameters had an effect on *A. poporum* in the field as well as the effects of temperature, salinity, and light on the growth of *A. poporum* in laboratory. The species revealed to grow on a wide range of temperature and salinity and was therefore generally well adapted to the highly variable field conditions observed in Shiwha

bay. Furthermore, the species revealed to be well adapted to low irradiance. The growth rates of *A. poporum* estimated in laboratory were also relatively high compared with other photosynthetic and mixotrophic dinoflagellates under photosynthetic growth. Such features do not explain the low abundances obtained from the field samples. However, *A. poporum* revealed to be more represented in the field when the concentrations of nitrite and nitrate, silicate, as well as chlorophyll a were lower and the transparency was higher. This suggests that *A. poporum* use reduced trophic state as windows of opportunity. Considering the low concentrations of *A. poporum* obtained from field samples during the survey of three years, these opportunities might represent a survival strategy in eutrophic environment.

The multifaceted studies cumulated in this thesis strengthen previous area of research related to the genus *Azadinium* and established new foundations in unexplored areas from which further studies can rise.

Keywords: morphology, rDNA, distribution, toxin, grazing, tolerance, salinity, temperature, light, pH, dissolved oxygen, transparency, nutrients, chlorophyll a

Student Number: 2009-31225

Contents

List of Tables

List of Figures

Chapter 1: Introduction

1.1 Generalities

The marine ecosystem food web relied on unicellular photosynthetic microscopic organisms. They can occupy the pelagic environment or be more closely related to the benthic zone. The different species co-exist to produce natural assemblages. Abiotic factors such as the temperature, the salinity, the light, and the nutrients, as well as biotic factors as grazing, cell contact, allelopathy, viruses, and parasites might affect the abundance of photosynthetic organisms. The hydrodynamics might also affect the distribution of a species and therefore its field dynamics. Occasionally, one or multiple species can dominate blooms that can last for weeks (Granéli & Turner 2006).

These blooms can be harmful. They can degrade the quality of the water, lower the concentration of oxygen, and/or obstruct fish gills. Some blooms are constituted of toxic microalgae. When the predator at the end of the food web is the human being, these blooms generate indirectly food poisoning of various types.

Of the approximately 25 000 species of known phytoplankton (Falkowski *et al*. 2004), only about 300 species are harmful for marine organisms and about 80 of these species are known to produce phycotoxins (Granéli & Turner 2006).

The marine phycotoxins are secondary metabolites produced by some prokaryotic or eukaryotic microalgae species. These metabolites are generally non-harmful for the producer organism and concentrate through the food web in

consumers. They move up the food web until they intoxicate the superior mammals. Among the consumers, protistan predators, zooplanktons, bivalve filter molluscs, gastropods, or herbivory fish will contaminate their predators.

In marine environment, the phycotoxins are mainly produced by the Dinophyceae (the dinoflagellates) and the Bacillariophyceae (the diatoms), but also the Prymnesiophyceae, the Raphidophyceae, and the Cyanophyceae (the cyanobacteria).

These toxins are classified based on their affinity, chemical structure, and the symptoms that they produced on human when seafood is consumed (Table 1.1). Based on their affinity, these toxins can be hydrophilic, lipophilic, or amphiphilic. The classification based on symptoms includes the paralytic shellfish poisoning (PSP), the diarrhetic shellfish poisoning (DSP), the amnesic shellfish poisoning (ASP), and the neurotoxic shellfish poisoning (NSP). Microalgae can produce toxins with different structures by slight variation of the main structure. Therefore, most of the groups of marine toxins also have numerous analogues.

Phytoplankton toxins can accumulate in shellfish and subsequently poison humans (Shumway 1990). The organisms at their origin can form blooms which have sometimes caused large-scale mortalities of finfish and shellfish and thus great losses to the aquaculture and tourist industries of many countries (Steidinger 1983, ECOHAB 1995, Burkholder *et al*. 1995). Phycotoxins can also affect higher trophic level through the food web as indicated by mortality of whales, dolphins, and seabirds (Geraci *et al*. 1989, Anderson & White 1992, Work *et al*. 1993). The distribution and dynamics of such species is of particular interest in order to have a

Table 1.1 The principal marine phycotoxins, their source, their affinity, their chemical formula, and the type of poisoning caused

Toxins	Abbreviation	Producers	Affinity	Formula	Poisoning
Domoic acid	DA	*Pseudo-nitzchia* spp.[1, 2, 3, 4]	Hydrophilic	$C_{15}H_{21}N_{O6}$	ASP
Okadaic acid	OA	*Dinophysis* spp.[5]	Lipophilic	$C_{44}H_{68}O_{13}$	DSP
		Prorocentrum spp.[6,7,8]			
Azaspiracid	AZA	*Azadinium* spp.[9, 10]	Lipophilic	$C_{47}H_{71}NO_{12}$	DSP
		Amphidoma languida [10]			
Brevetoxin-b	BTX	*Karenia brevis* [11, 12, 13, 14]	Lipophilic	$C_{50}H_{70}O_{14}$	NSP
		Chattonella spp.[15,16,17]			
Ciguatoxin-P	CTX	*Gambierdiscus toxicus*[18,19,20]	Lipophilic	$C_{60}H_{85}O_{16}$	NSP
Gymnodimine	GYM	*Karenia selliformis*[21,22]	Lipophilic	$C_{32}H_{45}NO_4$	NSP
Palytoxin	PLTX	*Ostreopsis* spp.[23]	Amphiphilic	$C_{129}H_{223}N_3O_{54}$	NSP
Pectenotoxin-2	PTX	*Dinophysis* spp.[24]	Lipophilic	$C_{47}H_{70}O_{14}$	DSP
Pinnatoxin	PnTX	*Vulcanodinium rugosum*[25]	Lipophilic	$C_{41}H_{61}NO_9$	NSP
Prorocentrolide	PCL	*Prorocentrum* spp.[26]	Lipophilic	$C_{56}H_{85}NO_{13}$	NSP

Table 1.1 (continued)

Toxins	Abbreviation	Producers	Affinity	Formula	Poisoning
Saxitoxin	STX	*Alexandrium* spp.[27, 28]	Hydrophilic	$C_{10}H_{17}N_7O_4$	PSP
		Gymnodinium catenatum[29]			
		Pyrodinium bahamense[29]			
Spirolide	SPX	*Alexandrium ostenfeldii*[30]	Lipophilic	$C_{41}H_{61}NO_7$	NSP
Yessotoxin	YTX	*Protoceratium reticulatum*[31]	Amphiphilic	$C_{55}H_{82}O_{21}S_2$	DSP
		Lingulodinium polyedrum[32]			
		Gonyaulax spinifera[33]			

Abbreviations used: paralytic shellfish poisoning (PSP), diarrhetic shellfish poisoning (DSP), amnesic shellfish poisoning (ASP), neurotoxic shellfish poisoning (NSP)

References. [1]Garrison *et al*. 1992, [2]Laycock *et al*. 1989, [3]Maranda *et al*. 1989, [4]Shimizu *et al*. 1989, [5]Yasumoto *et al*. 1980, [6]Dickey *et al*. 1990, [7]Hu *et al*. 1995, [8]Murakami *et al*. 1982, [9]Tillmann *et al*. 2009, [10]Krock *et al*. 2012, [11]Baden 1983, [12]Lin *et al*. 1981, [13]Prasad & Shimizu 1989, [14]Shimizu 1982, [15]Bourdelais *et al*. 2002, [16]Khan *et al*. 1995a, [17]Khan *et al*. 1995b, [18]Legrand *et al*. 1990, [19]Murata *et al*. 1990, [20]Yasumoto *et al*. 1977, [21]Seki *et al*. 1995, [22]Miles *et al*. 2000, [23]Usami *et al*. 1995, [24]Kamiyama *et al*. 2010, [25]Rhodes *et al*. 2011, [26]Torigoe *et al*. 1988, [27]Schantz *et al*. 1966, [28]Sommer & Meyer 1937, [29]FAO 2004, [30]Cembella *et al*. 2000, [31]Satake *et al*. 1997, [32]Tubaro *et al*. 1998, [33]Rhodes *et al*. 2006

better understanding of the factors implicated in their increase and decrease. Such knowledge will help to better predict the insurgence of blooms as well as to develop methods to prevent or decrease the effect of these blooms. The use of FISH (fluorescence *in situ* hybridization) and qPCR (quantitative polymerase chain reaction) as species-specific detection methods as well as the next generation high throughput sequencing is expected to increase our knowledge on these species.

1.2 Dinoflagellates

The number of living dinoflagellates is usually estimated to be approximately 2000, with 2500 named fossil species. In a recent revision Gómez (2005) recognized 1555 free-living marine species. Approximately 160 marine species are benthic (Taylor *et al*. 2008). Dinoflagellates are a highly diverse group of flagellates, consisting of both photosynthetic and non-photosynthetic taxa in equal proportions (Taylor 1987). Many of the photosynthetic members are mixotrophic, and the heterotrophs feed by a wide variety of mechanisms (Gaines & Elbrächter 1987, Schnepf & Elbrächter 1992). The phycotoxins are produced in most part by dinoflagellates (Table 1.1).

1.3 Ecology of toxic dinoflagellate

1.3.1 Biotic factors

As toxic dinoflagellates have potential impact on consumers, grazing on toxic dinoflagellate can have potential impact on preventing or terminating blooms. Toxic dinoflagellates can also graze on preys and thereafter maintain or increase

their abundance. Furthermore, allelopathy and cell contact are factors that can affect both toxic dinoflagellates and co-occurring species.

1.3.1.1 Toxic potency

Toxic dinoflagellates might contain mechanisms that able them to be recognized by predators and induced behavioral change. A toxic strain of *Alexandrium tamarense* inhibited feeding by *Favella* spp. (Hansen 1989). Some copepods are known to reject some toxic dinoflagellates (Huntley *et al*. 1983, 1986, Turner & Anderson 1983, Uye & Takamatsu 1990). Toxic dinoflagellates might also have mechanisms to reduce the growth or kill some predators after ingestion. *Strombidinopsis* sp. and *Tiarina fusus* did not grow on the toxic dinoflagellate *Amphidinium carterae* (Jeong *et al*. 1999, 2002). The toxic naked dinoflagellate *Gymnodinium aureolum* suppressed the growth of *F. ehrenbergii* (Hansen 1995). Some toxic dinoflagellate species that produce a paralytic shellfish poisoning toxin are harmful to *Oxyrrhis marina* and *Polykrikos kofoidii* (Matsuoka *et al*. 2000). Furthermore, some *Alexandrium* strains caused loss of motility and cell lysis of the heterotrophic dinoflagellates *Oblea rotunda* and *O. marina* by secretion of extracellular substances (Tillmann & John 2002). Therefore, the toxic potency of toxic dinoflagellates can act in various ways on predators.

1.3.1.2 Predation

Heterotrophic protists such as dinoflagellates and ciliates are known to feed on toxic dinoflagellates (Hansen 1989, Maneiro *et al*. 2000, Jeong *et al*. 2001, 2003a, Kamiyama & Arima 2001, Kamiyama *et al*. 2005, Adolf *et al*. 2007, Yoo *et al*. 2013). The heterotrophic dinoflagellate *Polykrikos kofoidii* grew well while

feeding on the toxic dinoflagellate *Gymnodinium catenatum*. Another heterotrophic dinoflagellate, *Oxyrrhis marina*, also grew well while feeding on the toxic dinoflagellates *Amphidinium carterae* and *Karlodinium veneficum*. Recently, *Gyrodinium moestrupii* was shown to feed and grow on toxic strains of *Alexandrium minutum*, *A. tamarense*, and *Karenia brevis*. Furthermore, the large tintinnid ciliates *Favella* spp. can feed well on *Alexandrium tamarense*, *A. catenella*, and *Dinophysis acuminate*. Several metazooplankters can also ingest toxic dinoflagellates without apparent harm (Calbet *et al*. 2003, Turner & Borkman 2005). This suggests that heterotrophic protists and metazoans can affect the dynamics of toxic dinoflagellates in the field.

1.3.1.3 Mixotrophy

Toxic dinoflagellates are known to be, in most cases, primarily photosynthetic. Many dinoflagellate species associated with toxin production were previously thought to be photosynthetic, but revealed to be mixotrophic (Jeong *et al*. 2005a b, Glibert *et al*. 2009, Blossom *et al*. 2012). Mixotrophy can enhance the growth of toxic dinoflagellates and therefore play a role in their dynamics.

1.3.1.4 Allelopathy and cell contact

Allelopathy or cell contact have been discussed as phenomena affecting phytoplankton bloom formation and are potential factors that can enhance or reduce the dynamics of toxic dinoflagellates.

Legrand *et al*. (2003) and Granéli & Hansen (2006) reviewed allelopathy in phytoplankton. Allelochemicals are generally characterized as specific metabolites

that stimulate or suppress growth of other organisms, or elicit other physiological responses in target cells. In marine environments, allelochemicals may function as chemical defence by deterring, incapacitating, and/or killing competitors or grazers (McClintock & Baker 2001, Cembella 2003, Legrand *et al*. 2003, Granéli & Hansen 2006).

Uchida (2001) reported the role of cell contact in some dinoflagellate species. Studies have previously reported the importance of cell contact in interactions involving dinoflagellates (Yamasaki *et al*. 2011, Qiu *et al*. 2012). However, while knowledge on allelopathy is increasing, further investigations on the role of cell contact are required in order to appreciate its relevance in the dynamics of dinoflagellates.

1.3.2 Abiotic factors

In marine environment, the temperature, the salinity, the light intensity, the turbulence, the pH, and the nutritional factors are important physicochemical factors for the regulation of growth and metabolism (enzymatic activity and secondary metabolite production).

1.3.2.1 Temperature

The temperature will influence the enzymatic activity of microalgae. The enzymes have an optimal temperature of operation under which the reaction speeds are slower and over which the enzymes degrade more quickly (Grzebyk & Séchet 2003). The temperature is then a parameter with an important effect on growth (Nielsen 1996, Matsubara *et al*. 2007, Xu *et al*. 2010).

1.3.2.2 Salinity

Unfavorable salinities to microalgae will act on enzymatic activity and on the consumption of energy allocated to the osmotic regulation (Grzebyk & Séchet, 2003). Salinity will therefore act on the cellular metabolism and on growth. The freshwater species will have a weak tolerance to variation of salinities, while estuarine species are euryhaline and the coastal and marine species have a wider tolerance to salinity variations in culture (Taylor & Pollingher 1987, Grzebyk *et al*. 2003, Nagasoe *et al*. 2006, Matsubara *et al*. 2007). However, some species are stenohaline and can be sensible to salinity variations (Kim *et al*. 2004a).

1.3.2.3 Light intensity

Photosynthetic dinoflagellates can adapt quickly to variations of light intensity. At weak light intensities, for example, dinoflagellates can increase the size and/or the number of photosynthetic units (Smayda 1997). This factor is the one affecting the most the nutrition of microalgae through the photosynthesis. An insufficient light can reduce or stop the growth (Grzebyk & Séchet 2003, Paz *et al*. 2006).

1.3.2.4 Turbulence

For multiple dinoflagellate species, the turbulence generated experimentally caused deleterious effects, notably a diminution of the cell division (Pollingher & Zemel 1981, Berdalet 1992, Sullivan *et al*. 2003), morphological changes (Zirbel *et al*. 2000), a modification of the swimming behavior (Karp-Boss *et al*. 2000,

Berdalet *et al*. 2007), or breaks of the cellular membrane (White 1976). Therefore, turbulence in the field might affect the dynamics and abundances of species.

1.3.2.5 pH

Knowledge on the effect of pH on dinoflagellates is limited and needs to be further assessed. The effect of pH on growth appears to be species specific. Furthermore, the pH might be implicated in species succession (Hansen 2002). Therefore, the effect of pH should be determined in order to have a better idea of species dynamics in the field.

1.3.2.6 Nutritional factors

1.3.2.6.1 Macronutrients

The macronutrients that are the most important to dinoflagellate growth are nitrogen and phosphorus. They affect the development of algal blooms (Paerl 1998, Sakka *et al*. 1999, Shi *et al*. 2005). Phosphorus is a component of ATP (adenosine triphosphate) as well as DNA (deoxyribonucleic acid), RNA (ribonucleic acid), and phospholipids. Since ATP can be used for the biosynthesis of many biomolecules, phosphorus is important for growth. Phosphorus can also be used to modify the activity of various enzymes by phosphorylation and can be used for cell signaling. The importance of nitrogen comes from its necessity as component of all proteins. The concentrations of these macronutrients as well as their interactions in the metabolism of toxic dinoflagellates will affect the dynamics of growth.

1.3.2.6.2 Micronutrients

A limited amount of data is available on the effect of micronutrients (vitamins and trace metals) on growth of dinoflagellates. If phosphorus and nitrogen are not limiting, the micronutrient will eventually limit growth. The micronutrients are implicated in the metabolism of microalgae as cofactor of enzymes or as metalloprotein involved in the photosynthesis and/or the assimilation of nitrogen (Grzebyk & Séchet 2003).

Micronutrients such as selenium and iron are required in the growth of some toxic dinoflagellates. Without addition of selenium, the growth rate of *Protoceratium reticulatum* is reduced and morphological changes are observed. Without addition of iron, the growth rate is also reduced (Mitrovic *et al*. 2004). The selenium was also observed to be essential for *Alexandrium minutum* and *Gymnodinium catenatum* (Doblin *et al*. 1999).

1.4 Study area

The Gyeonggi bay is located on the Korean West coast. The Gyeonggi bay is a shallow macrotidal and well-mixed estuary. The accumulation of organic matter is generally limited. The Gyeonggi bay is characterized by a broad shallow channel of 10-20 m depth flanked by tidal flats >3 km width (Choi & Shim 1986a). The macrotidal bay (tidal amplitude >10 m) is characterized by semi-diurnal strong tidal currents (1.2-2.3 and 0.9-1.9 m s^{-1} during spring and neap tides, respectively) and strong winter monsoon sweeps (3.77 m s^{-1}) that introduce vertical mixing causing the suspension of the bottom sediment (KMA 2010). Unpredictable discharges from Han River (55×10^6 m^3 d^{-1}) in the wet summer season bring nutrients into the system.

From 1986 to 1994, a 12.7 km sea dike was constructed within the Gyeonggi bay in order to create an artificial water body at proximity of Shiwha. This water body had a surface area of 42.3 km^2, a water storage capacity of 332 million tons, a maximum depth of 18 m, and a total seawater flux of 380 million tons per year (MOMAF 2006). The main tributaries of the Shiwha artificial water body consist of nine streams: the Okgu, Gunga, Jeongwang, Siheung, Singil, Ansan, Banweol, Dongwha, and Samwha streams (Oh *et al*. 2010). The Shiwha artificial water body was expected to transform into a freshwater lake and then be used for irrigation. However, the structures in place and the inputs from tributaries never enabled the establishment of a full freshwater body. Furthermore, eutrophication brought by the untreated sewage and wastewater flowing in from the Shiwha adjacent area caused a severe deterioration of the water quality in the middle of the 90s (Kim *et al*. 2004b).

The majority of the Gyeonggi bay shows a non-eutrophic state through the year. The reduced depth and mixing capacity of the system reduced stratification and the development of algal bloom. However, the Upper Gyeonggi bay and the Shiwha artificial water body show a eutrophic state in summer. These regions are characterized by enhanced nutrients and algal blooms. Moreover, strong stratification produced by freshwater inputs into the surface layer from precipitation and rainfall (NFRDI 2008) has accelerated harmful algal blooms and hypoxia.

The region is highly variable in regards of various environmental parameters such as the temperature, the salinity, the pH, the dissolved oxygen, the nutrients, and the phytoplankton biomass (i.e. chlorophyll a). The water temperature ranges

from 0.0 to 30.0 ºC with lower values during winter and maximum values in summer. Salinity variations are a reverse trend of temperature. Salinity ranges from 7.1 to 33.2 with lower values during the summer wet season and higher values in winter (Jahan *et al*. 2013). The pH is slightly higher in spring and autumn and dissolved oxygen concentrations are highest in winter. The nutrient concentrations are the highest in summer and eutrophic areas reaching values of approximately 50 µM dissolved inorganic nitrogen and 1 µM phosphate. In other seasons than summer, the system is characterized by lower nutrient concentrations. Chlorophyll a concentration can range from 0.7 to 210.7 µg L^{-1} (Jahan *et al*. 2013). The highest chlorophyll a concentrations are detected in summer in eutrophic areas which are considerably influenced by massive nutrient inputs. The chlorophyll a concentrations are considerably lower in other seasons than summer. The chlorophyll a experienced an increasing trend associated with an increase in dissolved inorganic nitrogen during the past decades (Park & Park 2000, NFRDI 2008).

The same tendencies observe in the region in regards of the temperature, the salinity, the nutrients, and the chlorophyll a are observed in the Shiwha artificial water body with the exception of both the pH and the dissolved oxygen for which there is no tendency (this study). The Shiwha artificial water body experiences similar water temperature ranging from 0.9 to 29.9 ºC and similar salinity ranging from 3.0 to 32.3 (this study). The nutrients reach higher concentrations than what is known for the region, the dissolved inorganic nitrogen getting up to 135.2 µM and the phosphate up to 3.8 µM. However, the phytoplankton biomass reaches lower value, the chlorophyll a getting up to 101.6 µg L^{-1} (this study).

The Upper Gyeonggi bay summer blooms are more dependent on physical processes rather than nutrients (Jahan *et al*. 2013). The huge discharges of the Han River not only deliver nutrients to the Upper Gyeonggi bay but also determine the hydrological properties of the water column, including high temperature, low salinity, vertical thermal stability, low turbidity as well as high light conditions. All of these properties trigger phytoplankton growth most likely by supplying proper temperature, increasing the light intensity, and retaining the algal cells in the euphotic zone. The Gyeonggi bay summer blooms are mostly dominated by the nano-size phytoplankton (2-20 μm). During 2000-2004, cryptomands (<5 μm) were the most dominant phytoplankton species associated with co-dominant diatoms, whereas the diatoms *Skeletonema costatum* and *Chaetoceros* spp. were the only dominant group in the past (1981-1982) (Choi & Shim 1986b).

The mechanism for summer blooms in the Shiwha artificial water body implicates huge freshwater inputs from the neighbouring municipal and industrial complexes through the adjacent streams. These inputs are large enough to offset the effects of tidal and wind stirring. As a result, the water column remains stratified at a depth range of 6-8 m for a period of time sufficient to promote phytoplankton growth and to generate frequent red tides indicating a hypertrophic condition (Choi *et al*. 1997, Han & Park 1999, Kim *et al*. 2004b). Summer harmful algal blooms are frequently caused by dinoflagellates (*Prorocentrum minimum*), cryptomonads, and Chrysophyceae, whereas diatoms (*Cyclotella atomas*, *Nitzchia* sp., and *Chaetoceros* sp.) are dominant in autumn and winter (Choi *et al*. 1997).

This study will particularly focus on the Shiwha artificial water body hereafter referred as Shiwha bay.

1.5 Context of the study

The azaspiracids (AZAs) were first identified following an outbreak of human illness in the Netherlands that was associated with ingestion of contaminated shellfish originating from Killary Harbour, Ireland (Twiner *et al*. 2008, Furey *et al*. 2010). Although the symptoms were typical of diarrhetic shellfish poisoning (DSP) toxins such as okadaic acid (OA) and dinophysistoxins (DTX), the levels of DSP toxins in these shellfish were well below the regulatory level. The shellfish were contaminated with a unique marine toxin, originally named Killary-toxin (Satake *et al*. 1998a). Thereafter, the toxin was renamed to azaspiracid (AZA) to more appropriately reflect its chemical structure: a cyclic amine, or aza group, with a tri-spiro assembly and carboxylic acid group (Satake *et al*. 1998a b).

To date, over 20 AZA analogues have been identified in phytoplankton and shellfish (Satake *et al*. 1998a b, Ofuji *et al*. 1999, Ofuji *et al*. 2001, Lehane *et al*. 2002, James *et al*. 2003a, Rehmann *et al*. 2008, McCarron *et al*. 2009, Jauffrais *et al*. 2012). The structure of these analogues was determined by using mass spectrometry in tandem mode and nuclear magnetic resonance (NMR) (Ofuji *et al*. 1999, Ofuji *et al*. 2001). The fragmentation of AZA molecules obtained by mass spectrometry produced characteristic ions of this molecular family (Brombacher *et al*. 2002, Diaz Sierra *et al*. 2003, James *et al*. 2003a, Rehmann *et al*. 2008). Only the AZA-1 to -5 were isolated and structurally confirmed by using NMR. The AZA-6 joined this list in 2012 (Kilcoyne *et al*. 2012).

AZAs have been reported in shellfish from many coastal regions of western Europe (James *et al*. 2002, Braña Magdalena *et al*. 2003, Furey *et al*. 2003, Amzil

et al. 2008**)**, South America (Álvarez *et al*. 2010, López-Rivera *et al*. 2010), and northern Africa (Taleb *et al*. 2006, Elgarch *et al*. 2008**)**. In addition, AZAs have been found in Scandinavian crabs (Torgersen *et al*. 2008) and Japanese sponges (Ueoka *et al*. 2009).

Since the first poisoning event in 1995, five new episodes of food poisoning occurred as the result of the consumption of contaminated Irish mussels (Table 1.2) in Irland, Italy, France, United kingdom and United States (Twiner *et al*. 2008, Klontz *et al*. 2009).

While the consumption of contaminated mussels by AZA caused multiple health problems, it is only in 2003 that the AZAs were detected for the first time in the phytoplankton species *Protoperidinium crassipes*, a dinoflagellate (James *et al*. 2003b). However, most of the toxin producers are photosynthetic or mixotrophic. Since *P. crassipes*, a heterotrophic dinoflagellate, is able to accumulate phycotoxins from its preys (Miles *et al*. 2004a), it was questionable whether it was a primary producer of AZA or not (Miles *et al*. 2004b, Hess *et al*. 2005). In 2007, in North Sea, a species producing AZA was isolated for the first time off Scotland (Krock *et al*. 2008). This organism was a producer of AZA-1 and -2 *in situ* and in axenic culture (Krock *et al*. 2009, Tillmann *et al*. 2009). The organism, a small thecal dinoflagellate (12-16 µm long; 7-11 µm wide), belonged to a new genus and was officially described as *Azadinium spinosum* (Tillmann *et al*. 2009).

Table 1.2 Food poisoning caused by azaspiracids and reported between 1995 and 2008

Poisoning location	Date	Poisoning source	Production location	Number of intoxication
The Netherlands[1,2]	November 1995	Mussels (*Mytilus edulis*)	Killary Harbour, Ireland	8
Ireland[1,2]	September/October 1997	Mussels (*Mytilus edulis*)	Arranmore Island, Ireland	ca. 20-24
Italy, Ravenna[1,2]	September 1998	Mussels (*Mytilus edulis*)	Clew bay, Ireland	10
France[1,2]	September 1998	Mussels (*Mytilus edulis*)	Bantry bay, Ireland	ca. 20-30
United Kingdom[1,2]	August 2000	Mussels (*Mytilus edulis*)	Bantry bay, Ireland	ca. 12-16
France[2,3]	April 2008	Mussels (*Mytilus edulis*)	Ireland	outbreak
United States[4]	July 2008	Mussels (*Mytilus edulis*)	Bantry bay, Ireland	2

References.[1]Twiner *et al*. 2008, [2]Furey *et al*. 2010, [3]RASFF 2008, [4]Klontz *et al*. 2009

Following the discovery of *Azadinium spinosum* as a source of AZA, multiple other species were discovered or transferred to this recently discovered genus, namely *A. obesum*, *A. poporum*, *A. caudatum*, and *A. polongum* (Tillmann *et al*. 2010, 2011, 2012a, Nézan *et al*. 2012). All species of the genus *Azadinium* are thecal. Most species of *Azadinium* are small (size of about 10-15 μm) and ovoid to elliptical in shape with a hemispherical hyposome. *A. caudatum* is distinctly larger and, with a characteristic biconical outline, significantly different in shape as well. In all species, the episome is larger than the hyposome. All species are photosynthetic and possess a presumably single chloroplast which is parietally arranged, lobed, and normally extends into both the epi- and hyposome. A compilation of distinctive features of the species of the genus *Azadinium* are compiled in Table 1.3.

The repartitions of AZAs (Fig. 1.1) and their progenitors (Fig. 1.2) in the multiple oceans of the world make these organisms a worldwide preoccupation. Knowledge on their classification, distribution, toxin analogues, field dynamics, interactions within the food web, and physiology is primordial to our understanding of their evolution and dynamics in the field.

In this context, this thesis aims to: (1) establish the occurrence of species of the genus *Azadinium* in Korea, (2) determine the AZA present in the species isolated, (3) determine the population dynamics of the species, (4) establish the growth and/or grazing capacity of protistan predators and copepods on the isolated species, and (5) assess the physiology of the species.

Table 1.3 Morphological features for species of the genus *Azadinium*

Feature	*Azadinium spinosum*[1]	*Azadinium obesum*[2]	*Azadinium poporum*[3]	*Azadinium caudatum*[4]		*Azadinium polongum*[5]
				var. *margalefii*	var. *caudatum*	
Length x Width (μm)	13.8 x 8.8	15.3 x 11.7	13.0 x 9.8	31.3 x 22.4[a]	41.7 x 28.7[a]	13.0 x 9.7
Length/Width ratio	1.6	1.3	1.3	1.2[b]	1.2[b]	1.3
Stalked pyrenoid(s) number	1 Central episome	0	≤ 4	0	0	0
Antapical projection	Small spine	No	No	Short horn Long spine	Long horn Short spine	Small spine
Location "ventral" pore	Left side of 1' (median position)	Left side of 1' (median position)	Left side of pore plate	Right side of pore plate	Right side of 1' (posterior position)	Left side, suture of 1'and 1" (slightly posterior)
Shape of pore plate	Round Ellipsoid	Round Ellipsoid	Round Ellipsoid	Round Elipsoid	Round Ellipsoid	Distinctly elongated

Table 1.3 (continued)

Feature	*Azadinium spinosum*[1]	*Azadinium obesum*[2]	*Azadinium poporum*[3]	*Azadinium caudatum*[4]		*Azadinium polongum*[5]
				var. *margalefii*	var. *caudatum*	
Contact of ventral precingulars with intercalaries	Ventral 1" in contact to 1a	No	Ventral 1" in contact to 1a	Ventral 1" in contact to 1a Ventral 6" in contact to 3a	Ventral 1" in contact to 1a, Ventral 6" in contact to 3a	Ventral 1" in contact to 1a
Shape of plate 4"	Similar size as other precingulars, in contact to 3a	Similar size as other precingulars, in contact to 3a	Similar size as other precingulars, in contact to 3a	Smaller than other precingulars, no contact to 3a	Smaller than other precingulars, no contact to 3a	Similar size as other precingulars, in contact to 3a
Azaspiracids	AZA-1,-2, -716	Not detected	Large strain variability, AZA-846, -876, -2 AZA new china	Not detected	No culture available, not analyzed yet	Not detected

[a]Cell length including antapical projection (horn and spine) [b]Length excluding antapical projection

References. [1]Tillmann *et al*. 2009; [2]Tillmann *et al*. 2010; [3]Tillmann *et al*. 2011, Krock *et al*. 2012; [4]Nézan *et al*. 2012 [5]Tillmann *et al*. 2012a

Fig. 1.1 Worldwide detection of azaspiracids

References. [1]Álvarez *et al*. 2010, [2]Amzil *et al*. 2008, [3]Braña Magdalena *et al*. 2003, [4]Taleb *et al*. 2006, [4]Elgarch *et al*. 2008, [5]Ueoka *et al*. 2009, [6]Vale *et al*. 2008, [7]James *et al*. 2002, [8]Furey *et al*. 2003, [9]López-Rivera *et al*. 2010, [10]Torgersen *et al*. 2008

Fig. 1.2 Worldwide distribution of *Azadinium* spp. and *Amphidoma languida*

References. [1]Tillmann *et al*. 2009, 2010, [2]Tillmann *et al*. 2011, [3]Salas *et al*. 2011, [3]Tillmann *et al*. 2012a, [4]Tillmann *et al*. 2012b, [5]Nézan *et al*. 2012, [6]Hernández-Becerril *et al*. 2012, [7]Akselman & Negri 2012, [8]Potvin *et al*. 2012, [9]Gu *et al*. 2013

This first chapter made a brief overview of the marine organisms producing phycotoxins, their toxins, and the main environmental factors as well as interspecies factors affecting the dynamics of toxic dinoflagellates.

The second chapter establishes the morphology with optical and scanning election microscopy, the phylogenetic position based on the SSU rRNA gene, the ITS rDNA region, and LSU rRNA gene, and if known AZA occurred in the strain of the genus *Azadinium* isolated from Shiwha bay, Korea.

The third chapter analyses, with a closer look, the content of AZA in the Korean strain of the genus *Azadinium* using triple quadrupole mass spectrometry in the precursor and product ion mode. The structure of a new compound related to AZA is proposed by interpretation of fragmentation patterns and high resolution mass measurements using Fourier transform ion cyclotron resonance-mass spectrometry (FTICR-MS).

The fourth chapter determines protistan and metazoan predators of the strain of the genus *Azadinium*, their physiology in regards of growth and/or grazing based on prey concentration, and their gross growth efficiency. Furthermore, qPCR is used to determine the population dynamics of the isolated species of the genus *Azadinium* from Shiwha bay for three years.

Finally, **the fifth chapter** looks at the tendency of various physical and chemical factors through time and seasons in Shiwha bay, the effect of some environmental factors on the growth of the strain in laboratory, and the

relationships between environmental factors and the occurrence of the strain of the genus *Azadinium* in the field.

Chapter 2: Taxonomy

First Report of the photosynthetic dinoflagellate genus *Azadinium* in the Pacific Ocean: morphology and molecular characterization of *Azadinium* cf. *poporum*

2.1 Abstract

A strain of a dinoflagellate belonging to the genus *Azadinium* was obtained by the incubation of sediments collected from Shiwha bay, Korea. This report of the genus *Azadinium* is the first outside of northern Europe and furthermore from the Pacific Ocean. The diagnostic morphological features of the isolate very closely resemble the recently described species *Azadinium poporum* isolated from the North Sea. However, the shape of the 3′ apical plate and the occasional morphological variations unreported from *A. poporum* bring minor distinctions between strains from different locations. The sequences of the SSU rDNA, ITS rDNA, and LSU rDNA differed by 0.2 %, 2.6 %, and 3.6 %, respectively, from those of *A. poporum*, whereas the COI gene was identical to those found in all strains of *Azadinium*. Phylogenetic analyses of the ribosomal DNA regions generally positioned the Korean strain as a sister taxon of *A. poporum*. However, the Korean isolate tends to occupy a basal position within *Azadinium* species with ITS rDNA and LSU rDNA. Using liquid chromatography coupled with tandem mass spectrometry, no known azaspiracids were detected. The slight but discernible morphological differences, the distinct rDNA sequences, and the tendency of the Korean strain to diverge phylogenetically based on ITS rDNA and LSU rDNA from *A. poporum* do not enable us to clearly assign the isolate to *A.*

poporum. It is therefore designated as *Azadinium cf. poporum*. The examination of more strains to find more diagnostic characteristics might enable the attribution of this material to a well-defined taxonomic position.

2.2 Keywords

Asia, azaspiracids, harmful algal blooms, rDNA, toxin

2.3 Introduction

Dinoflagellates are among the major components of marine ecosystems (Lessard 1991, Jeong 1999, Sherr & Sherr 2007, Terrado *et al*. 2009). Many dinoflagellate species cause red tides or harmful algal blooms (Lu & Hodgkiss 2004, Phlips *et al*. 2011). In particular, some toxic species are harmful to marine organisms and humans (Bagnis *et al*. 1980, Frangópulos *et al*. 2000, Prince *et al*. 2008, Tillmann & Hansen 2009, Tang & Gobler 2010, Pelin *et al*. 2011). Azaspiracids (AZAs) are the most recently discovered group of lipophilic marine biotoxins of microalgal origin associated with cases of shellfish poisoning in humans (Twiner *et al*. 2008). The heterotrophic dinoflagellate *Protoperidinium crassipes* was initially thought to be a causative species (James *et al*. 2003b), but further research identified a small phototrophic dinoflagellate as the source of the AZAs (Krock *et al*. 2009). This species, *Azadinium spinosum* Elbrächter *et* Tillmann, was assigned to a new genus (Tillmann *et al*. 2009). The relevance of this species attracted attention to species similar in morphology, size, and swimming pattern. Soon afterward, a new nontoxic species closely related to *A. spinosum* was discovered in the coastal waters off Scotland and described as *Azadinium obesum* Tillmann *et* Elbrächter (Tillmann *et al*. 2010). Recently,

another new nontoxic species of the genus *Azadinium* has been described as *Azadinium poporum* Tillmann *et* Elbrächter (Tillmann *et al*. 2011) from the North Sea off Denmark. Therefore, all the known species of the genus *Azadinium* were to date described from the North Sea.

The usual tabulation of the genus *Azadinium* follows the Kofoidian formula Po, cp, X, 4', 3a, 6", 6c, 5?S, 6‴, 2⁗. The distinctive morphological characters proposed so far for differentiating each species in this genus are the presence of an antapical spine, the location of a conspicuous pore (initially described as a ventral pore, but subsequently shown to occur apically on the Po plate depending of the species), the relative size of the anterior intercalary plates, the width of the first apical plate (1') in its lower part, the presence of stalked pyrenoids and the presence of a contact between the 1" and 1a plates (Tillmann *et al*. 2009, 2010, 2011).

The phylogenetic reconstructions support the separation of all three previously described species within the genus *Azadinium*. The genus *Azadinium* is stable and produces well-defined clades. *Azadinium spinosum* and *A. obesum* seem to be more closely related to each other than to *A. poporum* (Tillmann *et al*. 2011). Based on pairwise comparison of sequences when available, there is no intraspecific variability in actual species even though some stains were isolated from different locations such as *A. spinosum*.

We recently isolated a small dinoflagellate able to grow photosynthetically from Shiwha bay, Korea, and established a clonal culture. In this study, we report the morphological and genetic characteristics of this Korean strain and present phylogenetic trees based on SSU rDNA, ITS rDNA, and LSU rDNA. Furthermore, we test the occurrence of known AZAs. This is the first report of the genus

Azadinium in Korean waters and the Pacific Ocean.

2.4 Materials and methods

2.4.1 Collection and culturing of *Azadinium* cf. *poporum*

For the isolation and culture of *Azadinium* cf. *poporum*, surface sediment samples from Shiwha bay, Korea (37°18'N, 126°36'E), were collected in June 2010 using an Ekman grab (WILDCO,Wildlife Supply Company, Buffalo, NY), and stored in the dark at 4 °C. The sediment samples were sieved consecutively through 100 and 15 μm Nitex meshes. The fraction retained on the 15 μm Nitex mesh was used for further processing. Cells and particles of similar density were then separated from the gross sand by the application of a manual vortex in filtered seawater and the recovery of the suspended fraction. The clean sediment fraction was then incubated in F/2 medium-Si (Guillard & Ryther 1962) in a growth chamber at 20 °C under an illumination of 20 μE m^{-2} s^{-1} on a 14:10 h light: dark cycle. The incubated sediment was regularly observed for motile cells under a stereomicroscope (Olympus, SZX-12, Tokyo, Japan). Individual cells normally swimming at low speed and interrupted by short high-speed "jumps" in various directions, typical of the genus *Azadinium* (Tillmann *et al*. 2009), were isolated by micromanipulation in well plates (SPL Life Sciences, Pocheon, Korea). Each well contained ca. 360 μL F/2 medium-Si. When the cells reached a high density, they were isolated a second time and subsequently brought in 1 L volume.

2.4.2 Morphology of *Azadinium* cf. *poporum*

The morphology of living cells of *A.* cf. *poporum* was examined using a

transmitted light inverted microscope (Zeiss Axiovert 200M, Carl Zeiss Ltd., Göttingen, Germany) equipped with differential interference contrast optics at magnifications of 50-1000x. In addition, the length and width of cells were measured with a Zeiss AxioCam MRc5 digital camera (Carl Zeiss Ltd).

For scanning electron microscopy (SEM), cells from 50 mL of a dense culture were collected in conical centrifuge tubes (SPL Life Sciences) by centrifugation for 5 min at 2190 g (Hanil Science Industrial Co., Ltd., model FLETA 5, Incheon, Korea). The supernatant was removed and the cell pellet resuspended in 60 % ethanol for 1 h at 4 °C or room temperature to strip off the outer cell membrane similarly to Tillmann *et al*. (2011). Subsequently, the cells were pelleted by centrifugation and resuspended in 50 % filtered seawater for 30 min at 4 °C or room temperature. After centrifugation, the seawater supernatant was removed, and the cell pellet was resuspended and fixed in 50 % filtered seawater with 5 % (w/v) paraformaldehyde for 3 h at 4 °C. The cells were then collected on polycarbonate membrane filters (Whatman Nucleopore Track-Etch, 25 mm, 3 µm or 5 µm pore size, Dassel, Germany) in filter funnels without additional pressure. The cells were washed for 15 min with 50 % filtered seawater followed by 15 min of reverse osmosis purified water (Human RO 180, Human Corporation, Seoul, Korea). The washings were followed by a dehydration series in ethanol (i.e. 10 %, 30 %, 50 %, 70 %, 90 %, 100 % x 3). The filters were dried using a critical point dryer (BAL-TEC, CPD 030, Balzers, Liechtenstein). Finally, the filters were mounted on stubs, sputtercoated (BAL-TEC, SCD 005, Balzers) with gold-palladium and observed with a FE-scanning electron microscope (AURIGA®, Carl Zeiss). The specimens were photographed using a digital camera. Some SEM micrographs were presented on a black background using Adobe Photoshop CS4 Extended (Adobe Systems Inc., San Jose, CA). Measurements of detailed features

of the theca obtained from SEM pictures were made using the software Engauge Digitizer.

In describing the thecal plate tabulation, we employed the nomenclature of Kofoid (1909). The designation of the putatively subdivided thecal plates is adopted from Morrill & Loeblich (1981). The terminology used to describe plate modifications from the usual plate pattern followed Lefèvre (1932).

2.4.3 DNA extraction, PCR amplification, and sequencing

A 50 mL sample of an exponentially growing culture was filtered on a polycarbonate membrane (Whatman Nucleopore Track-Etch, 25 mm, 3 μm pore size) and resuspended by vortexing in sterile reverse osmosis purified water in a 1.5 mL microtube (Scientific Specialties Inc., Lodi, CA). The sample was subsequently centrifuged (DAIHAN Scientific Co., Ltd., WiseSpin® CF-10 Microcentrifuge, Namyangju, Korea) at 7500 g for 5 min at room temperature. The cells were immediately subjected to total DNA extraction using the AccuPrep® Genomic DNA extraction kit (Bioneer Corp., Daejeon, Korea) according to the manufacturer's instructions.

A thermal cycler (Eppendorf AG, Mastercycler® ep, model 5341, Hamburg, Germany) was used for PCR reactions. The final concentrations of PCR products were as follows: 1X PCR f-Taq buffer (SolGent Co., Ltd., fTaq DNA Polymerase, Daejeon, Korea), 0.2 mM of dNTP mix (SolGent Co., Ltd., fTaq DNA Polymerase), 0.4 μM of each primer, 0.025 U μL^{-1} of f-Taq DNA polymerase (SolGent Co., Ltd., fTaq DNA Polymerase), and 1.5 mM of $MgCl_2$. A volume of 1.0 μL of the DNA extraction was used as template in individual reactions, with a

final volume of 50 μL. The SSU rDNA, ITS rDNA, LSU rDNA, and COI mitochondrial DNA were obtained with these respective primer pairs: EukA (5'-CTG GTT GAT CCT GCC AG-3'; Medlin *et al*. 1988) and G23R (5'-TTC AGC CTT GCG ACC ATA C-3'; Litaker *et al*. 2003); G17F (5'-ATA CCG TCC TAG TCT TAA CC-3'; Litaker *et al*. 2003) and 5.8SR (5'-CAT CGT TGT TCG AGC CGA GAC-3'; Litaker *et al*. 2003); Euk 1209F (5'-CAG GTC TGT GAT GCC C-3') and ITSR2 (5'-TCC CTG TTC ATT CGC CAT TAC-3'; Litaker *et al*. 2003); 5.8SF (5'-CAT TGT GAA TTG CAG AAT TCC-3'; Litaker *et al*. 2003) and LSUB (5'-ACG AAC GAT TTG CAC GTC AG-3'; Litaker *et al*. 2003); and DINOCOX1F (5'-AAA AAT TGT AAT CAT AAA CGC TTA GG-3'; Lin *et al*. 2002) and DINOCOX1R (5'-TGT TGA GCC ACC TAT AGT AAA CAT TA-3'; Lin *et al*. 2002). The PCRs were produced as follows: one activation step at 95 °C for 2 min, followed by 35 cycles at 95 °C for 20 s, the selected annealing temperature (AT) for 40 s, and 72 °C for 1 min, and a final elongation step at 72 °C for 5 min. The AT was adjusted depending on the primers used according to the manufacturer's instructions.

Positive and negative controls were used for all amplification reactions. The purity of the amplicons was controlled by the migration of 3 μL of PCR products in 1.0 % agarose containing ethidium bromide and its observation under a UV lamp. The PCR products were purified using the AccuPrep® PCR purification kit (Bioneer Corp.) according to the manufacturer's instructions. The purified DNA was sent to the Genome Research Facility (School of Biological Science, Seoul National University, Korea) and sequenced with an ABI PRISM® 3700 DNA Analyzer (Applied Biosystems, Foster City, CA).

2.4.4 Sequence availability and phylogenetic analysis

Partial DNA sequences were combined with BioEdit v7.0.9.0 (Hall 1999). Sequences of taxa used to construct the phylogenies (Table 2.1) were aligned using CLUSTAL X v2.0 (Larkin *et al*. 2007). The alignment was refined manually to remove ambiguities. The matrix was then analyzed with PAUP v4.0b10 (Swofford 2002). Three phylogenetic methods were used with PAUP: neighbor joining (NJ); maximum parsimony (MP); and maximum likelihood (ML). The Kimura 2-parameter model (Kimura 1980) was used as a nucleotide substitution model for NJ analysis. Models of nucleotide substitution were determined for ML with Modeltest v7.3 (Posada & Crandall 1998) based on the Akaike information criterion (Posada & Buckley 2004). A heuristic tree search was used to determine the optimal trees for the MP and ML methods. The tree bisection-reconnection algorithm was used with 1000 and five random additions of sequences for MP and ML, respectively. The characters were equally weighted and spaces in the alignment were treated as missing data. RAxML v7.0.4 (Stamatakis 2006) was used to calculate ML bootstrap values using the default algorithm with the general time reversible + Γ model of nucleotide substitution and 1000 replicates.

The matrix was also analyzed with MrBayes v3.1.2 (Huelsenbeck & Ronquist 2001) for Bayesian analyses. The models previously selected by Modeltest 7.3 were used. Four independent Markov chain Monte Carlo simulations were run simultaneously for 2 000 000 generations. Trees were sampled every 1000 generations, and the first 800 trees were deleted to ensure that the likelihood had reached convergence. A majority-rule consensus tree was created from the remaining 1201 trees to examine the posterior probabilities of each clade.

Table 2.1 Taxa used to establish the phylogenies based on SSU rDNA, ITS rDNA, and LSU rDNA

	SSU rDNA	ITS rDNA	LSU rDNA
Akashiwo sanguinea	AY421770	-	AF260396 EF613348
Alexandrium affine	DQ166532	-	AY566190
Alexandrium catenella	-	-	AB196485
Alexandrium minutum	AJ535380	-	-
Alexandrium ostenfeldii	AJ535384	-	-
Alexandrium tamarense	-	-	AB196557
Alexandrium taylorii	AJ535385	-	-
Amphidinium herdmanii	AF274253	-	AY455675
Amphidinium semilunatum	AF274256	-	AY455678
Azadinium obesum 2E10	GQ914935	FJ766093	GQ914936
Azadinium poporum UTHD4	HQ324899	HQ324891	HQ324895
Azadinium poporum UTHC5	HQ324897	HQ324889	HQ324893
Azadinium poporum UTHC8	HQ324898	HQ324890	HQ324894
Azadinium spinosum 3D9	FJ217814	FJ217816	HQ324896
Azadinium spinosum UTHE2	HQ324900	HQ324892	HQ324896
Azadinium* cf. *poporum	FR877580	FR877580	FR877580
Calciodinellum albatrosianum	-	-	DQ167853
Calciodinellum levantinum	-	-	DQ167854
Ceratium fusus	AF022153	-	AF260390
Ceratium lineatum	-	-	AF260391
Crypthecodinium cohnii	-	-	-
Cryptoperidiniopsis sp.	-	-	AY436359
Dinophysis acuminata	EU130569	-	EF613351
Ensiculifera aff. *imariensis*	-	-	DQ167856
Ensiculifera cf. *loeblichii*	-	-	DQ167857
Fragilidium subglobosum	-	-	AF260387
Gonyaulax baltica	-	-	AF260388
Gonyaulax polygramma	AY775287	-	-
Gymnodinium aureolum	AJ415517	-	AY464687

Table 2.1 (continued)

	SSU rDNA	ITS rDNA	LSU rDNA
Gymnodinium catenatum	AY421785	-	AF200672
Gymnodinium fuscum	AF022194	-	AF200676
Gymnodinium impudicum	AF022197	-	AF200674
Gymnodinium instriatum	DQ847433	-	DQ847432
Gymnodinium mikimotoi	-	-	AF200682
Gymnodinium simplex	DQ388466	-	AF060901
Gymnodinium sp.	AF274260	-	-
Gyrodinium fissum	-	-	EF613353
Heterocapsa arctica	-	-	AY571372
Heterocapsa circularisquama	-	-	AB049709
Heterocapsa hallii	AF033865	-	AF033867
Heterocapsa niei	AF274265	-	-
Heterocapsa pygmaea	AF274266	-	-
Heterocapsa rotundata	AF274267	-	AF260400
Heterocapsa triquetra	AJ415514	-	AF260401 EF613355
Heterocapsa sp.	AB183639	-	AY371082 AF260399
Karenia brevis	AF274259	-	AY355459
Karenia umbella	-	-	AY266329
Karlodinium antarcticum	-	-	EF469234
Karlodinium micrum	AM494500	-	AF200675 AY263964
Lingulodinium polyedra	AF274269	-	-
Oxyrrhis marina	AF280077	-	EF613360
Pentapharsodinium tyrrhenicum	AF022201	-	DQ167859
Peridiniella catenata	-	-	AF260398
Peridiniopsis polonicum	AY443017	-	-
Peridinium aciculiferum	AY970653	-	-
Peridinium bipes f. *globosum*	EF058242	-	-
Peridinium cinctum	EF058245	-	-

Table 2.1 (continued)

	SSU rDNA	ITS rDNA	LSU rDNA
Peridinium limbatum	DQ980484	-	-
Peridinium palatinum	-	-	AF260394
Peridinium umbonatum	AF274271	-	-
Peridinium wierzejskii	AY443018	-	-
Peridinium willei	AF274280	-	-
Pernambugia tuberosa	-	-	DQ167860
Prorocentrum compressum	-	-	AY259169
Prorocentrum dentatum	DQ336057	-	AY833515
Prorocentrum donghaiense	DQ336054	-	-
Prorocentrum mexicanum	Y16232	-	DQ336183
Prorocentrum micans	AJ415519	-	EF613361
Prorocentrum minimum	DQ028763	AF352370	DQ662402
Prorocentrum triestinum	AB183673	-	AY863010
Protoceratium reticulatum	-	-	AF260386
Pseudopfiesteria shumwayae	AF080098	-	-
Pyrodinium bahamense	AF274275	-	-
Rhinodinium broomeense	-	-	DQ078782
Scrippsiella nutricula	U52357	-	-
Scrippsiella precaria	DQ847435	-	DQ167863
Scrippsiella rotunda	-	-	DQ167864
Scrippsiella sweeneyae	AF274276	-	AY628428
Scrippsiella trochoidea	AY421792	-	EF613366 DQ167865
Symbiodinium sp.	-	-	AF396626
Takayama cf. *pulchella*	AY800130	-	AY764178 U92254
Takayama tasmanica	-	-	AY284948
Togula britannica	AY443010	-	AY455679
Togula jolla	-	-	AY455680

2.4.5 Chemical analysis of azaspiracids

After approximately 3 wk of growth, 300 mL of *A.* cf. *poporum* culture was harvested at a concentration of 1.78 x 10^5 cells mL^{-1} determined by microscopical cell counts using a Sedgwick-Rafter chamber. The samples were centrifuged at 2190 g for 10 min in 50 mL conical centrifuge tubes (SPL Life Sciences). The cell pellets were combined in 1.5 mL microtubes (Scientific Specialties Inc.) and centrifuged again at 7500 g for 5 min. The cells were then frozen at 20 °C until analyzed.

A quantity of 250 µL of methanol was added to cells. The mixture was vigorously shaken and subsequently transferred to FastPrep vials containing 0.9 g lysing matrix D (Thermo-Savant, Illkirch, France). The procedure was repeated with another 250 µL of methanol, and corresponding samples were combined. The samples were homogenized by reciprocal shaking for 45 s at 6.5 m s^{-1}. The homogenates were centrifuged at 16 200 g for 15 min at 4 °C, and the supernatants were filtered through 0.45 µm cut-off spin filters by centrifugation for 30 s at 800 g. The filtrates were then transferred to HPLC vials and analyzed by liquid chromatography coupled to tandem mass spectrometry (LC-MS/MS) according to the methods described in detail by Tillmann *et al*. (2009). Selected reaction monitoring experiments were carried out in the positive ion mode for the most abundant AZA variants by selecting the following transitions (precursor ion > fragment ion): (1) AZA-1 and AZA-6: m/z 842 > 824 collision energy (CE): 40 V and m/z 842 > 672 CE: 70 V; (2) AZA-2 and Me-AZA-1: m/z 856 > 838 CE: 40 V and m/z 856 > 672 CE: 70 V; (3) AZA-3: m/z 828 > 810 CE: 40 V and m/z 828 > 658 CE: 70 V; and (4) Me-AZA-2: m/z 870 > 672 CE: 40 V and m/z 870 > 362 CE: 70 V. Precursor ion experiments were performed to detect putative unknown

AZA variants. Precursors of the characteristic AZA fragment m/z 362 were scanned in the range between m/z 300 and 1000.

2.5 Results

2.5.1 Morphology of *Azadinium* cf. *poporum*

The living cells of *A.* cf. *poporum* were ovoid and dorsoventrally compressed (Fig. 2.1 A-C). The hypotheca was generally semi-spherical and tended to be asymmetric, the left and right sides differing in length (Fig. 2.2 A-C). The hypotheca occasionally produced a protuberance at the antapex (Fig. 2.2 D). The episome was connected to the smaller hyposome by a deep and wide cingulum (Fig. 2.2 A-D). The large nucleus was spherical to slightly elongated and located in the central part of the cell (Fig. 2.1 A-B). Pyrenoids (> 1) were visible in most cells using light microscopy (Fig. 2.1 A). The exact number of pyrenoids was not determined. The antero-posterior (AP) length and width of cells fixed with Lugol's solution were 10.2-16.1 μm (mean ± standard deviation = 12.5 ± 0.9, n = 100) and 7.3-11.4 μm (mean ± SD = 9.2 ± 0.8, n = 100), respectively. The ratio of the AP length to the width of the cells was 1.17-1.53 (mean ± SD = 1.4 ± 0.1, n = 100).

The usual plate pattern of the Korean strain was arranged in the Kofoidian series Po, cp, X, 4', 3a, 6", 6C, 5(?)S, 6"', 2"" (Fig. 2.3 A-B). The episome ended with a conspicuous apical pore complex (APC) (Fig. 2.4 A-D). The round or slightly ellipsoid apical pore, located in the center of the pore plate (Po), was overlaid by a cover plate (cp) (Fig. 2.4 A-D). The length and width of the apical pore were 0.52-0.82 μm (mean ± SD = 0.71 ± 0.07, n = 27) and 0.39-0.63 μm (mean ± SD = 0.51 ± 0.06, n = 27), respectively. The X plate, which was connected

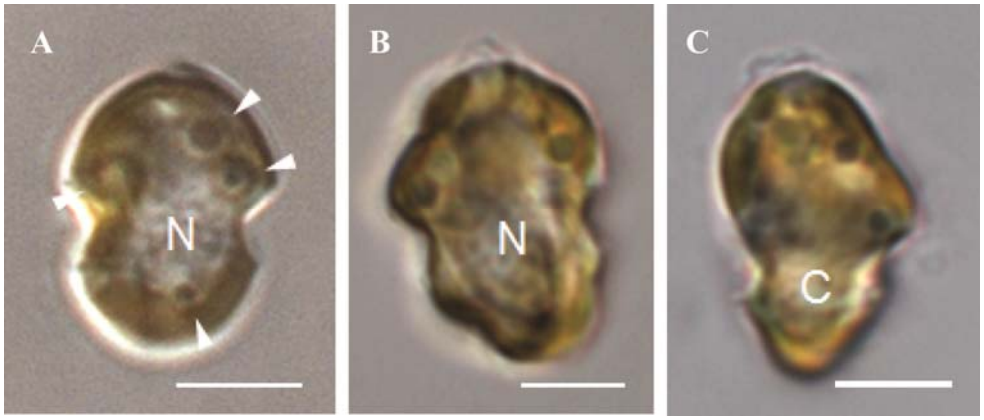

Fig. 2.1 Micrographs of cells of *Azadinium* cf. *poporum* taken using an inverted microscope. A-B. Mid-focus ventral view of live cells showing the nucleus and pyrenoids (white arrows) in both epitheca and hypotheca. C. Mid-focus lateral view of live cells showing the cingulum and the dorso-ventral compression. N: nucleus, C: cingulum. Scale bars = 5 μm

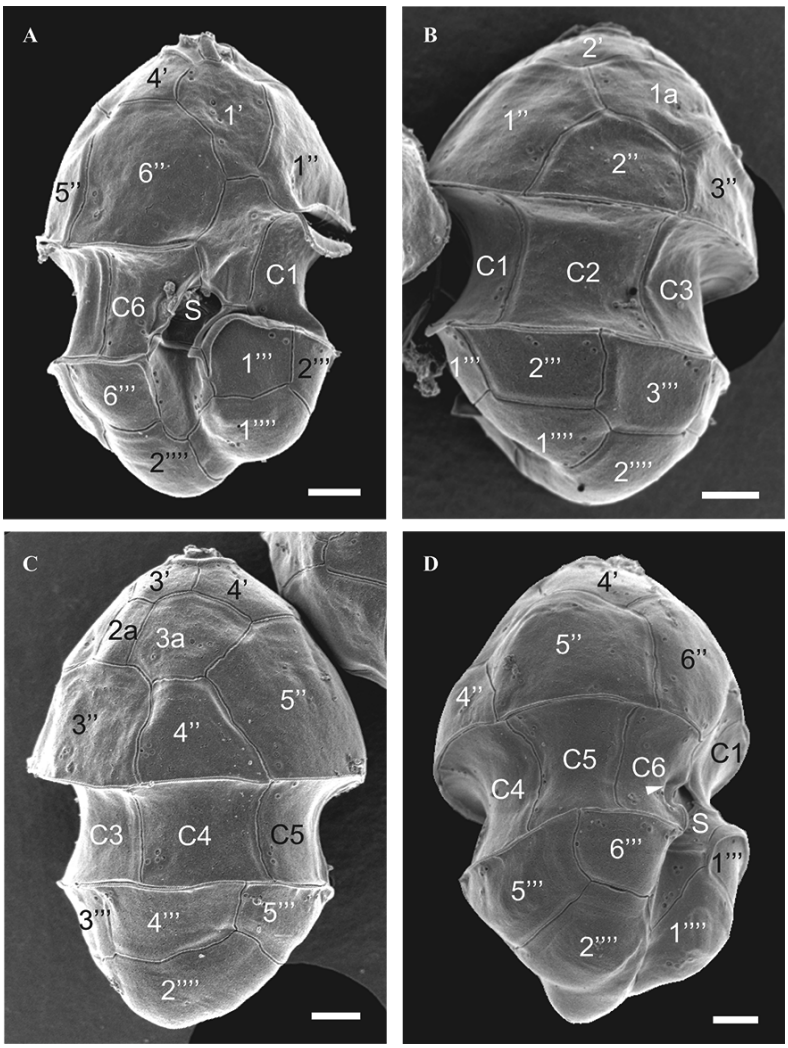

Fig. 2.2 Micrographs of cells of *Azadinium* cf. *poporum* taken using a scanning electron microscope. A. Ventral view. B. Left lateral view. C. Dorsal right lateral view. D. Right lateral view showing the sulcal list (arrow) and a protuberance at the antapex. The nomenclature of Kofoid (1909) was used to describe the thecal plate tabulation. S: sulcus. Scale bars = 1 μm

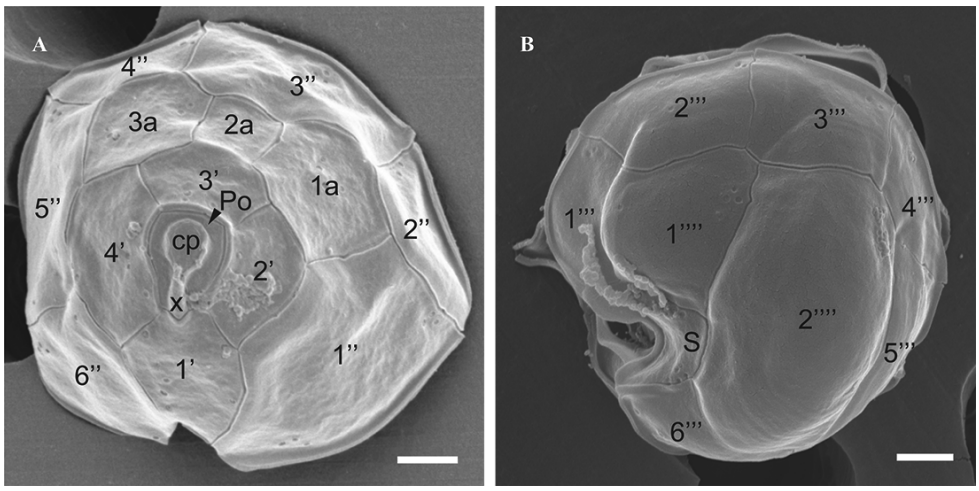

Fig. 2.3 Micrographs of cells of *Azadinium* cf. *poporum* taken using a scanning electron microscope. A. Apical view showing the whole series of epithecal plates. B. Antapical view showing the whole series of hypothecal plates. The nomenclature of Kofoid (1909) was used to describe the thecal plate tabulation. Po: pore plate, cp: cover plate, X: X plate, S: sulcus. Scale bars = 1 μm

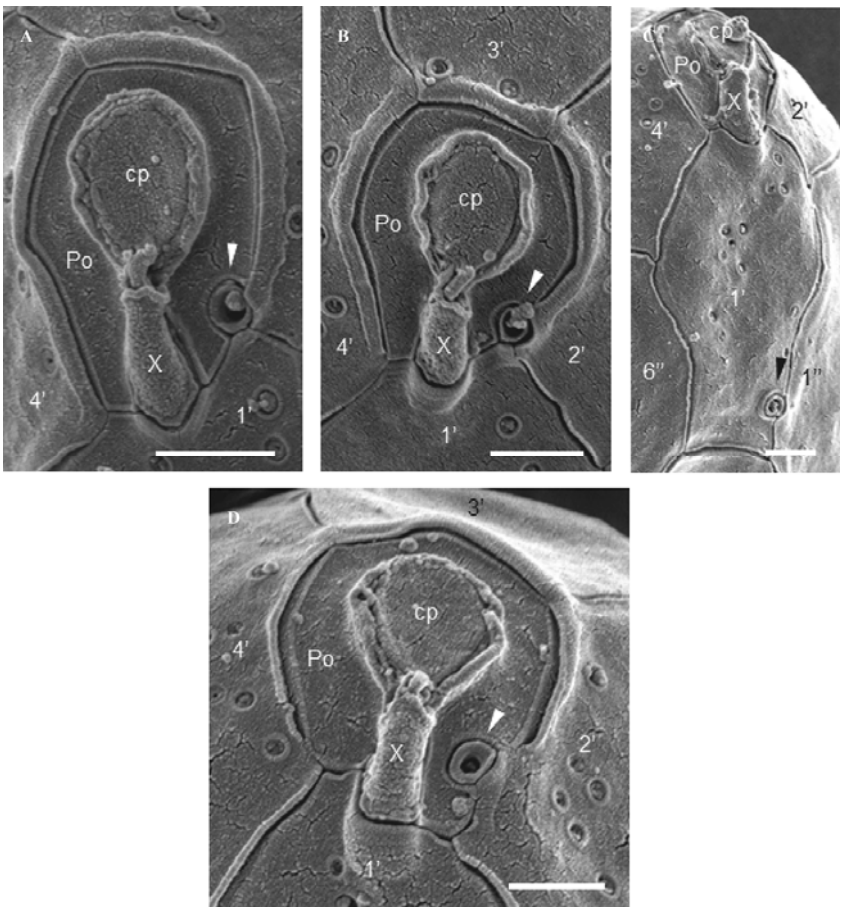

Fig. 2.4 Micrographs of cells of *Azadinium* cf. *poporum* taken using a scanning electron microscope showing the apical pore complex and other related features. A. Typical apical pore complex longer than wide with the ventral pore located at the intersection of the sutures of 1', 2' and Po (arrow). B. Apical pore complex almost as long as wide with the ventral pore located at the intersection of the sutures from 1', 2' and Po (arrow). C. Highly displaced ventral pore located unusually in a ventral position along the suture between 1' and 1" (arrow). D. Apical pore complex with a slightly displaced ventral pore located along the suture between 2' and Po (arrow). The nomenclature of Kofoid (1909) was used to describe the thecal plate tabulation. Po: pore plate, cp: cover plate, X: X plate. Scale bars = 0.5 μm

to the cp, was slightly intruded in the first apical plate (1') (Fig. 2.4 A-D). The Po was bordered by a conspicuous rim produced by the second, third, and fourth apical plates (Fig. 2.4 A-B) and was either elongated (Fig. 2.4 A) or of similar length and width (Fig. 2.4 B). The border of the Po was either sharply polygonal (Fig. 2.4 A) or rounded (Fig. 2.4 B-D). A conspicuous pore was usually located at the intersection of the Po, 1', and 2' plates (Fig. 2.4 A-B). This pore is assumed to be homologous to the ventral pore of *A. spinosum* and *A. obesum* (Tillmann *et al*. 2011). In the Korean strain, this pore was rarely located on the contact between the 2' plate and the Po plate of the APC (observed twice; Fig. 2.4 D) and found once on the contact between the 1' plate and 1" plate (Fig. 2.4 C). The length and width of the ventral pore, which was round or slightly ellipsoid (Fig. 2.4 A-D), were 0.20-0.34 μm (mean ± SD = 0.26 ± 0.04, n = 21) and 0.14-0.31 μm (mean ± SD = 0.22 ± 0.04, n = 21), respectively. Small pores were present on almost every plate. No pore was observed on the plates that formed the APC and the Sm and Sd plates of the sulcus. Small pores of different size were generally distributed randomly, but a group of small pores was often present on the 2"" plate (Fig. 2.3 B).

The first apical plate (1') touched the Po, X, 2', 4', 1", 6", and anterior sulcal (Sa) plates (Fig. 2.2 A). The 1' plate was slightly asymmetric. The contact with the 2' plate was smaller than the contact with the 4' plate. The size of the pentagonal 2' plate was similar to that of the hexagonal 3' plate, but smaller than the hexagonal 4' plate (Fig. 2.3 A). The quadrangular second anterior intercalary plate (2a), which touched the 3', 1a, 3a, and 3" plates, was usually smaller than the 1a and 3a plates (Fig. 2.3 A). The first precingular plate (1") was the biggest episomal plate (Fig. 2.3 A) and was in contact with the first intercalary plate 1a. The 3" and 5" plates were larger than the 2", 4", and 6" plates (Fig. 2.3 A).

The width of the left side of the cingulum (mean ± SD = 2.54 µm ± 0.21, n = 27) was similar to that of the right side (mean ± SD = 2.30 µm ± 0.19, n = 27). The cingulum was descending (Fig. 2.2 A), and was displaced by approximately half of its width (mean ± SD = 0.54 µm ± 0.15, n = 27) or by approximately one-tenth of cell length (mean ± SD = 0.13 ± 0.04, n = 27). Six cingular plates, similar to one another in size, were usually present (Fig. 2.2 A-D). In addition, narrow cingular lists were present (Fig. 2.2 A-D). A sulcal list was present at the right side of the cingulum and covered a part of the sulcal area (Fig. 2.5 A-D). Five sulcal plates occurred in a deeply concave sulcus: the anterior sulcal plate (Sa); the right sulcal plate (Sd); the left sulcal plate (Ss); the median sulcal plate (Sm); and the posterior sulcal plate (Sp). The Sa and Sp were much larger than the Sd and Sm, whereas the Ss was latitudinally extended (Fig. 2.5 A-D). The Sa, which extended toward the episome, touched the 1', 1", 6", C1, C6, and Ss plates and covered the Sm plate slightly (Fig. 2.5 A-D). The Ss plate, which touched the Sd, Sm, Sa, Sp, C6, and 1‴ plates, intruded the C1 plate (Fig. 2.5 A-D). The wide Sp touched the C6, Ss, 1‴, 6‴, 1⁗, and 2⁗ plates (Fig. 2.5 A-C).

The hypotheca was usually composed of six postcingular plates and two antapical plates. The 2⁗ was usually the biggest hyposomal plate (Fig. 2.3 B). Departures occurred from the usual tabulation pattern outlined above. Individual cells showed thecal modifications, including the fusion of plates (i.e. simplex modifications), the division of plates (i.e. complex modifications), and the displacement of sutures (i.e. travectum modifications) (see Fig. 2.6 A-H for examples). The plasticity was estimated to be ca. 40 % based on ca. 200 observations of scanning electron micrographs.

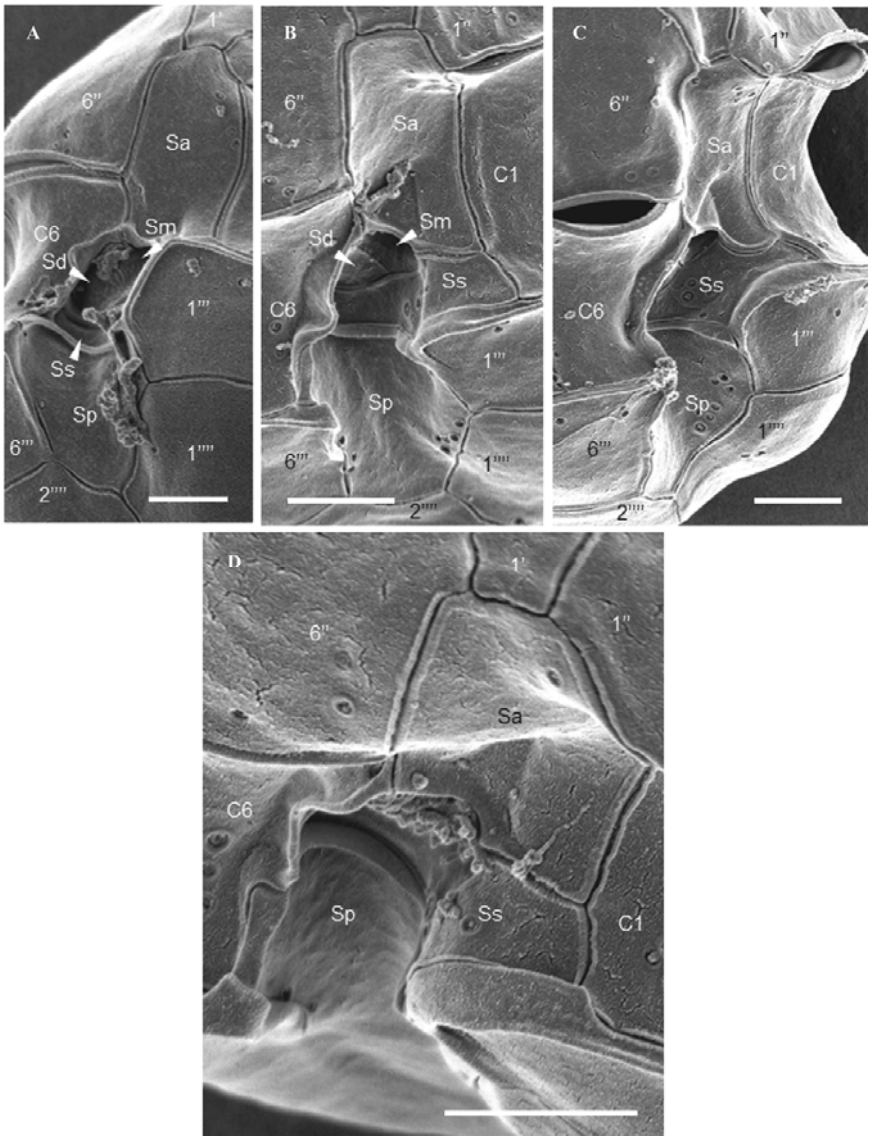

Fig. 2.5 Micrographs of cells of *Azadinium* cf. *poporum* taken using a scanning electron microscope showing the sulcal area. A. Right-lateral view of the sulcus. B. Ventral view of the sulcus. C. Left-lateral view of the sulcus. D. Apical view of the sulcus. The nomenclature of Kofoid (1909) was used to describe the thecal plate tabulation. Sa: anterior sulcal plate, Sd: right sulcal plate, Ss: left sulcal plate, Sm: median sulcal plate, Sp: posterior sulcal plate. Scale bars = 1 μm

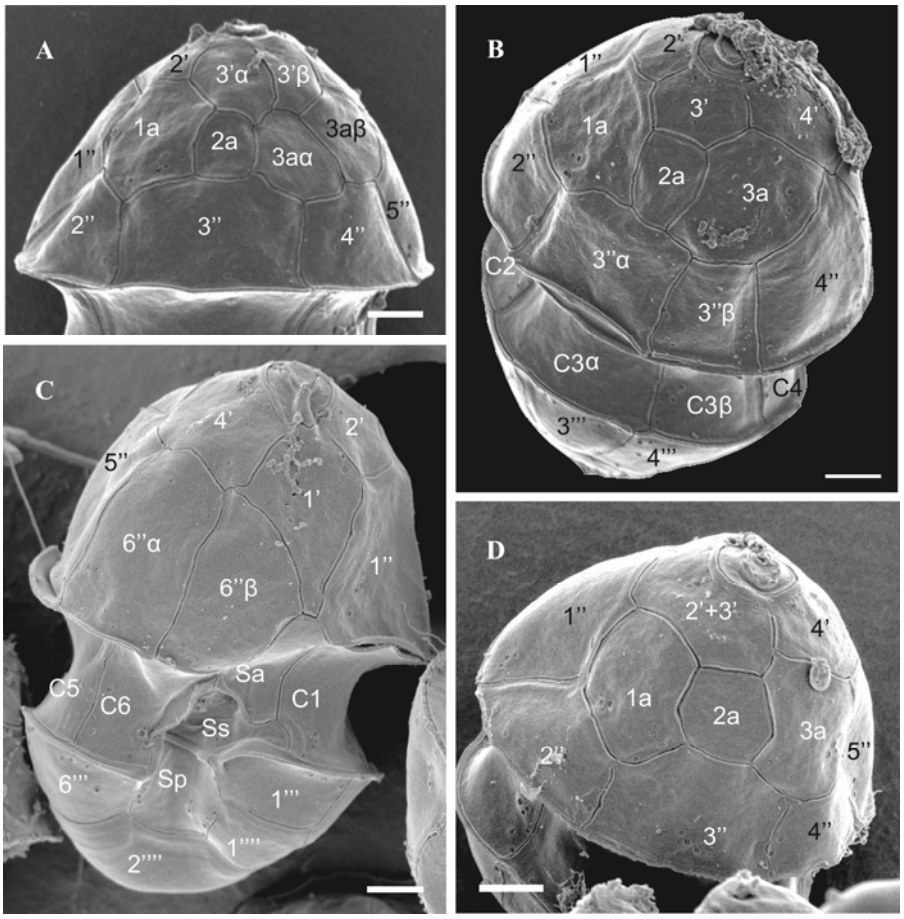

Fig. 2.6 Micrographs of cells of *Azadinium* cf. *poporum* taken using a scanning electron microscope showing plate modifications. A. Complex modification of the 3' and 3a plates producing a supplementary apical and anterior intercalary plate. B. Complex modifications of the 3" and C3 plates producing a supplementary precingular and cingular plate, respectively. C. Complex modification of 6" producing a supplementary precingular plate. D. Simplex modification involving 2' and 3' plates. The nomenclature of Kofoid (1909) was used to describe the thecal plate tabulation. Sa: anterior sulcal plate, Ss: left sulcal plate, Sp: posterior sulcal plate. Scale bars = 1 μm

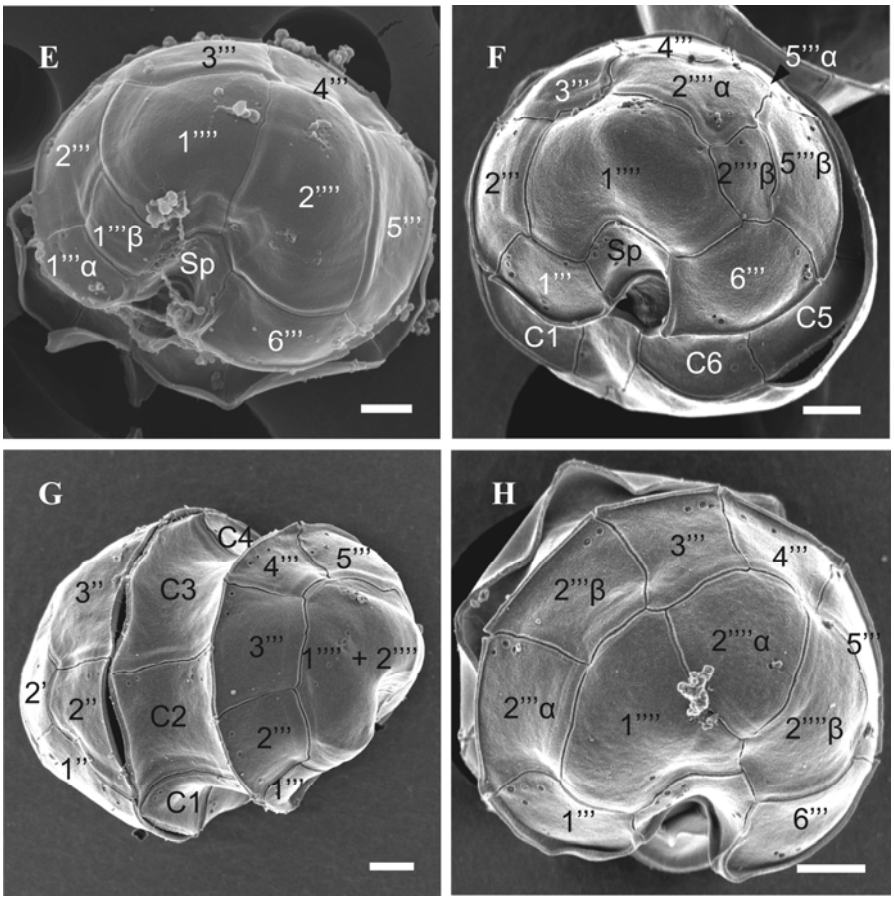

Fig. 2.6 (continued) E. Complex modification of the 1''' plate producing a supplementary intercalary plate. Travectum modification of the contact between 1'''' and 2'''' plates producing two antapical plates of similar size. F. Complex modifications of 5''' plate producing an additionnal postcingular plate. Travectum modification of 1'''' embedding all the Sp plate. Complex modification of the reduced 2'''' producing an additional antapical plate. G. Simplex modification reducing the number of antapical plate to one. H. Complex modification of the 2''' and 2'''' plates producing a supplementary postcingular and antapical plate. The nomenclature of Kofoid (1909) was used to describe the thecal plate tabulation. Sp: posterior sulcal plate. Scale bars = 1 μm

2.5.2 Molecular characterization of *Azadinium* cf. *poporum*

The partial SSU, ITS, and partial LSU rDNA of *A.* cf. *poporum* (GenBank accession number = FR877580) were analyzed and provided a sequence of 3267 bp. The mitochondrial gene COI of the Korean strain of *A.* cf. *poporum* (GenBank accession number = FR877581) was also analyzed and provided a sequence of 960 bp. The simplest measure of evolutionary distance in molecular phylogenetics is the number of nucleotide differences between species. We calculated nucleotide differences between strains of *Azadinium* (i.e. 3D9, UTHE2, 2E10, UTHD4, UTHC5, and UTHC8) for the SSU, ITS, and LSU rDNA, and COI mitochondrial DNA by pairwise comparison of aligned sequences. No intraspecific variability was found if we excluded ambiguous nucleotides. However, the interspecific DNA variability depended on the DNA region analyzed. The interspecific variability was < 0.4 % for the SSU rDNA, < 10.2 % for the ITS rDNA, < 6.3 % for the LSU rDNA, and nonexistent for the mitochondrial DNA gene COI. Therefore, the ITS rDNA and the LSU rDNA are more likely to resolve the relationships between species of the genus *Azadinium*. The rDNA sequences of the Korean strain of *A.* cf. *poporum* were more similar to *A. poporum* from the North Sea (Table 2.2).

In the phylogenetic tree based on the SSU rDNA, all the known species of the genus *Azadinium* formed a monophyletic clade with moderate support (Fig. 2.7). The three strains of *A. poporum* from the North Sea produced a polytomic clade that showed high support. All the phylogenetic methods used showed that the Korean strain of *A.* cf. *poporum* clustered with *A. poporum* from the North Sea as a sister taxon. The relationship between *A.* cf. *poporum* from Korea and *A. poporum* from the North Sea had low support with ML method and high support with Bayesian analysis. The relationships between species of the genus *Azadinium* other

Table 2.2 Dissimilarity matrix comparing *Azadinium* cf. *poporum* from Korea to other species in the genus *Azadinium*.[a] Gaps occurring in the alignment when sequences were compared were considered as dissimilarities. Ambiguous nucleotides were not considered as dissimilarities

DNA region	*Azadinium poporum*	*Azadinium spinosum*	*Azadinium obesum*
SSU rDNA	3/1410	4/1410	6/1410
	(0.2 %)	(0.3 %)	(0.4 %)
Gap	0/1410	0/1410	0/1410
	(0.0 %)	(0.0 %)	(0.0 %)
ITS rDNA	16/619	63/623	40/621
	(2.6 %)	(10.1 %)	(6.4 %)
Gap	5/619	21/623	13/621
	(0.8 %)	(3.4 %)	(2.1 %)
LSU rDNA	26/715	38/716	45/716
	(3.6 %)	(5.3 %)	(6.3 %)
Gap	1/715	2/716	2/716
	(0.1 %)	(0.3 %)	(0.3 %)
COI	0/913	0/913	0/913
	(0 %)	(0 %)	(0 %)
Gap	0/913	0/913	0/913
	(0 %)	(0 %)	(0 %)

[a]Sequences used in the comparison were obtained from Genbank

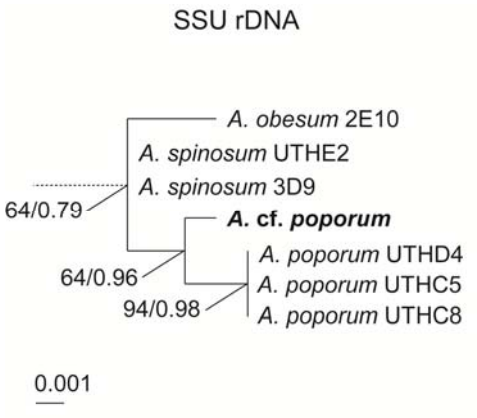

SSU rDNA. Tree based on 1080 aligned nucleotides of the nuclear SSU rDNA using the GTR+I+G model with *Oxyrrhis marina* as outgroup taxa. Alignment length includes gaps. The parameters were as follows: assumed nucleotide frequencies A=0.2819, C=0.1741, G=0.2551 and T=0.2890; substitution rate matrix with G-T=1.0000, A-C=0.8776, A-G=4.0977, A-T=1.3425, C-G=0.6189, C-T=10.2177; proportion of invariable sites=0.4176 and rates for variable sites assumed to follow a gamma distribution with shape parameter=0.5438.

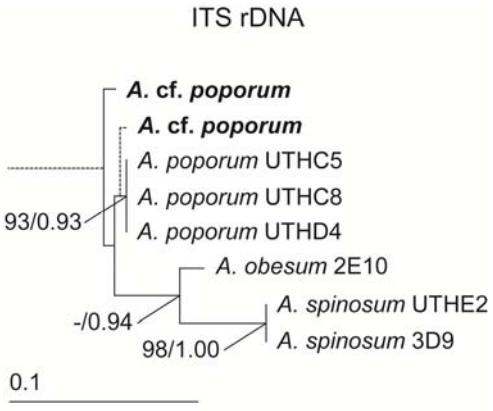

ITS rDNA. Tree based on 604 aligned nucleotides of the nuclear ITS rDNA using the K81uf+G model with *Prorocentrum minimum* as outgroup taxa. Alignment length includes gaps. The parameters were as follows: assumed nucleotide frequencies A=0.2065, C=0.2489, G=0.2469 and T=0.2976; substitution rate matrix with G-T=1.0000, A-C=1.0000, A-G=2.6949, A-T=0.3832, C-G=0.3832, C-T=2.6949; proportion of invariable sites=0 and rates for variable sites assumed to follow a gamma distribution with shape parameter=0.3807.

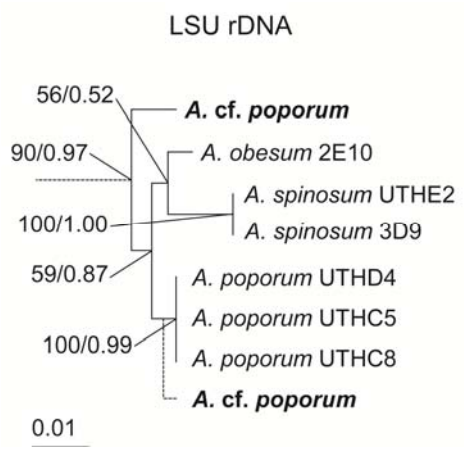

LSU rDNA. Tree based on 459 aligned nucleotides of the nuclear LSU rDNA using the GTR+I+G model with *Oxyrrhis marina* as outgroup taxa. Alignment length includes gaps. The parameters were as follows: assumed nucleotide frequencies A=0.2337, C=0.1959, G=0.2728 and T=0.2977; substitution rate matrix with G-T=1.0000, A-C=0.6504, A-G=2.2359, A-T=0.7607, C-G=0.5000, C-T=4.9494; proportion of sites assumed to be invariable=0.1178 and rates for variable sites assumed to follow a gamma distribution with shape parameter=0.8072.

Fig. 2.7 Maximum likelihood phylogenetic trees based on SSU rDNA, ITS rDNA, and LSU rDNA. The numbers at the nodes of the branches indicate the ML bootstrap (left) and Bayesian posterior probability (right) values; only values ≥ 50% or 0.5 are shown. The dashed line illustrate the alternative phylogenetic position of *Azadinium* cf. *poporum* as a sister taxon of *Azadinium poporum*.

than *A.* cf. *poporum* and *A. poporum* were not well defined. The sequences of the SSU rDNA in *Azadinium* species have a low number of variable characters (i.e. 0.6 % of variable sites based on 1410 aligned bp, including gaps) and therefore has a low resolution.

The ITS rDNA is more variable for the species of the genus *Azadinium* (i.e. 11.9 % of variable sites based on 631 aligned bp, including gaps) and relationships between species are likely to be better defined. The results based on the ITS rDNA positioned *A.* cf. *poporum* as a sister taxon of *A. poporum* with NJ and MP analyses. However, *A.* cf. *poporum* is in basal position among *Azadinium* species based on ML method (Fig. 2.7) and Bayesian analysis (not shown). In the two last mentioned methods, the strains of *A. spinosum*, *A. obesum*, and *A. poporum* produced a clade that was not supported. The relationship between *A. spinosum* and *A. obesum* was either not or highly supported depending on the method used. The three strains of *A. poporum* from the North Sea produced a polytomic clade that was well supported. However, the relationships between *Azadinium* species were unstable, *A.* cf. *poporum* being a sister taxon to the other strains of *A. poporum* in some occasions depending of the outgroup used.

The variability of the LSU rDNA is similar to the ITS rDNA for the species of the genus *Azadinium* (i.e. 9.6 % of variable sites based on 717 aligned bp, including gaps). The results based on the LSU rDNA positioned *A.* cf. *poporum* basal to *Azadinium* species with NJ method and basal to *Azadinium* species or occasionally as a sister taxon of *A. poporum* with MP method. *Azadinium* species generally produced a monophyletic clade based on ML method (Fig. 2.7) and Bayesian analysis (not shown). This clade was very well supported. The strains of *A. spinosum*, *A. obesum*, and *A. poporum* produced a clade that was weakly

supported. The relationship between *A. spinosum* and *A. obesum* was also weakly supported. The three strains of *A. poporum* from the North Sea produced a well-supported polytomic clade. The relationships between *Azadinium* species were, however, unstable as it also occurred for the ITS rDNA with ML method and Bayesian analysis. *A.* cf. *poporum* was either basal to all other known species in the genus *Azadinium* or a sister taxon to the other strains of *A. poporum* depending of the species included in the phylogeny. On one occasion, *Amphidinium herdmanii* was included in the clade composed of *Azadinium* species and thus made the genus paraphyletic (not shown).

2.5.3 Azaspiracids

No trace of known AZAs was detected. The limit of detection per cell as AZA-1 equivalents was estimated to be 4.9×10^{-7} pg, which is at least four orders of magnitude below the cell quota reported for *A. spinosum* (Krock *et al*. 2009). However, mass spectrometry yielded some indications that *A.* cf. *poporum* might contain some other potentially related compounds (not shown).

2.6 Discussion

2.6.1 Distribution

Species of the genus *Azadinium* have so far only been reported in northern Europe: from the North Sea (Tillmann *et al*. 2009, 2010, 2011) and the Irish coast of the eastern Atlantic (Salas *et al*. 2011). The type of the genus is the only species actually known to produce AZAs (Tillmann *et al*. 2009). These toxins were originally characterized from the shellfish *Mytilus edulis* of Ireland (Satake *et al*.

1998b). Following the development of sensitive LC-MS methods for the determination of AZAs, the toxins have been detected in additional locations, including Norway (James *et al*. 2002, Torgersen *et al*. 2008), England (James *et al*. 2002), Spain (Magdalena *et al*. 2003), France (Magdalena *et al*. 2003), Denmark (De Schrijver *et al*. 2002), Portugal (Vale 2004), Morocco (Taleb *et al*. 2006), Canada (Quilliam, M. pers. commun. in Twiner *et al*. 2008), and Sweden (Torgersen *et al*. 2008). It was therefore reasonable to suppose that the genus *Azadinium* had a more widespread distribution. This study is the first report of a species of the genus *Azadinium* from a locality other than northern Europe extending the latitudinal range of the genus further south.

2.6.2 Morphology

Azadinium cf. *poporum* can be easily differentiated from *A. spinosum* by multiple features, such as the absence of an antapical spine. Furthermore, its length to width ratio is lower than that of *A. spinosum*. A conspicuous pore, regarded as homologous to the ventral pore of *A. spinosum* and *A. obesum*, is located typically on the Po plate. *A.* cf. *poporum* can also be easily distinguished from *A. obesum* by the presence of pyrenoids, the location of the ventral pore on the Po plate, the presence of a contact between the 1" and 1a plates, the distinctive difference in the relative sizes of the anterior intercalary plates, and the absence of a narrow portion in the lower part of the 1' plate (Table 2.3).

Although the morphological differences between *A.* cf. *poporum* and *A. spinosum* or *A. obesum* are relatively easy to determine, the differentiation of *A.* cf. *poporum* from *A. poporum* is more difficult. The ovoid and dorsoventrally compressed shape of *A.* cf. *poporum* is very similar to that of *A. poporum* (Table

Table 2.3 Comparison of distinctive morphological and toxigenic features of species in the genus *Azadinium*. Y: the organism has. N: the organism does not have. Feature in bold distinguish *A.* cf. *poporum* from Korea and *A. poporum* from North Sea

Features	*Azadinium* cf. *poporum*	*Azadinium poporum*	*Azadinium spinosum*	*Azadinium obesum*
Localities (latitude, longitude)	Shiwha bay, Korea, (37°18'N, 126°36'E)	North Sea off Denmark (56°14.52'N, 07°27.54'E)	North Sea off Scotland[3] (57°3.9' N, 02°30.2' W) and Denmark[2] (56°14.52'N, 07°27.54'E)	North Sea, off Scotland (57°3.9'N, 02°30.2'W)
Shape	Ovoid and dorso-ventrally compressed	Ovoid and dorso-ventrally compressed	Elliptical, slightly elongated, and dorso-ventrally compressed	Ovoid and dorso-ventrally compressed
Cell length, μm (Median)	10.2-16.1 (12.5, n=100)	11.3-16.3 (13.0, n=48)	12.3-15.7 (13.8, n=73)	13.3-17.7 (15.3, n=36)
Cell width, μm (Median)	7.3-11.4 (9.2, n=100)	8.0-11.6 (9.8, n=48)	7.4-10.3 (8.8, n=73)	10.0-14.3 (11.7, n=36)
Median ratio of length to width	1.4 (1.2-1.5) (n=100)	1.3 (n=48)	1.6 (n=73)	1.3 (n=36)
Ratio of cingulum width to cell length	0.19-0.27 (n=27)	ca. 0.20	ca. 0.25	ca. 0.20

Table 2.3 (continued)

Features	*Azadinium* cf. *poporum*	*Azadinium poporum*	*Azadinium spinosum*	*Azadinium obesum*
Displacement relative to cingulum width	0.22-0.84 (n=27)	ca. 0.5	ca. 0.5	ca. 0.5
Antapical spine	N	N	Y	N
Pyrenoids (number)	Y (>1 ?)	Y (>1 2-4?)	Y (1)	N (0)
Location of ventral pore	Po[a]	Po	1'	1'
1" plate in contact with 1a plate	Y	Y	Y	N
1a and 3a plates large	Y	Y	Y	N
Lower part of 1' plate narrow	N	N	N	Y
3' plate symmetry	**Antero-posterior and lateral axes**	**Antero-posterior axis**	**Antero-posterior axis**	**Antero-posterior axis**
Azaspiracid production	N	N	Y	N
References	(1)	(2)	(2), (3)	(4)

[a]The ventral pore has been occasionally observed along the 1' plate

References. [1]This study, [2]Tillmann *et al*. 2011, [3]Tillmann *et al*. 2009, [4]Tillmann *et al*. 2010

2.3). The AP length and width of the cells of *A.* cf. *poporum* (10-16 and 7-11 µm, respectively) are highly similar to the corresponding dimensions of *A. poporum* (11-16 and 8-12 µm, respectively). The median of the ratio of the AP length to width of *A.* cf. *poporum* (1.4) is also highly similar to that of *A. poporum* (1.3). The absence of an antapical spine, the presence of pyrenoids, the usual location of the ventral pore on the Po plate, the contact between the 1'' and 1a plates, the relative size of 1a and 3a plates in the anterior intercalary plate series, and the absence of a narrow portion in the lower part of the 1' plate are features shared by both *A.* cf. *poporum* and *A. poporum* (Table 2.3). However, the 3' apical plate is usually symmetric on the AP and lateral axes for *A.* cf. *poporum*, whereas it is only symmetric on the AP axis for *A. poporum* (Table 2.3 and Fig. 2.8). This feature allows distinction between the strains from Korean waters and the North Sea.

Variations from the usual plate pattern were quite common in the cultured strain of *A.* cf. *poporum*. The number of plates was observed to vary in all plate series, beside the sulcal series. Individual variations in shape were observed for many plates, with the exceptions of the first apical plate, many precingular plates, and a few postcingular plates. A high variability in plate patterns seems to be a common feature of all *Azadinium* cultures so far (Tillmann *et al*. 2009, 2010, 2011). The observed variability for *A.* cf. *poporum* is higher than the variability of *A. poporum* described by Tillmann *et al*. (2011). However, it is unknown whether the presence and/or degree of variability is an inherited feature of the genus *Azadinium*, is distinct at the strain or species level or is simply a culture artifact. Clearly, detailed morphological investigations of field populations are needed to answer these questions.

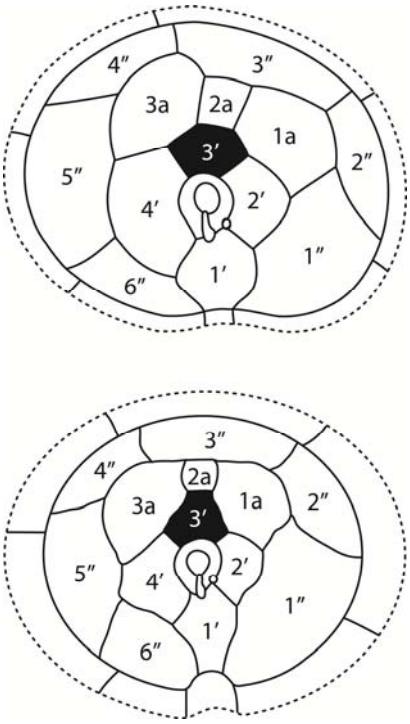

Fig. 2.8 Comparison between the shape of the third apical plate of *Azadinium* cf. *poporum* from Korea (top) and *Azadinium poporum* from North Sea (bottom; from Tillmann *et al*. 2011). The nomenclature of Kofoid (1909) was used to describe the thecal plate tabulation.

2.6.3 Molecular characterization

The Korean isolate revealed haplotypes of SSU rDNA, ITS rDNA, and LSU rDNA not previously reported. The haplotypes of the previously described *Azadinium* species are similar, but they are distinct even if the species occur in the same geographical area. Moreover, the defined species are morphologically distinguishable. These observations suggest that each previously defined species is biologically distinct. The high stability of each haplotype observed when multiple strains were available (i.e. *A. spinosum* and *A. poporum*) further suggests distinct biological species. Therefore, the distinct haplotype from Korea might represent a recently diverged or new species or a different strain inhabiting a distinct geographical area.

The position of *A.* cf. *poporum* is variable among DNA regions. The SSU rDNA showed a close relationship between *A.* cf. *poporum* and *A. poporum*. The rate of evolution of the SSU rDNA is much slower than that of the ITS rDNA and the D1/D2 region of the LSU rDNA. The relationships between species based on SSU rDNA can therefore be misleading and analyses based on the ITS rDNA and the LSU rDNA are more likely to reveal proper relationships among *Azadinium* species.

The ITS rDNA region has been used before to infer phylogenetic relationships among strains of the same or closely related species. The relatively rapid divergence rates of the ITS rDNA make this region useful for inferring genetic relationships at the inter and intraspecific level (Adachi *et al*. 1996, 1997, Coleman & Mai 1997, LaJeunesse 2001). This region has also been used to suggest the existence of cryptic species (Montresor *et al*. 2003). The genetic relationships

based on ITS rDNA also reflected in some occasions biogeographical patterns (Montresor *et al*. 2003). Phylogenetic relationship based on LSU rDNA have also shown to reflect biogeographical aspects (John *et al*. 2003). The ITS and LSU rDNA depict the same relationships between species in the genus *Azadinium* including the variable position of *A.* cf. *poporum*. Strains from the same species from different biogeographical areas are expected to produce a monophyletic clade in phylogenetic analyses. This condition is not respected with *A. poporum* from North Sea and *A.* cf. *poporum* from Korea when the latter adopts a basal position among *Azadinium* species. The unstable position of *A.* cf. *poporum* and the occasional absence of monophyly between strains from different localities suggest that *A. poporum* and *A.* cf. *poporum* are recently diverged species.

2.6.4 Azaspiracids

No trace of known AZAs was detected. However, both toxic and nontoxic species of the genus *Azadinium* are known to co-occur in the same geographical area. It is therefore likely that other species of the genus *Azadinium* could be present at proximity of Korea. The recent detection of AZAs in Japan (Ueoka *et al*. 2009) underscores the need to look further for the presence of other *Azadinium* species in Asia.

On morphological grounds, the Korean isolate is apparently associated more closely with the species *A. poporum* described by Tillmann *et al*. (2011). However, differences in morphology, DNA sequences, and phylogenetic relationships, particularly those derived from the ITS rDNA and the LSU rDNA regions, led us to designate the Korean strain as *A.* cf. *poporum*. The characterization of further strains belonging to the genus *Azadinium* is likely to bring more reliable diagnostic

features that might help to stabilize the taxonomic position of *A.* cf. *poporum*.

Chapter 3: Azaspiracid

New azaspiracids in Amphidomataceae (Dinophyceae)

3.1 Abstract

Azaspiracids (AZAs) are a group of lipophilic polyether toxins implicated in incidents of shellfish poisoning in humans, particularly in northern Europe, which are produced by the small marine dinoflagellate *Azadinium spinosum*. Other related species/strains of the Amphidomataceae have not been proven to date to contain any of the known azaspiracids. Closer analyses of these species/strains by triple quadrupole mass spectrometry in the precursor and product ion mode now revealed a new compound with high similarity to azaspiracids, with a characteristic m/z 348 fragment but with absence of the m/z 362 fragment. This compound was detected in the Korean isolate of *A. poporum* (molecular mass: 857.5 Da). Cell quota of roughly 2 fg per cell was in the same range as found for AZA-1 and -2 in *A. spinosum*. Structure for the compound was proposed by interpretation of fragmentation patterns and high resolution mass measurements using Fourier transform ion cyclotron resonance-mass spectrometry (FTICR-MS).

3.2 Keywords

Azaspiracids, *Azadinium poporum*, LC-MS/MS, Phycotoxin

3.3 Introduction

Azaspiracids (AZAs) are a group of lipophilic polyether toxins at first associated with the diarrhetic shellfish poisoning (DSP) syndrome, based upon provisional epidemiological and etiological characteristics. AZAs consist of a six-membered cyclic imine ring and – like most polyketides – of a linear carbon chain, which is cyclized at several points in the molecule by ether bridges (Satake *et al*. 1998b, Nicolaou *et al*. 2006). The first azaspiracid poisoning (AZP) event was recorded after eight people in the Netherlands became ill in November 1995 after consumption of mussels from the Irish west coast. Symptoms of the affected persons – nausea, vomiting, severe diarrhea and stomach cramps – were typical for DSP. The mouse bioassay for DSP toxicity was also strongly positive, however, the DSP toxins in the mussels (okadaic acid and dinophysistoxin-2) were present at only very low concentrations, and thus could not account for the observed severe intoxications (McMahon & Silke 1996).

A few years after this unattributed toxic incident, the first member of a novel group of marine biotoxins designated as "azaspiracid" (AZA) was isolated and characterized from shellfish (as AZA-1) (Satake *et al*. 1998b) and later structurally revised (Nicolaou *et al*. 2006). Following confirmation of AZA-1 as the cause of human poisoning, other cases of intoxication from consumption of mussels from Ireland, France, and Italy were also unambiguously attributed to the AZP syndrome (James *et al*. 2000). Detailed global surveys on the biogeographical distribution of AZA toxins have not been conducted, but AZA-contaminated mussels have been found on the east coast of England and along the Norwegian west coast (Lehane *et al*. 2002). Reported AZA occurrences outside of northern European waters, include the coast of Portugal (Vale *et al*. 2008), Morocco (Taleb *et al*. 2006) and Chile (Álvarez *et al*. 2010), but monitoring of lipophilic phycotoxins in mussels from the White Sea, northern Russia did not reveal the presence of AZAs (Vershinin *et al*.

2006). So far, shellfish from areas outside Europe have not caused yet cases of human intoxication due to AZP.

Although most research has focused on AZA-1 as the first discovered and most accessible AZA analogue, other structural variants have been isolated and characterized from shellfish (Ofuji *et al*. 1999, 2001, James *et al*. 2003a b). The current list comprises two dozen naturally occurring structural variants of AZA-1 (Rehmann *et al*. 2008) (Fig. 3.1), of which only AZA-1, AZA-2 and AZA-3 have been found in plankton samples (James *et al*. 2003a b), while all other variants were detected in shellfish and are regarded as shellfish metabolites.

Recently an AZA producing organism was isolated (Krock *et al*. 2009) and identified as *Azadinium spinosum* Elbrächter *et* Tillmann (Tillmann *et al*. 2009). Several strains from the Scottish east coast, the Danish west coast, and the Irish west coast showed all similar toxin profiles consisting only of AZA-1 and AZA-2 (Salas *et al*. 2011). Subsequently, a number of new species of the genus *Azadinium* were described from the North Sea (Tillmann *et al*. 2010, 2011). Nevertheless, *Azadinium* species probably have a worldwide distribution. We now have a strain available from Korean coastal waters, which morphologically closely resembles *A. poporum* but in relation to their ITS and LSU rDNA sequences differs considerably. This strain at present has been designated as *A.* cf. *poporum* (Potvin *et al*. 2012).

No known AZAs were previously detected in *A.* cf. *poporum* (Potvin *et al*. 2012). However, we now detected a compound that shows fragmentation patterns with high similarities to those of AZAs. Here we summarize structural information of this new compound and propose its structure by mass spectrometric techniques.

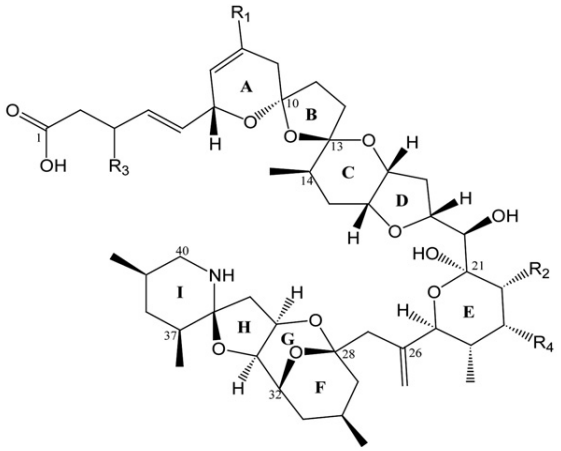

Toxin	R_1	R_2	R_3	R_4	$[M+H]^+$
AZA-1	H	CH_3	H	H	842
AZA-2	CH_3	CH_3	H	H	856
AZA-3	H	H	H	H	828
AZA-4	H	H	OH	H	844
AZA-5	H	H	H	OH	844
AZA-6	CH_3	H	H	H	842
AZA-7	H	CH_3	OH	H	858
AZA-8	H	CH_3	H	OH	858
AZA-9	CH_3	H	OH	H	858
AZA-10	CH_3	H	H	OH	858
AZA-11	CH_3	CH_3	OH	H	872

Fig. 3.1 Structures of the fully structurally characterized azaspiracids AZA-1 to AZA-11. The m/z values are given for the $[M+H]^+$ ions.

3.4 Materials and methods

3.4.1 Algal culture

The alga was grown as described in detail by Potvin *et al*. (2012) for *A.* cf. *poporum*. A dense culture was sampled for cell counts (inverted microscope) and approx. 500 000 cells were harvested by centrifugation (15 min, 16 100 x g). The cell pellet was stored at -20 °C until use.

3.4.2 Toxin extraction and preparation

The cell pellet was suspended in 300 µL acetonitrile, and subsequently transferred into a FastPrep tube containing 0.9 g of lysing matrix D (Thermo Savant, Illkirch, France). The sample was homogenized by reciprocal shaking at maximum speed (6.5 m s^{-1}) for 45 s in a Bio101 FastPrep instrument (Thermo Savant, Illkirch, France). After homogenization, the sample was centrifuged (Eppendorf 5415 R, Hamburg, Germany) at 16 100 x g at 4 °C for 15 min. The supernatant (250 µL) was transferred to a 0.45 µm pore-size spin-filter (Millipore Ultrafree, Eschborn, Germany) and centrifuged for 30 s at 800 x g. The filtrate was transferred into an LC autosampler vial for LC-MS/MS analyses.

3.4.3 Multiple reaction monitoring (MRM) measurements

Water was deionized and purified (Milli-Q, Millipore, Eschborn, Germany) to 18 MΩ cm^{-1} or better quality. Formic acid (90 %, p.a.), acetic acid (p.a.) and ammonium formate (p.a.) were purchased from Merck (Darmstadt, Germany). The solvents, methanol and acetonitrile, were high performance liquid chromatography (HPLC) grade (Merck, Darmstadt, Germany).

Mass spectral experiments were performed to survey for a wide array of AZAs. The analytical system consisted of an ABI-SCIEX-4000 Q Trap, triple quadrupole mass spectrometer equipped with a TurboSpray® interface coupled to an Agilent model 1100 LC. The LC equipment included a solvent reservoir, in-line degasser (G1379A), binary pump (G1311A), refrigerated autosampler (G1329A/G1330B), and temperature-controlled column oven (G1316A).

Separation of the AZA (5 µl sample injection volume) was performed by reverse-phase chromatography on a C8 phase. The analytical column (50 x 2 mm) was packed with 3 µm Hypersil BDS 120 Å (Phenomenex, Aschaffenburg, Germany) and maintained at 20 °C. The flow rate was 0.2 mL min^{-1} and gradient elution was performed with two eluants, where eluant A was water and B was acetonitrile/water (95:5 v/v), both containing 2.0 mM ammonium formate and 50 mM formic acid. Initial conditions were 8 min column equilibration with 30 % B, followed by a linear gradient to 100 % B in 8 min and isocratic elution until 18 min with 100 % B then returning to initial conditions until 21 min (total run time: 29 min).

AZA profiles were determined in one period (0-18) min under mass spectrometer conditions: curtain gas: 10 psi, CAD: medium, ion spray voltage: 5500 V, temperature: ambient, nebulizer gas: 10 psi, auxiliary gas: off, interface heater: on, declustering potential: 100 V, entrance potential: 10 V, exit potential: 30 V). MRM experiments were carried out in positive ion mode by selecting the following transitions (precursor ion > fragment ion): 1) AZA-1 and AZA-6: m/z 842 > 824 collision energy (CE): 40 V and m/z 842 > 672 (AZA-1 only) CE: 70 V), 2) AZA-2: m/z 856 > 838 CE: 40 V and m/z 856 > 672 CE: 70 V, 3) AZA-3: m/z

828 > 810 CE: 40 V and m/z 828 > 658 CE: 70 V, 4) AZA-4 and AZA-5: m/z 844 > 826 CE: 40 V, 5) AZA-7, AZA-8, AZA-9 and AZA-10: m/z 858 > 840 CE: 40 V, 6) AZA-11 and AZA-12: m/z 872 > 854 CE: 40 V and 7) new compound and their methyl esters 816 > 798 CE: 40 V, 816 > 348 CE: 70 V, 830 > 812 CE: 40 V, 830 > 348 CE: 70 V, 844 > 826 CE: 40 V 846 > 828 CE: 40 V, 846 > 348 CE: 70 V, 858 > 348 CE: 70 V, 860 > 842 CE: 40 V and 872 > 854 CE: 40 V.

3.4.4 Precursor ion experiments

Precursors of the fragment m/z 348 were scanned in the positive ion mode from m/z 400 to 950 under the following conditions: curtain gas: 10 psi, CAD: medium, ion spray voltage: 5500 V, temperature: ambient, nebulizer gas: 10 psi, auxiliary gas: off, interface heater: on, declustering potential: 100 V, entrance potential: 10 V, collision energy: 70 V, exit potential: 12 V.

3.4.5 Product ion spectra

Product ion spectra were recorded in the Enhanced Product Ion (EPI) mode in the mass range from m/z 150 to 860. Positive ionization and unit resolution mode were used. The following parameters were applied: curtain gas: 10 psi, CAD: medium, ion spray voltage: 5500 V, temperature: ambient, nebulizer gas: 10 psi, auxiliary gas: off, interface heater: on, declustering potential: 100 V, collision energy spread: 0, 10 V, collision energy: 70 V.

3.4.6 FTICR-MS measurements

Mass spectra were acquired with a Solarix 12T with Dual source Fourier transform ion cyclotron resonance-mass spectrometer (FTICR-MS; Bruker Daltonik GmbH, Bremen, Germany) equipped with a 12 T refrigerated actively shielded superconducting magnet (Bruker Biospin, Wissembourg, France) and Infinity ICR analyzer cell. The sample was ionized using a dual ion source in electrospray positive ion mode (Bruker Daltonik GmbH, Bremen, Germany). The sample solution was continuously infused using a syringe at a flow rate of 2 µL min^{-1}. The detection mass range was set to m/z 150-3000. Ion accumulation time was set to 0.1 s. Data sets were acquired with 4 MW data points resulting in a resolving power of 450 000 at m/z 400. Spectra were zero-filled to process size of 8M data points before sine apodization.

Mass spectra were calibrated with arginine cluster using a linear calibration. A 10 µg mL^{-1} solution of arginine in 50 % methanol was used to generate the clusters. For MS/MS experiments accumulation time was up to several seconds, the isolation window was 0.5 Da and collision energy set to 30 eV.

3.4.7 Methylation of AZAs

50 µL of a 2 M ethereal solution of trimethylsilyl diazomethane (TMSDM, Sigma-Aldrich, Steinheim, Germany) were added to 50 µL sample extract. The mixture was vortexed every 5 min for half an hour. Subsequently 5 µL acetic acid (100 %, Merck KGaA, Darmstadt, Germany) were added and the sample was vortexed again. The sample was taken to dryness in a gentle nitrogen stream and taken up again in 50 µL methanol prior to LCMS analyses.

3.5 Results and discussion

A MRM scan of the Korean strain of *A.* cf. *poporum* revealed a peak at the ion trace m/z 858 > 840, which is characteristic for AZA-7, -8, -9 and -10 (Fig. 3.1). However, this finding was unexpected because these AZAs are regarded as shellfish metabolites and not as original phycotoxins as they are found in shellfish (McCarron *et al*. 2009) but they could not be detected by passive water samplers in environmental samples (Fux *et al*. 2009, Rundberget *et al*. 2009) and in planktonic samples (Krock *et al*. 2009). Consequently we recorded a product ion spectrum of the compound (Fig. 3.2) and found very similar fragment clusters as in AZA-1, but clearly not identical with those of AZA-7, -8, -9 and -10 (Rehmann *et al*. 2008). All fragment clusters of AZA-1 were present in the spectrum of the new compound, but shifted 14 mass units to lower masses. The estimated cell quota of the new compound is in the same order of magnitude as of AZA-1 and -2 in *A. spinosum*, namely 2 fg $cell^{-1}$ (estimated as AZA-1 equivalent).

A common structural element of all AZAs is a free carboxylic group at the end of the side chain (Fig. 3.3). In order to prove the presence of carboxylic groups in the new compound, we treated the extracts with trimethylsilyl diazomethane (TMSDM), which is a specific methylation reagent for carboxylic groups. After TMSDM treatment the ion traces of the compound disappeared and peaks at 14 Da higher masses and longer retention times appeared instead, which is consistent with methylation (Fig. 3.4). By this experiment the presence of a carboxylic group in the compound could be corroborated.

CID mass spectra of AZAs are characterized by cleavages at certain points of the polyketide chain and subsequent water losses of each of these fragments, so

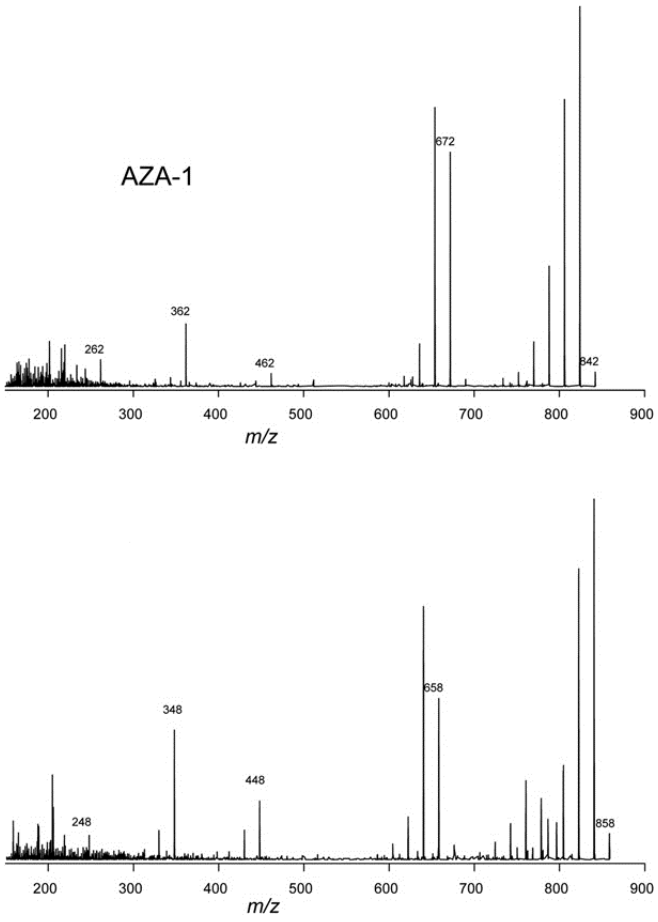

Fig. 3.2 Product ion scan of AZA-1 (m/z 842) (top) and the compound (m/z 858) (bottom)

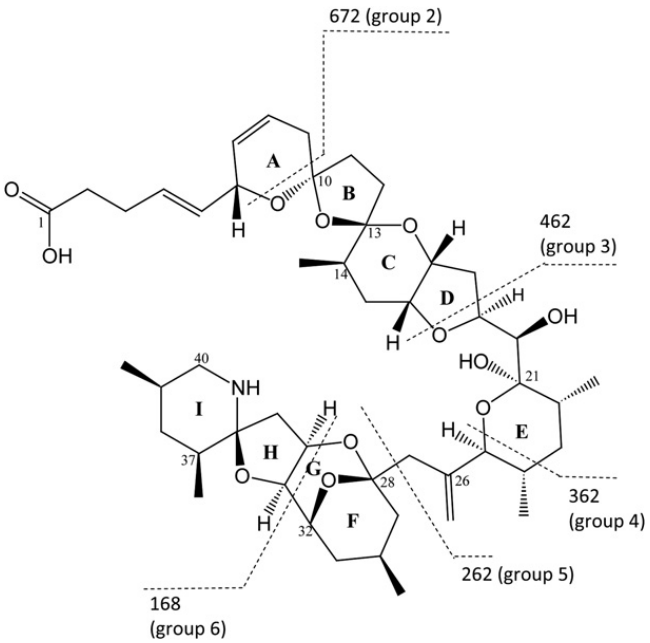

Fig. 3.3 Structure of AZA-1 and CID cleavage sites

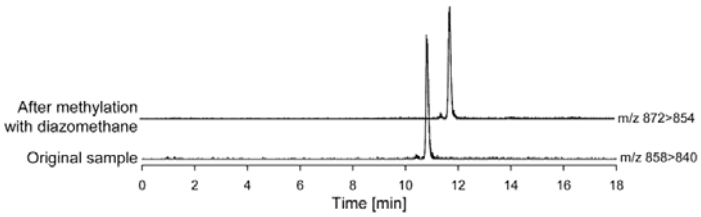

Fig. 3.4 Ion traces of the $[M + H]^+$ ion masses of the compound and the corresponding methylated compound

that each chain cleavage results in a fragment cluster with m/z 18 differences. Main cleavages of AZAs include a pseudo Retro-Diels-Alder reaction (RDA) of ring A of the molecule (Rehmann *et al*. 2008) resulting in a simultaneous cleavage between C6 and the A-ring O and C9 and C10, respectively. The remaining fragment is detected at m/z 672 in the case of AZA-1. Other characteristic cleavages are between C18 and C19 resulting in m/z 462, a second pseudo RDA of ring E resulting in m/z 362, the cleavage between C27 and C28 (m/z 262) and another pseudo RDA of ring G resulting in m/z 168 (Fig. 3.3). All known AZAs show these fragmentation patterns (Brombacher *et al*. 2002, Rehmann *et al*. 2008). These fragmentation patterns are also observed in the compound with the only difference that fragment groups 3–6 are shifted to 14 Da smaller m/z values (Table 3.1). The CID spectra of the compound will be discussed in more detail.

The molecular ion $[M+H]^+$ of the compound is m/z 858 (Fig. 3.2), which is 16 Da more than that of AZA-1. FTICR-MS results in a molecular formula of $C_{47}H_{71}NO_{13}$ with 13 double bond equivalents (Koch & Dittmar 2006) for the compound, which confirms this assumption (Table 3.1). Group 2 fragment (Fig. 3.3) of the compound is m/z 658 and all other fragments are 14 Da smaller than the corresponding group 2 - 6 fragments of AZA-1. This means that a methyl (or methylene) group is missing in the part of the molecule consisting of ring H and I. This methyl (or methylene) group instead must be located at carbon atoms 2-9 of the carboxylic side chain and part of ring A. Furthermore, the presence of an additional oxygen atom could be also deduced from the molecular formula.

But there is another obvious difference between the CID spectra of AZA-1 and the compound: whereas the $[M+H]^+$ peak of AZA-1 shows only 5 subsequent

Table 3.1 Exact masses of $[M+H]^+$ ions and characteristic group fragments of AZA-1 and the compound

		Group 1	Group 2	Group 3	Group 4	Group 5	Group 6
AZA-1	m/z	842	672	462	362	262	168
	Composition	$C_{47}H_{72}NO_{12}$	$C_{38}H_{58}NO_{12}$	$C_{27}H_{44}NO_5$	$C_{22}H_{36}NO_3$	$C_{16}H_{24}NO_2$	$C_{10}H_{18}NO$
Compound	Observed	858.4998	658.3950	448.3058	348.2533	248.1645	154.1227
	Composition	$C_{47}H_{72}NO_{13}$	$C_{37}H_{56}NO_9$	$C_{26}H_{42}NO_5$	$C_{23}H_{34}NO_3$	$C_{15}H_{22}NO_2$	$C_9H_{16}NO$
	±ppm	0.0	0.0	0.0	0.1	0.1	0.4

Note that there is no consistent fragment group numbering in the literature

water losses, the $[M+H]^+$ ion cluster of the compound is more complex (Fig. 3.5 A). Besides the water losses of the $[M+H]^+$ ion there is an additional loss of CO_2 (mass difference of m/z 44) followed by water losses, which is not observed in any of the known AZAs. The fact that the compound eliminates CO_2 under CID conditions, but known AZAs do not, is strong evidence that chemistry in close vicinity of the carboxylic function of the compound differs in relation to the known AZAs. Another interesting difference in the molecular ion cluster of the compound is the mass difference of m/z 78 also followed by water losses, which is also unique for the compound and absent in all described AZAs to date. FTICR-MS measurement of fragment $[M+H]^+$ gave a mass formula of $C_{45}H_{66}NO_{10}$, which represents a difference of $C_2H_6O_3$. Such unusual fragments have been observed for the CID of hexoses without any further interpretation (Zhu & Sato 2007). The elimination of a fragment $C_2H_6O_3$ cannot easily be explained. However, with an additional hydroxyl group at C2 and a methyl group at C3, a cyclic transition state can be postulated, which could be stabilized by a simultaneous elimination of a molecule of water and a $C_2H_4O_2$ unit under formation of an allylic system (Fig. 3.6) and thus explain the m/z 78 mass difference. In summary, the compound is proposed to be a 37- or 39-demethyl variant of AZA-1 with an additional hydroxyl group at C2 and an additional methyl group at C3 of the carboxylic side chain (Fig. 3.7). However, the location of these substitutions as well as the site of demethylation cannot unambiguously be assigned by MS alone, but needs confirmation by nuclear resonance spectroscopy (NMR).

Very little is known about the biosynthesis of AZAs by marine plankton. However, in analogy to other polyketides like spirolides (Kalaitzis *et al*. 2010) it is assumed that an amino acid, which delivers the amine nitrogen, is prolonged by polyketide synthases via the addition of acetic acid units to form a linear carbon

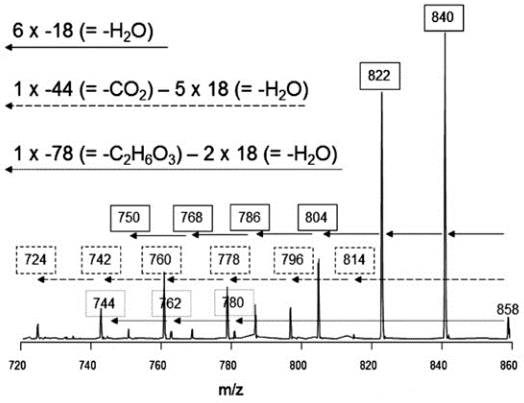

Fig. 3.5 Enlargements of the $[M+H]^+$ ion clusters of the product ion spectrum of the compound. m/z values in lined boxes belong to the water loss series, m/z values in dashed boxes belong to the CO_2 loss series and m/z values in dotted boxes belong to the $C_2H_6O_3$ loss series.

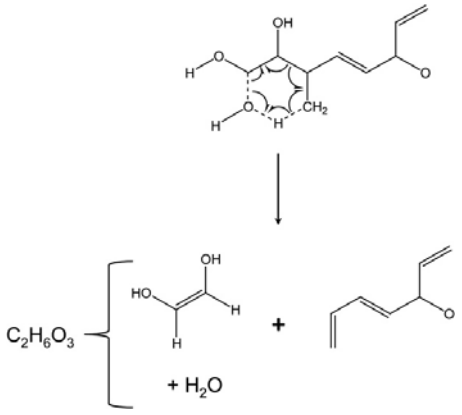

Fig. 3.6 Proposed fragmentation scheme for the elimination of $C_2H_6O_3$ from the compound

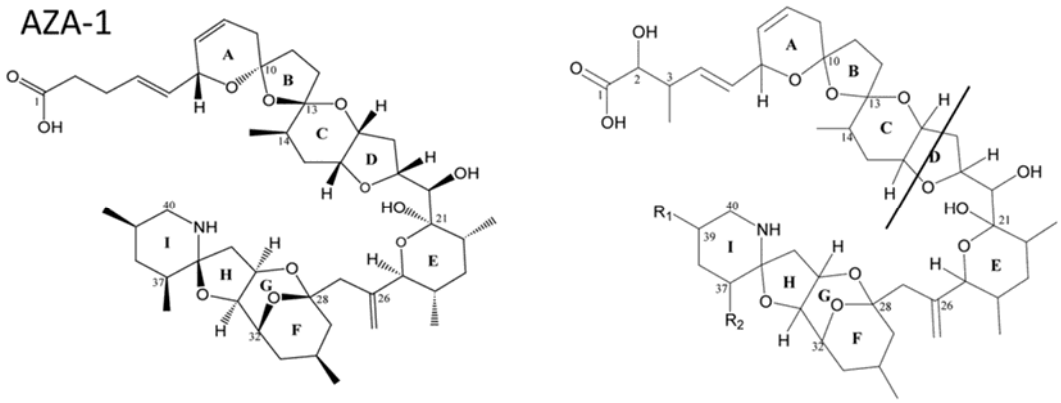

Fig. 3.7 Structure of AZA-1 (left) and proposed structure for the compound (right); R_1 = H and R_2 = CH_3 or R_1 = CH_3 and R_2 = H

chain, which is subsequently cyclized by the formation of ether bridges (MacKinnon *et al*. 2006). Interestingly, AZA-1 and AZA-2, which are to date the only two AZAs known to be produced by phytoplankton, differ only in a methyl group at C8 in the upper part of the molecule. The same applies to the new compound, whose lower parts with the cyclic imine function and E-I ring system are highly conserved and modifications only occur in the upper part (carboxylic side chain and A-C ring system) of the molecule between C2 and C14. The only exception is the missing methyl group at C37 or C39 of the compound in comparison to the known AZAs.

Even though mass spectrometry alone in most cases is not sufficient for complete structural elucidation of new compounds, thorough analysis of CID spectra, especially in combination with high resolution mass measurements and comparison to spectra of related compounds with known structures, delivers useful structural information, which allows for the prediction of structural elements of unknown compounds with low uncertainty or variability of structural variants. The state-of-the-art method for full structural elucidation is NMR spectroscopy. However, unlike mass spectrometry, which is orders of magnitude more sensitive and can operate with raw extracts, NMR requires fully purified material in the µg to mg range. This is a big challenge for the examination of planktonic secondary metabolites in general, but especially for metabolites of small dinoflagellates like *Azadinium* spp. which contain AZAs in the lower fg $cell^{-1}$ range. The isolation of sufficient material for NMR analyses requires the production, extraction and purification of several hundreds of liters of algal cultures. This effort will be subject of future work for the full characterization of the compound. Another open question remains the toxicity of the new AZA. It is reasonable to assume that the

new AZA provokes comparable cellular responses and human illness as the known AZAs due to their high structural similarity, but this has to be tested empirically. As NMR measurements and toxicity tests require pure compound in high amount, the strategy to address these questions will be to collect and purify enough material for NMR measurements. After NMR the same material will be used for toxicity assays.

Chapter 4: Predation

Feeding by heterotrophic protists and copepods on the photosynthetic dinoflagellate *Azadinium* cf. *poporum* from western Korean waters

4.1 Abstract

We explored the interactions between the photosynthetic dinoflagellate *Azadinium* cf. *poporum* isolated from Korean waters and potential predators, including engulfment feeders, a pallium feeder, peduncle feeders, and filter feeders. We measured the growth and/or ingestion rates of *Oxyrrhis marina*, *Strobilidium* sp., and *Acartia* spp. on *A.* cf. *poporum* as a function of prey concentrations. We also calculated grazing coefficients by using field data on abundance of *Strobilidium* sp.-sized naked ciliates co-occurring with *A.* cf. *poporum* and laboratory data on ingestion rates obtained in this study. Most of the tested organisms were able to feed on *A.* cf. *poporum*, but only *O. marina*, *Strobilidium* sp., and *Acartia* spp. showed sustained growth and/or ingestion on *A.* cf. *poporum*. Thus, some heterotrophic dinoflagellates using engulfment and filter feeders, such as ciliates and copepods, are likely to be optimal predators, while peduncle-feeding heterotrophic dinoflagellates are unlikely to efficiently feed due to the handling of the theca. The predators had low ratios of maximum growth rate to maximum ingestion rate on *A.* cf. *poporum,* as well as low gross growth efficiencies. Therefore, *A.* cf. *poporum* appears to be a low-quality prey for the predators tested. Grazing coefficients ranged between 0.052 and 0.446 d^{-1}, suggesting that *Strobilidium* sp.-sized naked ciliates may sometimes have a high impact on *A.* cf. *poporum* populations, leading to the removal of up to 36 % of the population in 1 d. However, the low quality of the prey and predator

selectivity in a more complex microbial community may reduce this impact.

4.2 Keywords

Azadinium, Azaspiracids, Toxins, Seasonal dynamics, Grazing, Predation, Ingestion, Growth

4.3 Introduction

The azaspiracids (AZAs) are the most recently discovered group of lipophilic marine biotoxins of microalgal origin associated with cases of shellfish poisoning in humans (Twiner *et al*. 2008). The production of AZAs was previously associated with a small photosynthetic dinoflagellate (Krock *et al*. 2009), designated as *Azadinium spinosum* Elbrächter *et* Tillmann and assigned to a new genus (Tillmann *et al*. 2009). The genus *Azadinium* is now composed of 4 well defined species, namely *A. spinosum* Elbrächter *et* Tillmann (Tillmann *et al*. 2009), *A. obesum* Tillmann *et* Elbrächter (Tillmann *et al*. 2010), *A. poporum* Tillmann *et* Elbrächter (Tillmann *et al*. 2011), and *A. caudatum* (Halldal) Nézan *et* Chomérat (Nézan *et al*. 2012). Undefined species were also described as *A.* cf. *poporum* (Potvin *et al*. 2012) and *A.* cf. *spinosum* (Akselman & Negri 2012). Until recently, *A. spinosum* was the only known planktonic source of AZAs. However, new AZAs have since been discovered in *A. poporum*, *A.* cf. *poporum*, and the closely related species *Amphidoma languida* Tillmann, Salas *et* Elbrächter (Krock *et al*. 2012, Tillmann *et al*. 2012b). *A. obesum* and *A. caudatum* are the only members of the genus *Azadinium* established in culture for which no AZA has been detected. While the AZAs produced by *A. spinosum* have been shown empirically to be toxic (Ito *et al*. 2002, Román *et al*. 2002, Colman *et al*. 2005, Twiner *et al*. 2005,

Alfonso *et al*. 2006, Kulagina *et al*. 2006, Vale *et al*. 2007), research is pending for the new AZAs.

The population dynamics of the species of the genus *Azadinium* are not well known. These species apparently seem to either remain at low density, such as *A. caudatum*, which was not observed to exceed 1.3 cells L^{-1} (Nézan *et al*. 2012), or are able to bloom (e.g. *A.* cf. *spinosum)* and can reach up to 9.03×10^3 cells mL^{-1} (Akselman & Negri 2012).

Grazing pressure sometimes plays an important role in population dynamics (Watras *et al*. 1985). Heterotrophic dinoflagellates (HTDs), ciliates, and copepods are integral parts of marine planktonic food webs (Jeong *et al*. 2010a). HTDs and ciliates can be found everywhere and can sometimes dominate in abundance and/or biomass, while copepods can similarly dominate the mesozooplankton (Brownlee & Jacobs 1987, Lessard 1991, Jeong 1999, Turner *et al*. 2005). These 3 groups sometimes have considerable grazing impact on populations of diverse prey (Painting *et al*. 1993, Strom *et al*. 1993, Sherr & Sherr 2007). In particular, grazing by heterotrophic protists is believed to contribute to the decline of blooms (Kim & Jeong 2004). In order to investigate grazing pressure by predators, growth and ingestion need to be studied. No study extensively exploring predation on species of the genus *Azadinium* is currently available.

In order to determine which predators are more likely to grow and feed actively on *Azadinium* spp., we explored feeding of HTDs *(Polykrikos kofoidii*, *Gyrodinium dominans*, *G. moestrupii*, *Oxyrrhis marina*, *Oblea rotunda*, *Stoeckeria algicida*, *Pfiesteria piscicida*, and *Gyrodiniellum shiwhaense)*, a ciliate (*Strobilidium* sp.) and the copepods *Acartia* spp. on *Azadinium* cf. *poporum*. We

found that *O. marina*, *Strobilidium* sp., and *Acartia* spp. fed well on *A.* cf. *poporum*. Therefore, we measured their growth and/or ingestion rates on *A.* cf. *poporum* as a function of prey concentration. Furthermore, we calculated grazing coefficients by using field data on abundance of *Strobilidium* sp.-sized naked ciliates co-occurring with *A.* cf. *poporum* and laboratory data on ingestion rate obtained in this study. Our results provide a basis for understanding interactions between *Azadinium* spp. and common heterotrophic protists and copepods.

4.4 Materials and methods

4.4.1 Preparation of experimental organisms

For the isolation and culture of *Azadinium* cf. *poporum* (GenBank accession number = FR877580), surface sediment samples from Shiwha bay, a highly eutrophic saline bay in Korea (37° 18' N, 126° 36' E), were incubated in F/2 medium-Si (Guillard & Ryther 1962) in a growth chamber at 20 °C under an illumination of 20 μE m^{-2} s^{-1} of cool white fluorescent light on a 14:10 h light: dark cycle. The monoclonal culture was established as described in detail by Potvin *et al*. (2012).

For the isolation and culture of potential protistan predators, plankton samples collected with water samplers were taken from the Korean coastal waters off Shiwha, Masan, Saemankeum, Karorim, and Jinhae between 2007 and 2011 (Table 4.1). A clonal culture of each predator was established as in Kim & Jeong (2004), Jeong *et al*. (2003a b, 2005c, 2006, 2011a), Kang *et al*. (2011), and Yoon *et al*. (2012). *Oblea rotunda* was brought into culture as *Gyrodinium* spp. in Kim & Jeong (2004; Table 4.1). The cultures were maintained on a wheel rotating at 0.9 rpm in a growth chamber at 20 °C under an illumination of 20 μE m^{-2} s^{-1} of cool

Table 4.1 Isolation and maintenance conditions of the experimental organisms. Sampling location in Korea and time, field water temperature (T, °C), and salinity (S) from which species were isolated, and prey species and concentrations (cells mL^{-1}) for maintenance. All organisms are heterotrophic dinoflagellates, except *Strobilidium* sp., a ciliate

Organism	Location	Year (month)	T	S	Prey species	Concentration
Gyrodiniellum shiwhaense	Shiwha bay	2009 (09)	24.5	24.0	*Amphidinium carterea*	20 000
Gyrodinium dominans	Masan bay	2007 (04)	15.1	33.4	*Amphidinium carterea*	8000
Gyrodinium moestrupii	Saemankeum bay	2009 (10)	21.2	31.0	*Alexandrium minutum*	3000−5000
Oblea rotunda	Shiwha bay	2010 (08)	26.8	23.7	*Prorocentrum minimum*	30 000
Oxyrrhis marina	Karorim	2010 (05)	19.5	33.0	*Amphidinium carterea*	8000
Pfiesteria piscicida	Jinhae	2010 (02)	24.5	12.6	*Amphidinium carterea*	20 000−30 000
Polykrikos kofoidii	Shiwha bay	2010 (03)	9.2	23.4	*Scrippsiella trochoidea*	8000
Stoeckeria algicida	Masan bay	2007 (08)	24.5	29.7	*Heterosigma akashiwo*	30 000
Strobilidium sp.	Shiwha bay	2011 (08)	27.0	15.0	*Heterocapsa rotundata*	50 000−60 000

white fluorescent light on a 14:10 h light: dark cycle. Fresh prey cells were provided every 1 to 3 d.

The copepods *Acartia* spp. were collected from Kunsan port with a 303 μm mesh net in May 2011 when water temperature and salinity were 16.8 °C and 18.9, respectively. The copepods were acclimated in a room at 20 °C, with *Prorocentrum minimum* provided as prey. Species of the genus *Acartia*, which co-occur in coastal waters off western Korea, can be very similar and impossible to distinguish from each other when they are alive (e.g. Soh & Suh 2000). Therefore, we had to use a mixture of adult *Acartia* spp.

The mean equivalent spherical diameter (ESD) of live *Azadinium* cf. *poporum* was measured (ESD = 10.0 μm) by an electronic particle counter and size analyzer (model Z2, Beckman Coulter). The shape of a sphere was used to estimate the volume of *A.* cf. *poporum* based on the ESD. *Oxyrrhis marina* and *Strobilidium* sp. were measured in order to estimate their volume in the different predator-prey combinations at the end of the incubation. Measurements were made with specimens fixed in 5 % acid Lugol's solution using a transmitted light inverted microscope (Zeiss Axiovert 200M, Carl Zeiss) at a magnification of 400x with a Zeiss AxioCam MRc5 digital camera (Carl Zeiss). The shape of *O. marina* was estimated as 2 cones joined at their bases. The shape of *Strobilidium* sp. was estimated as a sphere, cylinder, or cone depending of the shape of the specimen. Carbon content was estimated from the cell volume according to Menden-Deuer & Lessard (2000).

4.4.2 Feeding

Expt 1 was designed to test whether *Polykrikos kofoidii*, *Gyrodinium dominans*, *G. moestrupii*, *Oxyrrhis marina*, *Oblea rotunda*, *Stoeckeria algicida*, *Pfiesteria piscicida*, *Gyrodiniellum shiwhaense*, *Strobilidium* sp., and *Acartia* spp. were able to feed on *Azadinium* cf. *poporum* (Table 4.2).

Azadinium cf. *poporum* (10 000 cells mL^{-1} final concentration) was added to 80 mL polycarbonate (PC) bottles, followed by the addition of each of the other HTDs (100 to 3000 cells mL^{-1} final concentration), the ciliates (20 cells mL^{-1} final concentration), or the copepods (0.025 ind. mL^{-1} final concentration). Duplicates were established for each predator put into contact with *A.* cf. *poporum*. One control bottle (without prey) was set up for each experiment. The bottles were placed on a plankton wheel rotating at 0.9 rpm in a growth chamber at 20 °C under an illumination of 20 μE m^{-2} s^{-1} of cool white fluorescent light on a 14:10 h light: dark cycle.

Aliquots (5 mL) were removed from each bottle after 1, 2, 6, and 24 h of incubation and then transferred into 6-well plate chambers or onto microscopic slides. Approximately 200 cells of each predator were observed using a transmitted light inverted microscope (Zeiss Axiovert 200M, Carl Zeiss) at a magnification of 100x to 630x to determine whether the predators were able to feed on *Azadinium* cf. *poporum*. Cells of predators containing ingested *A.* cf. *poporum* cells were photographed using a Zeiss AxioCam MRc5 digital camera at a magnification of 630x. To confirm the absence of prey ingestion, higher prey concentrations were provided.

Table 4.2 Experimental design to assess predation by various planktonic predator species on the prey species *Azadinium* cf. *poporum*. The numbers in prey and predator columns are the actual initial concentrations (cells or ind. mL^{-1}) of prey and predator. In each experiment, the lowest *A.* cf. *poporum* concentration was tested against the lowest predator concentration, the next lowest against the next lowest, etc. Values within parentheses in the prey and predator columns are the corresponding prey and predator concentrations in the predator-only control bottles. Feeding occurrence of each predator on *A.* cf. *poporum* in Expt 1 is represented by Y (feeding observed) or N (no feeding observed)

Expt	Prey concentration	Species	Predator concentration	Feeding
1	10 000	*Gyrodiniellum shiwhaense*	1000	Y
		Gyrodinium dominans	500	Y
		Gyrodinium moestrupii	500	Y
		Oblea rotunda	500	N
		Oxyrrhis marina	3000	Y
		Pfiesteria piscicida	3000	Y
		Polykrikos kofoidii	100	N
		Stoeckeria algicida	1000	N
		Strobilidium sp.	20	Y
		Acartia spp.	0.025	Y
2	44, 282, 1223, 2991, 9600, 22 758 (0)	*Oxyrrhis marina*	5, 12, 24, 36, 53, 106 (7, 261)	
3	62, 558, 2415, 5536, 11 771, 22 919, 59 267 (0)	*Strobilidium* sp.	6, 6, 6, 15, 13, 13, 29 (7, 28)	
4	52, 151, 492, 1895, 6553, 27 070, 52 332 (0)	*Acartia* spp.	0.02, 0.02, 0.02, 0.02, 0.02, 0.02, 0.02 (0.02)	

4.4.3 Growth, ingestion, and gross growth efficiency

Expts 2 and 3 were designed to measure the growth and ingestion rates of *Oxyrrhis marina* and *Strobilidium* sp. as a function of the prey concentration when fed on *Azadinium* cf. *poporum* (Table 4.2). Only this HTD and this ciliate were shown to feed and to have sustained growth on *A.* cf. *poporum* among the protists tested.

Two weeks before the experiments were conducted, dense cultures of *Oxyrrhis marina* and *Strobilidium* sp. growing on algal prey listed in Table 4.1 were transferred into 500 mL PC bottles containing *Azadinium* cf. *poporum* (ca. 20 000 cells mL^{-1} final concentration). These predator cultures were transferred to 500 mL PC bottles of fresh prey (ca. 20 000 cells mL^{-1} final concentration) every 1 to 3 d. The bottles were filled to capacity with freshly filtered seawater, capped, and placed on plankton wheels rotating at 0.9 rpm and incubated under the conditions described above. To monitor the conditions and interactions between the predator and prey species, the cultures were periodically removed from the rotating wheels, examined through the surface of the capped bottles by using a stereomicroscope (Olympus, SZX-12), and then returned to the rotating wheels. Once the target prey cells in ambient water were no longer detectable, predators were routinely inspected until the prey cells were no longer observed in the cytoplasm. This was carried out to minimize possible residual growth resulting from the ingestion of prey during batch culture. Once the predators were starved, the cultures were then used to conduct the experiments.

For each experiment, the initial concentrations of protists were established using an autopipette to deliver predetermined volumes of known cell

concentrations to the bottles. Triplicate 42 mL (for the HTD) or 80 mL (for the ciliate) experimental bottles (mixtures of predator and prey) and triplicate control bottles (prey only) were set up for each predator-prey combination. Triplicate control bottles containing only predators were also established at 2 predator concentrations. F/2 medium-Si (5 mL for the HTD, 10 mL for the ciliate) was added to all PC bottles. To obtain similar water conditions, the water of the predator culture was filtered through a 0.7 μm GF/F filter and then added to the prey control bottles in the same amount as the volume of the predator culture added to the experiment bottles for each predator-prey combination. Culture of *Azadinium* cf. *poporum* was filtered and added to the predator control bottles in the same way as for the prey control bottles. All bottles were then filled to capacity with filtered seawater and capped. To determine the actual protist concentrations at the beginning of the experiment, a 5 or 6 mL aliquot was taken from each bottle for the HTD and ciliate, respectively. The bottles were refilled to capacity with freshly filtered seawater, capped, and placed on rotating wheels under the conditions described above. Dilution of the cultures associated with refilling was considered when calculating growth and ingestion rates. Another aliquot of the same volume as before was taken from each bottle after 48 or 24 h for the HTD and ciliate, respectively. The aliquots were fixed with 5 % acid Lugol's solution (final concentration). The abundances of predator and prey were determined by counting all or >300 cells in 3 Sedgwick-Rafter chambers (SRCs, 1 mL). The conditions of the predator and its prey were assessed using a stereomicroscope as described above before subsampling.

Expt 4 was designed to measure only the ingestion and clearance rates of *Acartia* spp. on *Azadinium* cf. *poporum* as a function of the prey concentration (Table 4.2). Adult female *Acartia* spp. were used.

The initial concentration of *Acartia* spp. was determined by the individual transfer of the copepods using a Pasteur pipette with a stereomicroscope (Olympus, SZX-12). Triplicate 500 mL experimental bottles (mixtures of predator and prey) and triplicate control bottles (prey only) were set up for each predator-prey combination. Triplicate control bottles containing only predators were also established at 1 predator concentration. F/2 medium-Si (50 mL) was added to all PC bottles. To obtain similar water conditions, the same procedures described above were followed. Furthermore, the actual protist concentrations at the beginning and end of the experiment were determined as before by taking a 10 mL aliquot. The final concentration of *Acartia* spp. was determined by direct counting with a stereomicroscope (Olympus, SZX-12).

The specific growth rate of predators, μ (d^{-1}), was calculated as:

$$\mu = [\mathrm{Ln}\ (P_t/P_0)]/t \quad (1)$$

where P_0 and P_t are the concentrations of predators at 0 and 48 h for the HTD, and at 0 and 24 h for the ciliate, and t is the time elapsed during the experiment.

Growth rates were fit to the Michaelis-Menten model (Michaelis & Menten 1913). The equation for growth rate data is:

$$\mu = \mu_{max}\ (X - X')/[K_{GR}+(X - X')] \quad (2)$$

where μ_{max} is the maximum growth rate (d^{-1}); X is the prey concentration (cells mL^{-1} or ng C mL^{-1}), X' is the threshold prey concentration (the prey concentration where $\mu = 0$), K_{GR} is the prey concentration sustaining half of μ_{max}. Data were iteratively fitted to this regression type using DeltaGraph® (Delta Point) and the Levenberg-Marquardt algorithm, which minimizes the sum of squares of differences between the dependent variables in the equation and the observed data.

Ingestion and clearance rates were calculated using the equations of Frost (1972) and Heinbokel (1978). The incubation times for calculating ingestion and clearance rates were the same as those for estimating growth rates. The data on the ingestion rates were fit to the Michaelis-Menten model or a simple linear regression model depending of the functional response. The Michaelis-Menten equation for ingestion rate (IR) data is:

$$IR = I_{max} (X)/[K_{IR}+(X)] \quad (3)$$

and the simple linear regression equation is:

$$IR = C1(X) + C2 \quad (4)$$

where I_{max} is the maximum ingestion rate (cells $predator^{-1}$ d^{-1} or ng C $predator^{-1}$ d^{-1}); X is the prey concentration (cells mL^{-1} or ng C mL^{-1}), K_{IR} is the half saturation constant (the prey concentration sustaining half of I_{max}), and C1 and C2 are constants.

Gross growth efficiency (GGE), defined as predator biomass produced (+) or lost (−) per prey biomass ingested, was calculated from estimates of carbon content per cell based on cell volume for each mean prey concentration.

4.4.4 Field data

Water samples were obtained at least at monthly intervals in ice-free conditions from January 2009 to December 2011 in Shiwha bay, Korea, at different stations from the surface and 1 m above the bottom (Fig. 4.1). To quantify cells based on optical microscopy, samples were fixed with 5 % acid Lugol's solution (final concentration) and used to determine the abundance of *Oxyrrhis marina* and *Strobilidium* sp.-sized naked ciliates. *Azadinium* cf. *poporum* cannot be differentiated easily from species of its own genus and other species highly similar morphologically based on optical microscopy. Therefore, qPCR (quantitative polymerase chain reaction) was used to estimate its concentration in the field. Field samples were concentrated by the filtration of 100 mL of seawater with a 25 mm GF/C glass microfiber filter (Whatman™) and immediately frozen on dry ice. Filters were subsequently stored at -20 °C until further processing.

Fixed field samples were settled for 48 h. They were then concentrated by gently removing the surface water. To determine the concentration of *Oxyrrhis marina* and *Strobilidium* sp.-sized naked ciliates, an aliquot was removed from each concentrated field sample and examined with a compound microscope to determine their abundances by enumerating the cells in three 1 mL SRCs. The protists were enumerated at 40x to 200x magnification.

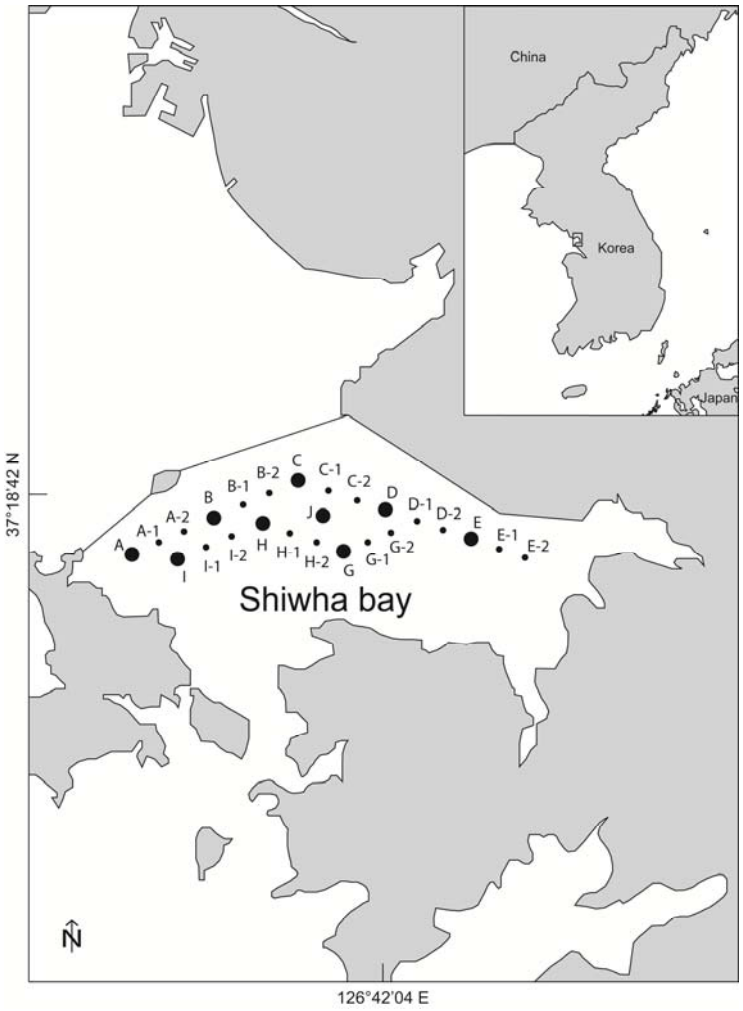

Fig. 4.1 Shiwha bay, Korea, and fixed stations where water samples were collected. Surface water samples used for protistan determination and qPCR were taken at every station, while bottom water samples were only taken at stations represented by enlarged circles.

After the filters stored at -20 °C had defrosted, cells were resuspended by adding TE buffer (Tris HCl pH 8.0 10 mM, EDTA 1 mM, Bioneer) and grinding the filters in 2 mL tubes (GenePole). The suspension was subsequently boiled at 100 °C for 5 min and cooled at room temperature for 20 min. We added 850 µL of 25:24:1 phenol: chloroform: isoamyl alcohol (Bioneer) and mixed by vortexing. The samples were subsequently centrifuged (Hanil Science, model MICRO 17TR) at 17 640 x g (30 min at 20 °C). The supernatant was transferred to a DNA binding column (Bioneer) and subsequently centrifuged at 2250 × g (1 min at 20 °C). We then added 700 µL of 99.5 % ethanol (Merck) at -20 °C and 30 µL 3M sodium acetate (pH 7.0, Bioneer) to the binding column. The mixture was subsequently incubated at −20 °C for 1 h. The mixture was then centrifuged at 2250 × g (1 min at 4 °C). The pellet was then washed twice by the addition of 70 % ethanol (Merck) followed by centrifugation at 2250 × g (1 min at 4 °C). The pellet contained in the binding column was subsequently dried at 50 °C for 1 h. TE buffer (200 µL) was added to the binding column. The binding column was left to stand for more than 10 min in order to resuspend the DNA. Finally, the binding column was centrifuged at 1440 × g (5 min) followed by 17 640 × g (5 min). The crude extracts and 1:10 dilutions were stored at -20 °C until further use in qPCR assays. A preliminary survey was done with the undiluted and diluted extracts for each sample collected. Each positive assay of this survey was measured in triplicate.

The design of the primers and the probe was based on the ITS rDNA region sequences of all species of the genus *Azadinium* available from GenBank. Sequences were aligned using the program Clustal X2 (Larkin *et al*. 2007). Manual searches of the alignment were conducted to determine unique sequences and to develop an *A.* cf. *poporum* specific qPCR assay. The primers and probe sequences as well as their general properties were determined with Primer 3 (Rozen &

Skaletsky 2000). Their secondary structures were analyzed with OligoCalc (Kibbe 2007). Subsequently, the primers and probe were synthesized by Biosearch Technologies (Novato, CA). The probe was dual-labeled with the fluorescent dye FAM and the BHQ-1 quencher at the 5' and 3' ends, respectively. The sequences of the primers and probe were checked against published sequences in GenBank by BLAST homology search. BLAST searches showed that the sequences of the selected primers and probe matched only with the sequences of *A.* cf. *poporum*. The specificity was further assessed with the DNA from 22 dinoflagellate cultures (Table 4.3) extracted as in Potvin *et al*. (2012). Agarose gel analysis of the PCR products showed only amplicons of the expected size (94 bp) for *A.* cf. *poporum* and no product for other species. qPCR experiments showed that the primers-probe set was specific to the target for which it was designed.

To achieve optimal performance, series of primers and probe concentrations as well as annealing-extension times and temperatures were tested by qPCR assays. The tested primers and probe concentrations ranged from 200 to 1000 and 100 to 500 nM, respectively. The tested annealing-extension times and temperatures ranged from 45 to 85 s and 56 to 64 °C, respectively. The conditions that provided the lowest cycle threshold (CT) value and the highest fluorescence were selected. PCR assays were performed on a Rotor-Gene 6000 (Corbett Research). The following reagents were added in the reaction mixture: 5 µL of 2x SensiMix II Probe (GenePole), forward (5'-GGG AAC CTT CGC ATC AAT CAA C-3') and reverse (5'-CAC GAA GCA GCC TTG GGT TT-3') primers each at a final concentration of 0.2 µM, probe (5'-TGA GTG TCT TTG ATA CCA TCT GTT GCA-3') at a final concentration of 0.15 µM, l µL of template DNA, and nuclease-free water (GenePole) to a final volume of 10 µL. The thermal cycling

Table 4.3 Isolation conditions of the dinoflagellates used in the qPCR specificity test. Sampling location and time, field water temperature (T, °C), and salinity (S) are shown. na: not available

Dinoflagellate	Location	Year (month)	T	S
Azadinium cf. *poporum*	Shiwha bay, Korea	2010 (06)	24.1[a]	26.7[a]
Bysmatrum caponii	Karorim, Korea	2010 (05)	19.5	33.0
Cryptoperidiniopsis brodyi	Pamlico River, USA	1992 (07)	na	na
Dinophysis acuminata	Masan bay, Korea	2005 (12)	na	na
Gymnodinium aureolum	Kunsan, Korea	2008 (03)	10.0	30.5
Gymnodinium simplex	Shiwha bay, Korea	2009 (09)	25.1	24.0
Gyrodiniellum shiwhaense	Shiwha bay, Korea	2009 (09)	24.5	24.0
Gyrodinium moestrupii	Saemangum bay, Korea	2009 (10)	21.2	31.0
Heterocapsa rotundata	Kunsan, Korea	2002 (05)	16.6	22.0
Heterocapsa triquetra	Masan bay, Korea	2008 (06)	20.2	29.0
Karenia brevis	Gulf of Mexico, USA	1999 (09)	na	na
Karlodinium veneficum	Shiwha bay, Korea	2011 (08)	27.1	7.2
Oxyrrhis marina	Karorim, Korea	2010 (05)	19.5	33.0
Paragymnodinium shiwhaense	Shiwha bay, Korea	2006 (05)	18.8	30.4
Pfiesteria piscicida	Jinhae, Korea	2010 (02)	24.5	12.6
Prorocentrum donghaiense	Jeju, Korea	2010 (06)	na	na

Table 4.3 (continued)

Dinoflagellate	Location	Year (month)	T	S
Prorocentrum micans	Shiwha bay, Korea	2009 (10)	16.8	27.0
Prorocentrum minimum	Shiwha bay, Korea	2009 (01)	1.2	30.3
Scrippsiella precaria	Shiwha bay, Korea	2009 (06)	22.8	27.6
Scrippsiella sweeneyae	Masan bay, Korea	2009 (08)	27.0	31.5
Stoeckeria algicida	Masan bay, Korea	2007 (08)	24.5	29.7
Woloszynskia cincta	Shiwha bay, Korea	2009 (06)	22.0	29.3

[a]Isolated from sediment

conditions consisted of 10 min at 95 °C followed by 50 cycles of 10 s at 95 °C and 65 s at 60 °C. Fluorescence data were collected at the end of each cycle, and determination of the cycle threshold line was carried out automatically by the instrument. PCR products that were positive were further analyzed by gel electrophoresis to confirm the amplicon size. Three samples that gave positive qPCR results were reamplified without the probe. The PCR products were purified using the AccuPrep® PCR purification kit (Bioneer) according to the manufacturer's instructions. The purified DNA was sent to the Genome Research Facility (School of Biological Science, Seoul National University, Korea) and sequenced with an ABI PRISM® 3700 DNA Analyzer (Applied Biosystems). All sequences obtained corresponded to *Azadinium* cf. *poporum*.

A standard curve using cell numbers was constructed from *Azadinium* cf. *poporum* culture. Cell numbers (100 000 cells) were estimated by counting 3 SRCs, and genomic DNA was extracted the same way as for the field samples. Ten-fold serial dilutions of the DNA extract were used to construct the standard curve. A strong linear relationship between the CT values and the log of the cell numbers was established, with a correlation coefficient (r^2) of 0.999. The cell number of *A.* cf. *poporum* in field samples was determined from CT values and comparison with the standard curve.

4.4.5 Grazing impact

We calculated grazing coefficients by using field data on the abundance of *Strobilidium* sp.-sized naked ciliates (25 to 60 μm in length) co-occurring with *Azadinium* cf. *poporum* and laboratory data on ingestion rate. We assumed that the

ingestion rates of *Strobilidium* sp.-sized naked ciliates on *A.* cf. *poporum* were the same as those obtained in this study.

The grazing coefficients (g, d^{-1}) were calculated as:

$$g = CR \times GC \times 24 \quad (5)$$

where CR is the clearance rate (mL $predator^{-1}$ h^{-1}) of a predator on *Azadinium* cf. *poporum* at a given prey concentration, and GC is the grazer concentration (cells mL^{-1}). CRs were calculated as:

$$CR = IR/X \quad (6)$$

where IR is the ingestion rate (cells eaten $predator^{-1}$ h^{-1}) of the predator on the prey and X is the prey concentration (cells mL^{-1}). CRs were corrected using Q_{10} = 2.8 (Hansen *et al*. 1997) because *in situ* water temperatures and the temperature used in the laboratory for the experiments (20 °C) were sometimes different.

4.4.6 Swimming speed

A culture of *Azadinium* cf. *poporum* (ca. 20 000 cells mL^{-1}) growing at 20 °C under an illumination of 20 µE m^{-2} s^{-1} of cool white fluorescent light on a 14:10 h light: dark cycle in F/2 medium-Si was added to a 50 mL cell culture flask and allowed to acclimate for 30 min. The video camera focused on 1 field seen as 1 circle in a cell culture flask under a stereomicroscope (Olympus, SZX-12) at 20 °C, and swimming of *A.* cf. *poporum* cells was then recorded at a magnification of 40x using a video analyzing system (Samsung, SV-C660) and a CCD camera (Hitachi,

KP-D20BU). The swimming speed was calculated based on the linear displacement of cells in 1 s. The average swimming speed was calculated based on the measures of 30 cells during single-frame playback. The swimming of individual cells was interrupted by short and high-speed 'jumps' in various directions typical of the genus *Azadinium* (Tillmann *et al*. 2009). These 'jumps' were excluded from the measurements.

4.5 Results

Among the predators tested, *Gyrodinium dominans*, *G. moestrupii*, *Oxyrrhis marina*, *Pfiesteria piscicida*, *Gyrodiniellum shiwhaense*, *Strobilidium* sp., and *Acartia* spp. were able to feed on *Azadinium* cf. *poporum* (Fig. 4.2), while *Polykrikos kofoidii*, *Oblea rotunda*, and *Stoeckeria algicida* were not. Only the HTD *O. marina* and the ciliate *Strobilidium* sp. showed sustained growth on *A.* cf. *poporum*.

4.5.1 Growth rate

The growth rate of *Oxyrrhis marina* on *Azadinium* cf. *poporum* rapidly increased up to ca. 5.2×10^3 cells mL^{-1} (669 ng C mL^{-1}), but became saturated at the higher prey concentrations (Fig. 4.3 A). When the data were fitted to Eq. (2), the maximum growth rate (μ_{max}) of *O. marina* on *A.* cf. *poporum* was 0.497 d^{-1} and the threshold prey concentration for the growth of the predator was 4 cells mL^{-1} (0.509 ng C mL^{-1}). The prey concentration sustaining half of μ_{max} was 619 cells mL^{-1} (79.4 ng C mL^{-1}).

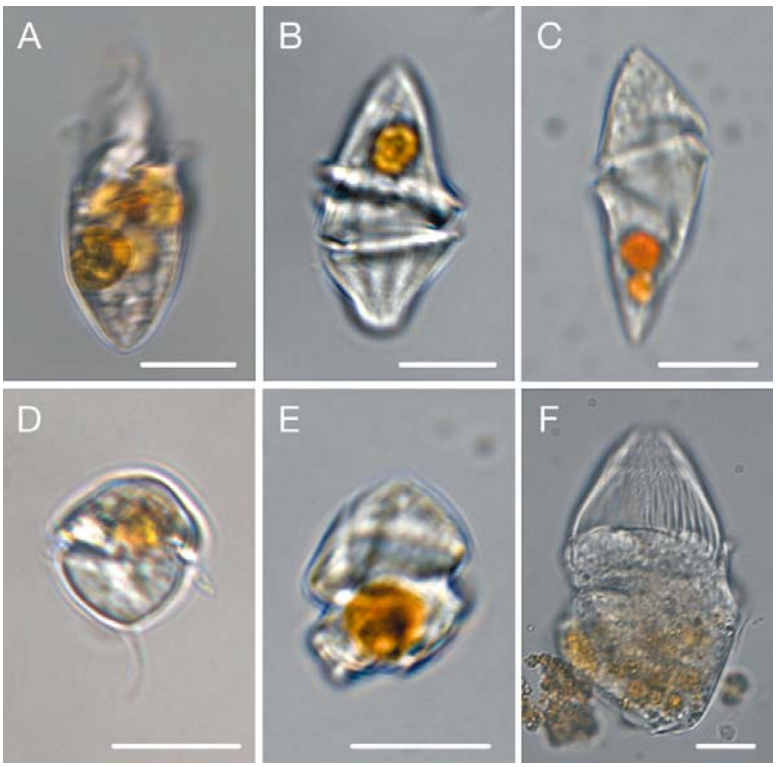

Fig. 4.2 Feeding by (A−E) heterotrophic dinoflagellates and (F) a ciliate on *Azadinium* cf. *poporum*. (A) *Oxyrrhis marina* with several ingested *A.* cf. *poporum* cells, (B) *Gyrodinium dominans* with an ingested *A.* cf. *poporum* cell, (C) *Gyrodinium moestrupii* with 2 ingested *A.* cf. *poporum* cells, (D) *Pfiesteria piscicida* with an ingested *A.* cf. *poporum* cell, (E) *Gyrodiniellum shiwhaense* with an ingested *A.* cf. *poporum* cell, (F) *Strobilidium* sp. with several ingested *A.* cf. *poporum* cells. All photographs were taken by means of an inverted microscope using Zeiss AxioCam MRc5 digital camera at a magnification of 630x. Scale bars = 10 μm

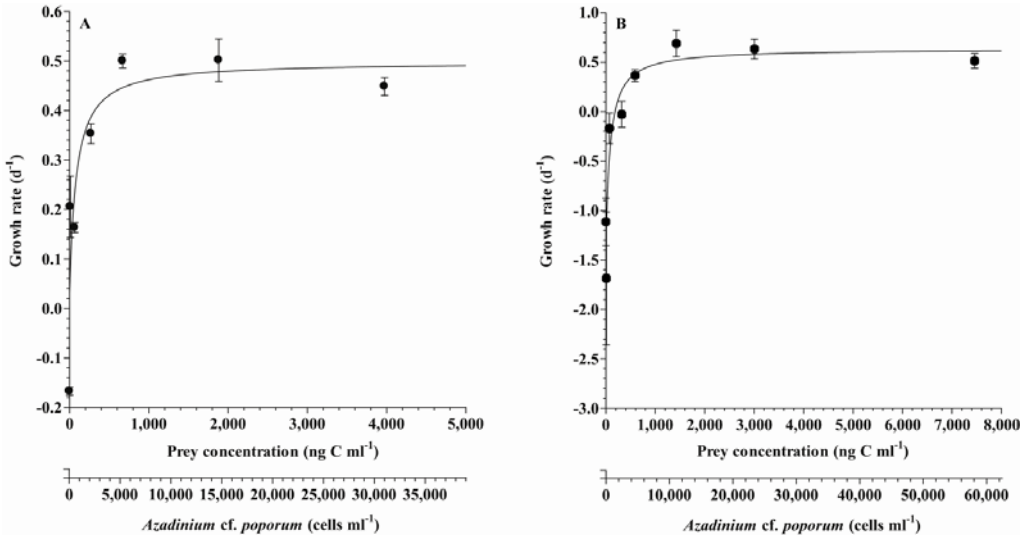

Fig. 4.3 *Oxyrrhis marina* and *Strobilidium* sp. Specific growth rate (μ, d^{-1}) of (A) the heterotrophic dinoflagellate and (B) a ciliate feeding on the dinoflagellate *Azadinium* cf. *poporum* as a function of mean prey concentration (X). Symbols represent treatment means ± 1 SE. A Michaelis-Menten equation (Eq. 2) was used to produce curves for (A) and (B) for all treatments in the experiments. (A) $\mu = 0.497(X - 0.509)/[79.4 + (X - 0.509)]$, $r^2 = 0.776$; (B) $\mu = 0.636(X - 185)/[268 + (X - 185)]$, $r^2 = 0.744$

The growth rate of *Strobilidium* sp. on *Azadinium* cf. *poporum* rapidly increased up to ca. 4.6×10^3 cells mL^{-1} (590 ng C mL^{-1}), but became saturated at the higher prey concentrations (Fig. 4.3 B). When the data were fitted to Eq. (2), the μ_{max} of *Strobilidium* sp. on *A.* cf. *poporum* was 0.636 d^{-1} and the threshold prey concentration for the growth of the predator was 1.4 x 10^3 cells mL^{-1} (185 ng C mL^{-1}). The prey concentration sustaining half of μ_{max} was 2.1 x 10^3 cells mL^{-1} (268 ng C mL^{-1}).

4.5.2 Ingestion rate

The ingestion rate of *Oxyrrhis marina* on *Azadinium* cf. *poporum* increased rapidly with mean prey concentration up to ca.5.2×10^3 cells mL^{-1}(669 ng C mL^{-1}), but became saturated at higher concentrations (Fig. 4.4 A). When the data were fitted to Eq. (3), the maximum ingestion rate (I_{max}) of *O. marina* on *A.* cf. *poporum* was 39 cells $predator^{-1}$ d^{-1} (4.99 ng C $predator^{-1}$ d^{-1}). The prey concentration sustaining half of I_{max} was 2.2×10^3 cells mL^{-1} (287 ng C mL^{-1}). The maximum clearance rate of *O. marina* on *A.* cf. *poporum* was 8.85 µL $predator^{-1}$ d^{-1}.

The ingestion rate of *Strobilidium* sp. on *Azadinium* cf. *poporum* increased rapidly with mean prey concentration up to ca. 4.6×10^3 cells mL^{-1} (590 ng C mL^{-1}). The ingestion rate continued to increase until the maximum prey concentration was reached at 5.8×10^4 cells mL^{-1} (7.5×10^3 ng C mL^{-1}), but at a slower rate (Fig. 4.4 B). When the data were fitted to Eq. (3), the I_{max} of *Strobilidium* sp. on *A.* cf. *poporum* was 1.4×10^3 cells $predator^{-1}$ d^{-1} (179 ng C $predator^{-1}$ d^{-1}). The prey concentration sustaining half of I_{max} was 4.8×10^3 cells mL^{-1} (608 ng C mL^{-1}). The maximum clearance rate of *Strobilidium* sp. on *A.* cf. *poporum* was 346 µL $predator^{-1}$ d^{-1}.

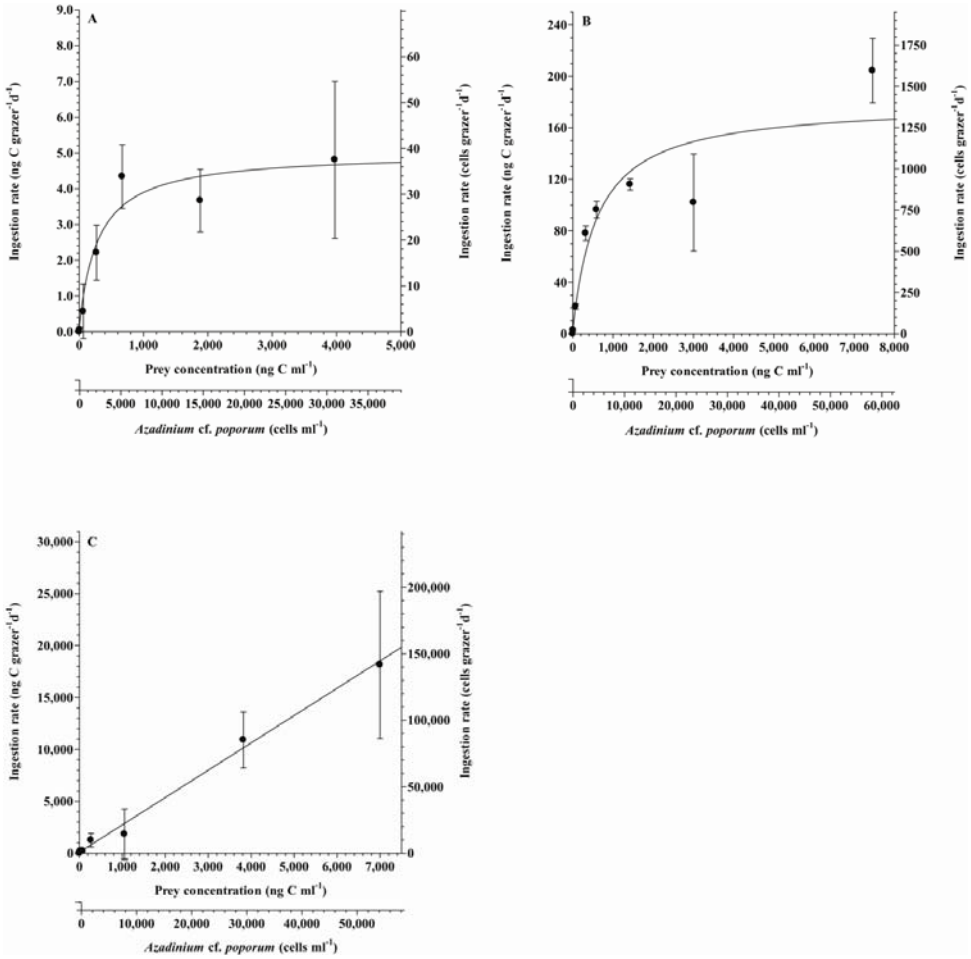

Fig. 4.4 *Oxyrrhis marina*, *Strobilidium* sp., and *Acartia* spp. Ingestion rate (IR) of (A) the heterotrophic dinoflagellate, (B) a ciliate, and (C) copepods feeding on the dinoflagellate *Azadinium* cf. *poporum* as a function of mean prey concentration (X). Symbols represent treatment means ± 1 SE. A Michaelis-Menten equation (Eq. 3) was used to produce the curves for (A) and (B), while a simple linear regression equation (Eq. 4) was used to produce the curve for (C) for all treatments in the experiments. (A) IR = 4.99 X/(287 + X), $r^2 = 0.581$; (B) IR = 179 X/(608 + X), $r^2 = 0.777$; (C) IR = 2.63 X + 55.6, $r^2 = 0.707$

The ingestion rate of *Acartia* spp. on *Azadinium* cf. *poporum* increased linearly up to ca. 5.5 x 10^4 cells mL^{-1} (7.0 x 10^3 ng C mL^{-1}), the maximum prey concentration used (Fig. 4.4 C). When the data were fitted to Eq. (4), the I_{max} of *Acartia* spp. at the maximum prey concentration tested was 1.4 x 10^5 cells $predator^{-1}$ d^{-1} (1.9 x 10^4 ng C $predator^{-1}$ d^{-1}). The maximum clearance rate of *Acartia* spp. on *A.* cf. *poporum* was 8.4 mL $predator^{-1}$ d^{-1}.

4.5.3 Gross growth efficiency

The mean GGEs by predator-prey combination of *Oxyrrhis marina* on *Azadinium* cf. *poporum* generally increased with the mean prey concentrations. The GGEs were 6 to 11 % at the prey concentrations for which ingestion rate was saturated (Fig. 4.5 A). The mean GGEs by predator-prey combination of *Strobilidium* sp. on *A.* cf. *poporum* generally increased from the first mean prey concentration to 2.4 x 10^4 cells mL^{-1} (3.01 x 10^3 ng C mL^{-1}), the mean prey concentration preceding the last. However, *Strobilidium* sp. underwent a decrease of GGE at the last mean prey concentration (5.8 x 10^4 cells mL^{-1}, 7.5 x 10^3 ng C mL^{-1}), likely caused by incomplete digestion, a phenomenon referred as 'superfluous feeding' (Straile 1997). The GGEs were 2 to 6 % at prey concentrations $\geq 4.6 \times 10^3$ cells mL^{-1} (590 ng C mL^{-1}; Fig. 4.5 B).

4.5.4 Dynamics of *Azadinium* cf. *poporum*

The 36 mo field survey conducted in Shiwha bay showed that *Azadinium* cf. *poporum* cell concentrations were generally low (Fig. 4.6). The DNA of

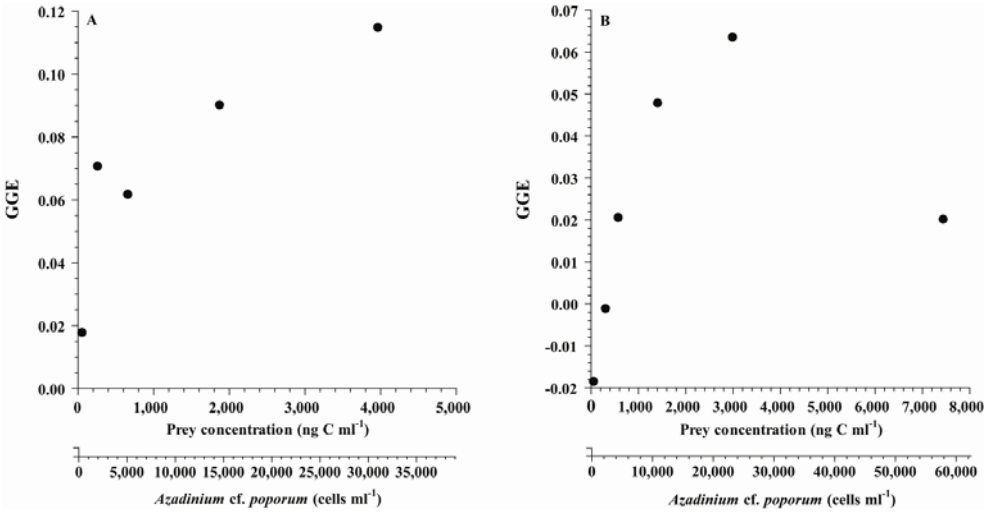

Fig. 4.5 *Oxyrrhis marina* and *Strobilidium* sp. Mean gross growth efficiencies (GGEs) of (A) the heterotrophic dinoflagellate and (B) a ciliate on *Azadinium* cf. *poporum* as a function of mean prey concentration. The GGEs at the first mean prey concentration are not illustrated since they were highly negative.

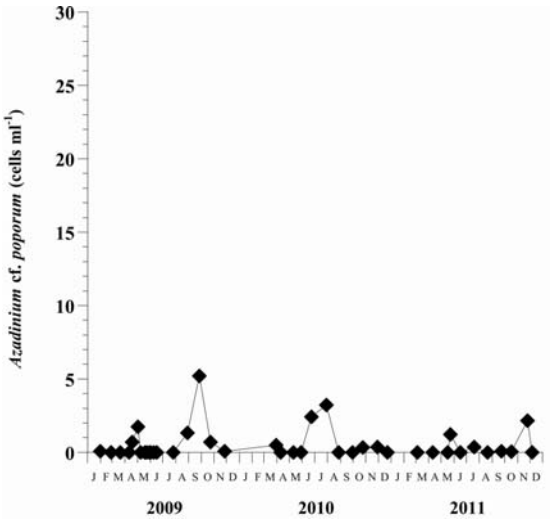

Fig. 4.6 *Azadinium* cf. *poporum.* Dynamics of abundances quantified by qPCR in Shiwha bay, Korea, from 2009 to 2011. The highest values obtained at each sampling date are reported. The presence of ice prevented sampling in some months. J: January, F: February, M: March, A: April, M: May, J: June, J: July, A: August, S: September, O: October, N: November, D: December

A. cf. *poporum* was detected each year of the survey. *A.* cf. *poporum* reached its highest concentration in September 2009 at 5.2 cells mL^{-1}.

4.5.5 Grazing impact

The grazing impact of *Oxyrrhis marina* was not possible to assess with the data provided by this study, since *Azadinium* cf. *poporum* and *O. marina* were not found to co-occur. However, *Strobilidium* sp.-sized naked ciliates (25 to 60 μm in length) were observed to co-occur with *A.* cf. *poporum* in Shiwha bay, Korea, between January 2009 and December 2011. Grazing coefficients were variable in a narrow range of concentrations for *A.* cf. *poporum* (0.2 to 3.2 cells mL^{-1}) and *Strobilidium* sp.-sized naked ciliates (0.1 to 1.0 cells mL^{-1}). Assuming that the ingestion rates of all *Strobilidium* sp.-sized naked ciliates on *A.* cf. *poporum* were the same as that of *Strobilidium* sp. obtained in this study, the grazing coefficients ranged between 0.052 and 0.446 d^{-1} (n = 7; Fig. 4.7).

4.5.6 Swimming speed

The average (±SE, n = 30) and maximum swimming speeds of *Azadinium* cf. *poporum*, excluding the short and high-speed 'jumps' in various directions, at the given conditions were 416 (± 13) and 550 μm s^{-1}, respectively.

4.6 Discussion

4.6.1 Feeding

This study is the first extensive report of feeding by HTDs, ciliates, and copepods on a species of the genus *Azadinium*. The engulfment feeders used in this

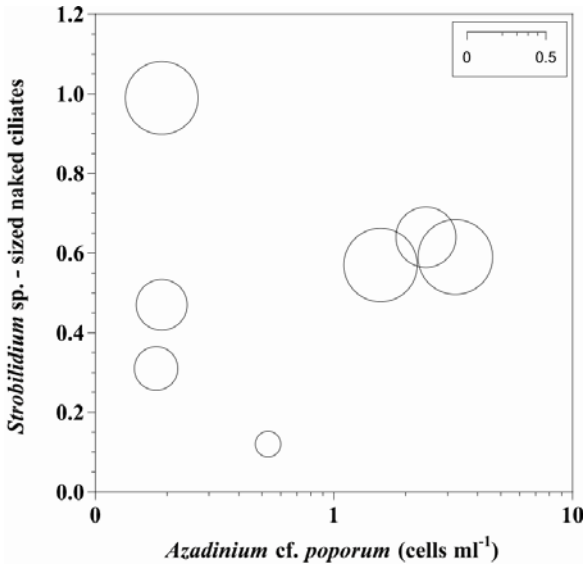

Fig. 4.7 *Strobilidium* sp.-sized naked ciliates (25 to 60 µm in length). Calculated grazing coefficients of the ciliates (n = 7) in relation to the concentration of co-occurring *Azadinium* cf. *poporum* (see Eqs. 5 & 6 for calculation). Clearance rates were corrected with a Q10 = 2.8 (Hansen *et al*. 1997) because *in situ* water temperatures and the experimental temperature used in the laboratory (20°C) were sometimes different. Inset shows the scale of the circles that represent grazing coefficients (g, d^{-1}).

study are raptorial feeders (Fenchel 1987, Sleigh 1989). These predators usually prefer prey approaching their size (Hansen *et al*. 1994). While the biggest engulfment feeder, *Polykrikos kofoidii*, did not feed on *Azadinium* cf. *poporum*, *Gyrodinium* spp. were of intermediate size and occasionally fed on *A.* cf. *poporum*. *Oxyrrhis marina* was the smallest engulfment feeder used in this study and revealed to be the most efficient on *A.* cf. *poporum*. Therefore, size is likely to be an important factor affecting the feeding of predators using engulfment on *Azadinium* spp. A particular case is *G. fusus*, which was previously suggested to be an important grazer on *A.* cf. *spinosum* (Akselman & Negri 2012). Akselman & Negri (2012) claimed that *G. fusus* is able to develop a hyaline cytoplasmic extension or feeding veil from its hypocone that reaches up to twice its length. This particularity was not observed with *Gyrodinium* spp. in our study and might explain the feeding efficiency of *G. fusus* on small prey such as *A.* cf. *spinosum* despite the difference in size. While size appears to be a relevant factor in feeding on *A.* cf. *poporum* for engulfment feeders, speed is unlikely to be a critical factor. For example, *P. kofoidii* is known to feed on prey of similar speed (e.g. *Gymnodinium catenatum* mean speed: 450 μm s^{-1}, maximum speed: 615 μm s^{-1}; Yoo *et al*. 2010, this study).

Peduncle feeders can be highly specialized, such as *Stoeckeria algicida* which is only known to feed on *Heterosigma akashiwo* among algal prey (Jeong *et al*. 2005d, 2011b, this study). However, these predators are usually generalists and are able to feed on a wide range of dinoflagellates, but are restricted in size regarding thecal dinoflagellates. Peduncle feeders do not seem to have peduncles that are strong enough to efficiently penetrate the theca of dinoflagellates. Therefore, the theca might explain the absence of growth by both *Pfiesteria*

piscicida and *Gyrodiniellum shiwhaense* despite the occurrence of feeding. Peduncle feeders are therefore unlikely to be effective predators on *Azadinium* spp.

The pallium feeder *Oblea rotunda* was not able to feed on *Azadinium* cf. *poporum*. *O. rotunda* responds to chemosensory, but not to mechanosensory stimulation (Strom & Buskey 1993). Therefore, the lack of chemosensory stimulation from *A.* cf. *poporum* might explain the lack of feeding by *O. rotunda*. *P. crassipes*, for which AZA-1, AZA-2, and AZA-3 have been detected (James *et al*. 2003b), is likely to feed on *Azadinium* spp. or closely related species. Therefore, it is worthwhile to study feeding by pallium feeders on *Azadinium* spp. further in order to assess the potential of such predators.

The filter feeders *Strobilidium* sp. and *Acartia* spp. were both able to feed on *Azadinium* cf. *poporum*. However, not all filter feeders are likely to feed on *Azadinium* spp. The ciliate *Laboea strobila* as well as 3 unidentified oligotrich ciliate species were previously observed to co-occur with *A.* cf. *spinosum*. Among them, only 1 oligotrich ciliate was suggested to feed (Akselman & Negri 2012). The facility of filter feeders to capture prey of smaller size (Hansen *et al*. 1994) might partly explain their success. However, more factors are apparently implicated in their capacity to feed on *Azadinium* spp.

Based on the results of the present study, the dynamics of HTDs that engulf their prey and are not disproportionately larger than *Azadinium* spp., as well as ciliates which use filtration, are more likely to be affected by the occurrence of *Azadinium* spp. than HTDs that feed using their peduncle.

4.6.2 Growth and ingestion rates

The μ_{max} of the predators of *Azadinium* cf. *poporum* were the lowest among known photosynthetic or mixotrophic prey enabling growth (Fig. 4.8 A, 4.9 A; Goldman *et al*. 1989, Montagnes 1996, Jeong *et al*. 2001, 2003b, Tillmann & Reckermann 2002, Chen *et al*. 2010, Yoo *et al*. 2010), while the I_{max} values were the highest (Fig. 4.8 B, 4.9 B, 4.10; Houde & Roman 1987, Goldman *et al*. 1989, Jeong *et al*. 2001, 2003b, Besiktepe & Dam 2002, Tillmann & Reckermann 2002, Broglio *et al*. 2003, Cohen *et al*. 2007, Chen *et al*. 2010, Yoo *et al*. 2010). The low ratios of maximum growth rate to maximum ingestion rate, or RMGI, and GGEs obtained by predators in this study suggest that *A.* cf. *poporum* is a low-quality prey. The energy necessary to capture, handle, and digest this prey is higher than for other prey species, or the conversion of ingested *A.* cf. *poporum* carbon to predator body carbon is low. This can lead the predators to compensate for the low quality of *A.* cf. *poporum* by feeding more and explains the high ingestion rates obtained in the laboratory experiments. *A.* cf. *poporum* is the only known photosynthetic or mixotrophic thecate prey species for *Oxyrrhis marina* and *Strobilidium* sp. for which we have quantitative data on growth and ingestion rates. The theca of *A.* cf. *poporum* might be partly responsible for its reduced quality as prey. It is also possible that the azaspiracid produced by *A.* cf. *poporum* (Krock *et al*. 2012) lowers its quality as prey.

4.6.3 Dynamics of *Azadinium* cf. *poporum*

The survey of *Azadinium* cf. *poporum* by qPCR revealed that the species is always in low concentration in Shiwha bay. In this respect, it appears that *A.* cf. *poporum* acts similarly to *A. caudatum* (Nézan *et al*. 2012). The reasons explaining

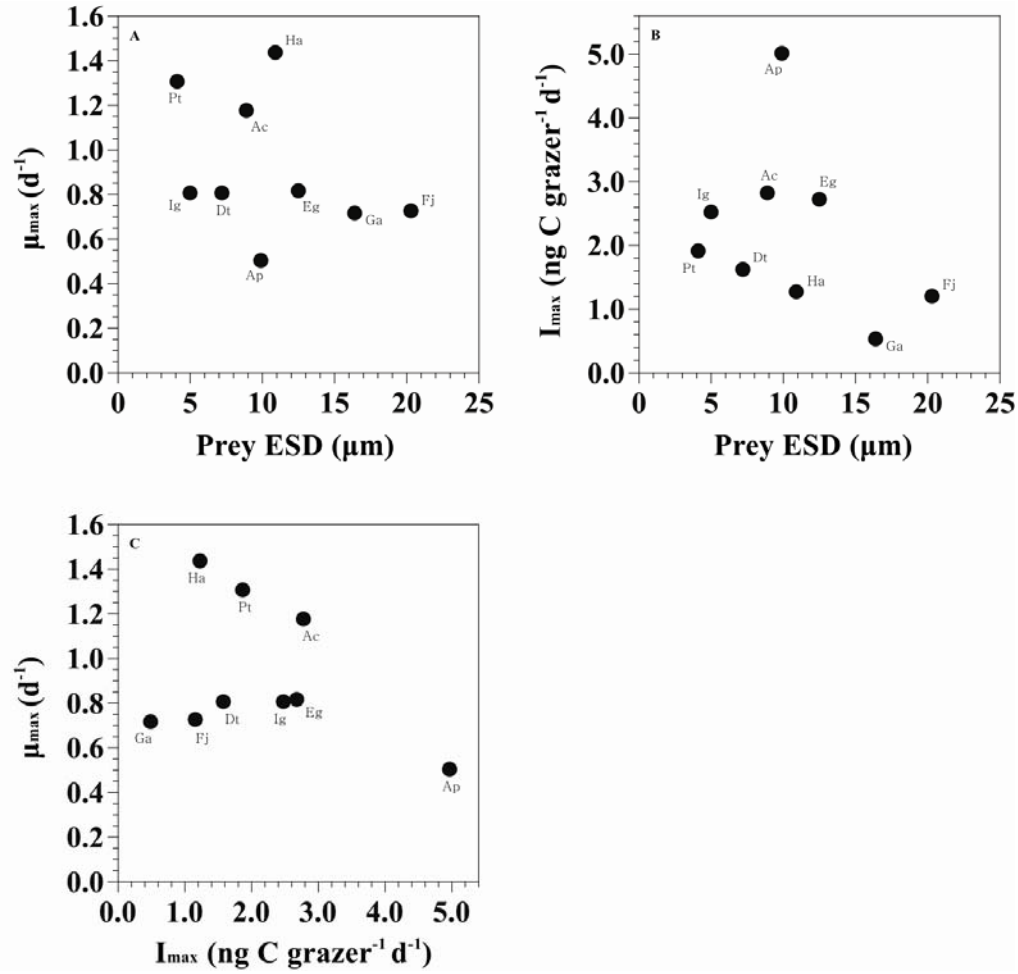

Fig. 4.8 *Oxyrrhis marina.* (A) Maximum growth (μ_{max}, d^{-1}) and (B) ingestion rates (I_{max}, ng C $predator^{-1}$ d^{-1}) of the heterotrophic dinoflagellate feeding on photosynthetic or mixotrophic algal prey as a function of prey size (equivalent spherical diameter, ESD, μm), and (C) μ_{max} as a function of I_{max}. ESDs were estimated based on prey volume or carbon content converted to prey volume according to Menden-Deuer & Lessard (2000) if not provided. Ingestion rates from Goldman *et al*. (1989) were converted from cell to carbon according to Menden-Deuer & Lessard (2000). Control laboratory experiments were made at 20°C. Ac: *Amphidinium carterae*, Ap: *Azadinium* cf. *poporum*, Dt: *Dunaliella tertiolecta*, Eg: *Eutreptiella gymnastica*, Fj: *Fibrocapsa japonica*, Ga: *Gymnodinium aureolum*, Ha: *Heterosigma akashiwo*, Ig: *Isochrysis galbana*, Pt: *Phaeodactylum tricornutum*.

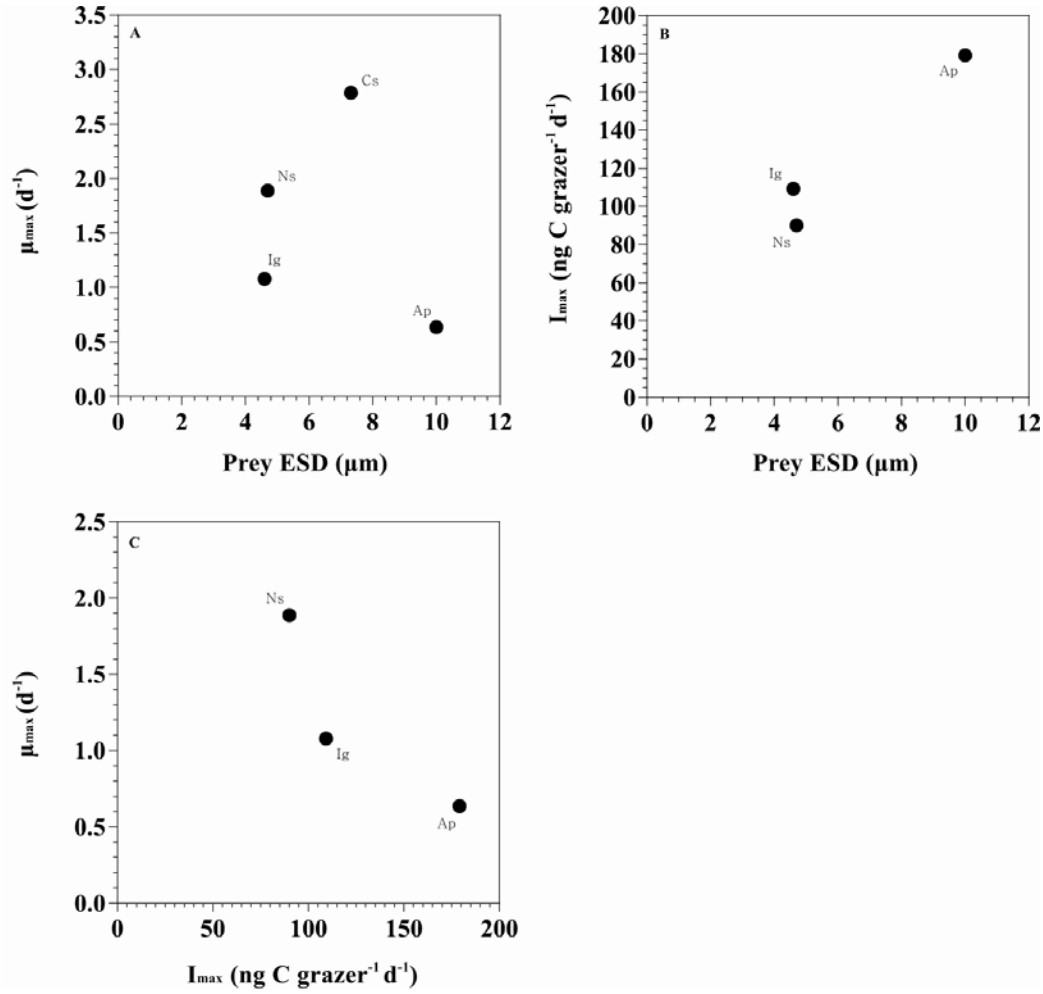

Fig. 4.9 *Strobilidium* spp. (A) Maximum growth (μ_{max}, d^{-1}) and (B) ingestion rates (I_{max}, ng C $predator^{-1}$ d^{-1}) of the ciliates feeding on photosynthetic or mixotrophic algal prey as a function of prey size (equivalent spherical diameter, ESD, μm) and (C) μ_{max} as a function of I_{max}. Rates were corrected with a Q10 = 2.8 (Hansen *et al*. 1997) if control laboratory experiments were made at a temperature different than 20°C. ESDs were estimated based on carbon content converted to prey volume according to Menden-Deuer & Lessard (2000) if not provided. Ap: *Azadinium* cf. *poporum*, Cs: *Chroomonas salina*, Ig: *Isochrysis galbana*, Ns: *Nannochloropsis* sp.

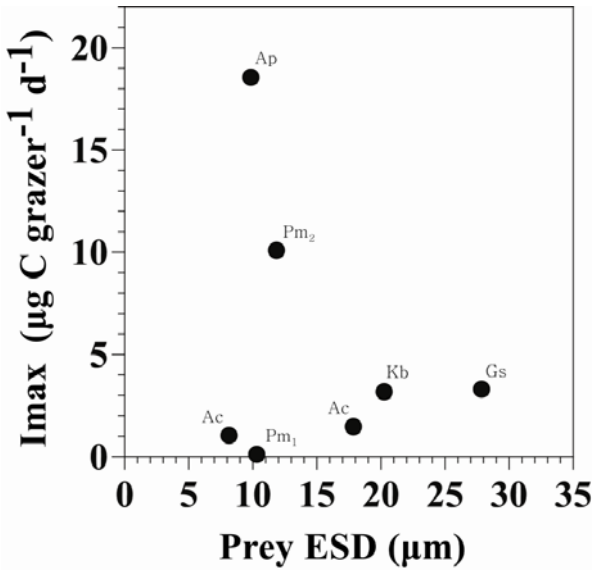

Fig. 4.10 *Acartia* spp. Maximum ingestion rate (I_{max}, µg C predator^{-1} d^{-1}) of the copepods on photosynthetic or mixotrophic algal prey as a function of prey size (equivalent spherical diameter, ESD, µm). Rates were corrected with a Q10 = 2.8 (Hansen *et al*. 1997) if control laboratory experiments were unambiguously made at a temperature different than 20°C. ESDs were estimated based on carbon content converted to prey volume according to Menden-Deuer & Lessard (2000) if not provided. *Maximum value obtained. Ac: *Amphidinium carterae**, Ap: *Azadinium* cf. *poporum**, Gs: *Gymnodinium sanguineum**, Kb: *Karenia brevis**, Pm1* and Pm2: *Prorocentrum minimum*.

these observations are unknown. Predation on *A.* cf. *poporum* as well as the physiology of the species can result in such dynamics.

4.6.4 Grazing impact

The grazing coefficients obtained by using field data on abundance of *Strobilidium* sp.-sized naked ciliates (25 to 60 μm in length) co-occurring with *Azadinium* cf. *poporum* as well as laboratory data on ingestion rates suggest that up to 36 % of the *A.* cf. *poporum* population could be removed by *Strobilidium* sp.-sized naked ciliates in 1 d. However, it is unclear whether such an impact is reflected in the field with a more complex microbial food web. The high ingestion rates obtained in laboratory experiments, as mentioned above, might be influenced by compensatory feeding. Furthermore, oligotrich ciliates are known to select food based on size (Kivi & Setälä 1995). However, ciliates have also shown selectivity at the species level (Stoecker *et al*. 1981, Verity 1988). Therefore, it is questionable to what extent the grazing impacts obtained in this study reflect what is actually happening in the field.

4.6.5 Ecological implications

Many predators are able to feed on *Azadinium* cf. *poporum*. However, only 2 predators used in this study responded with acute growth on *A.* cf. *poporum*. Furthermore, *A.* cf. *poporum* appears to be a low-quality prey for the planktonic predators tested here based on the RMGI and GGEs obtained. If this can be generalized at the genus level, it suggests that only a few predators are likely to feed efficiently on *Azadinium* spp. The abundances of *A.* cf. *poporum* in the field revealed to be below or slightly above the threshold prey concentration of the

predators. Therefore, *A.* cf. *poporum* is unlikely to affect the dynamics of these predators in the field. This is reflected by the absence or low co-occurrence of the protistan predators with *A.* cf. *poporum* over the 3 yr of monitoring. Factors other than predation are likely to be implicated in the determination of the abundance of *A.* cf. *poporum* in the field. Further research is required to determine these factors.

Chapter 5: Physiology

Effect of environmental factors on *Azadinium* cf. *poporum* from western Korean waters

5.1 Abstract

In order to determine the causes explaining the low dynamics of *Azadinium poporum* in Shiwha bay, an eutrophic area, we assessed the tendency of some parameters through time such as the temperature, the salinity, the pH, the dissolved oxygen, the Secchi depth, the concentration of nutrients, and the concentration of chlorophyll a. We also determined the effects of temperature, salinity, and light on the growth of *A. poporum* in laboratory as well as relationships between environmental parameters and *A. poporum* in the field. The species revealed to grow on a wide range of temperature and salinity and was therefore generally well adapted to the high variability observed in Shiwha bay. *A. poporum* was also adapted to low light condition. The growth obtained in laboratory studies when compared to other photosynthetic or mixotrophic dinoflagellates was not particularly low. *A. poporum* revealed to be more represented in the field when the concentrations of nitrite and nitrate, silicate, and chlorophyll a were low and the transparency was high. These parameters correspond to a reduced trophic state. This suggests that *A. poporum* use these reduced trophic states as windows of opportunity to thrive and survive in a eutrophic environment.

5.2 Keywords

Azadinium poporum, Shiwha bay, growth, tolerance, temperature, salinity, light, pH, dissolved oxygen, nutrients, chlorophyll a

5.3 Introduction

Investigations of the factors that account for the population dynamics and the spatial distribution of phytoplankton in aquatic systems often focus on growth responses. Growth and related metabolic activities are typically dependent on various environmental factors. Among these factors, temperature, salinity, light, and nutrients might affect dinoflagellate growth (Flynn *et al*. 1996, Parkhill & Cembella 1999, Hwang & Lu 2000, Maclean *et al*. 2003, Hu *et al*. 2006, Gedaria *et al*. 2007, Lartigue *et al*. 2009, Xu *et al*. 2010).

The temperature will influence the enzymatic activity of microalgae. The enzymes have an optimal functional temperature under which the speed reaction are slower and over which the enzymes degrade more quickly (Grzebyk & Séchet 2003). Therefore, the temperature is a factor having a significant effect on growth until the reach of an optimum (Nielsen 1996, Matsubara *et al*. 2007, Xu *et al*. 2010, Laabir *et al*. 2011).

Unfavorable salinities to microalgae will affect enzymatic activity by modifying the energetic consumption allocated to osmotic regulation (Grzebyk & Séchet 2003). Therefore, the salinity will have an effect on the cellular metabolism and growth. The euryhaline estuarine species and the marine coastal species have a large tolerance to salinity variation (Taylor & Pollingher 1987, Grzebyk *et al*. 2003, Nagasoe *et al*. 2006, Matsubara *et al*. 2007, Laabir *et al*. 2011). However, some marine species are stenohaline and can be sensible to

salinity variation (Kim *et al*. 2004a).

The photosynthetic dinoflagellate species can adapt quickly to variations of light intensities. For example, they can, at low light intensity, increase their size and/or number of photosynthetic units (Smayda 1997). This factor is the one that affect the most the nutrition of microalgae. An insufficient light reduced or stop the growth (Grzebyk & Séchet 2003, Paz *et al*. 2006).

Nutritional factors are of high relevance in the determination of the dynamics of growth. Dinoflagellates respond differently to various nutrients as well as their concentrations. The diversity of responses is partly responsible of the species dynamics in the field.

The population dynamics of the species of the genus *Azadinium* is not well known. These species apparently seem to either keep a low density such as *A. caudatum* which was not observed exceeding 1.3 cells L^{-1} (Nézan *et al*. 2012), while others are able to bloom such as *A.* cf. *spinosum* and reached up to 9.03×10^3 cells mL^{-1} (Akselman & Negri 2012). The survey of *A. poporum* by qPCR (quantitative polymerase chain reaction) revealed that the species is always in low concentration in Shiwha bay (Potvin *et al*. 2013). The reasons resulting in such dynamics are unknown.

In order to determine the factors implicated in the low abundance of *A. poporum*, we explored the trends of various factors in the field, the effect of environmental factors such as temperature, salinity, and light on the growth, as well as the distribution of the species in relation to various abiotic and biotic factors. The results of the present study provide a basis to understand the effects

of environmental factors on the dynamics of *Azadinium* spp. in a highly eutrophic area.

5.4 Materials and methods

5.4.1 Study area

Shiwha bay was created artificially by the reclamation of an intertidal flat on the west coast of Korea from December 1986 to January 1994. This saline bay was expected to transform into a freshwater body and to be used for irrigation purposes. However, the drainage structure of the bay did not allow the entrapment of the Yellow Sea water and the full replacement by freshwater from its hinterland. Eutrophication progressed due to untreated sewage and wastewater flowing in from Shiwha adjacent area (Kim *et al*. 2004b). The severe deterioration of the water quality in the middle of the 90s prompted a more pronounced monitoring of the bay in order to assess the environmental impacts (Park *et al*. 2003, Yoo *et al*. 2009)

5.4.2 Field data

Water samples were obtained at least at monthly intervals in ice-free conditions from January 2009 to December 2011 in Shiwha bay, Korea, at different stations (Potvin *et al*. 2013). Temperature and salinity were measured using a YSI pH-meter (model 63-10FT) with a detection limit of 0.1 and 0.1, respectively. pH and DO were measured using a Handylab pH 11 (Schott Instruments, Mainz, Germany) and a Oxi 197i (WTW GmbH, Weilheim, Germany), respectively. The Secchi depth was measured using a Secchi disk. Water samples for analyzing nutrient concentrations were gently filtered through

GF/F filters and stored frozen at -20 °C until the concentrations of ammonium (NH_4^+), nitrate plus nitrite ($NO_3^- + NO_2^-$), phosphate (PO_4^{3-}), and silicate (SiO_3^{2-}) were measured using a nutrient auto-analyzer system (Quattro; Seal Analytical Gmbh, Norderstedt, Germany). The chlorophyll a was measured as in APHA (1995). The correlation coefficients between various physical, chemical, and biological properties were calculated using Pearson's correlation (Conover 1980, Zar 1999).

5.4.3 Maintenance of the experimental organism

A. poporum was isolated from surface sediment samples from Shiwha bay, an highly eutrophic bay from Korea (37° 18' N, 126° 36' E) as in Potvin *et al*. (2012) and cultivated in F/2 medium-Si (Guillard & Ryther 1962) in a growth chamber at 20 °C under an illumination of 20 μE m^{-2} s^{-1} of cool white fluorescent light on a 14:10 h light-dark cycle.

5.4.4 Effect of temperature, salinity, and light on growth

In order to determine the effect of temperature on growth, *A. poporum* was cultured at different temperatures (11, 12, 13, 14, 15, 20, 23, 25, 27, 30 °C), while the irradiance was kept at 20 μE m^{-2} s^{-1} of cool white fluorescent light on a 14:10 h light: dark cycle and the salinity kept at 31±1.

To determine the effect of salinity on growth, *A. poporum* was cultured at different salinities (10, 15, 20, 25, 30, 35, 40, 45, 50), while the irradiance was kept at 20 μE m^{-2} s^{-1} of cool white fluorescent light on a 14:10 h light: dark cycle and the temperature kept at 20±1 °C.

To assess the effect of light on growth, *A. poporum* was cultured at different irradiances (0, 5, 10, 20, 50, 100, 200, 300 µE m^{-2} s^{-1}) of cool white fluorescent light on a 14:10 h light: dark cycle, while the temperature was kept at 20±1 °C and the salinity at 31±1. Bottles were wrapped with aluminum foil for darkness and with layers of neutral density filter (fiberglass mesh) to set the proper light intensity.

A stock culture was adapted in F/2 medium-Si for at least 2 generations. Thereafter, the stock culture was diluted every second day with new F/2 medium-Si of the respective temperature and salinity keeping the cells in exponential growth phase. The last generation, obtained within a week, was used as inoculum for the experiments.

The following formula, modified from Lenderman and Tett (Lenderman & Tett 1981) was used to describe the relationship between growth rate and irradiance:

$$\mu = \mu_{max} (I-I_0) / (K_s-I_0) + (I-I_0)$$

where μ_{max} is the maximum growth rate (d^{-1}), I is the irradiance (µE m^{-2} s^{-1}), I_0 is the compensation irradiance (µE m^{-2} s^{-1}), and K_s is the irradiance sustaining half the maximum growth rate. Data were iteratively fitted to the model using DeltaGraph® (Delta Point).

All experiments were carried out in polycarbonate bottles (500 mL) in standing condition. Each experiment was initiated by the inoculation of about

1000 to 2500 cells mL^{-1} (final concentration) and allowed to run for 6 to 8 d. Subsamples (37.5 mL) were taken for the enumeration of phytoplankton cells every second day. After subsampling, the bottles were refilled to capacity with F/2 medium-Si of the respective salinity and temperature. The condition of *A. poporum* was assessed using a stereomicroscope (Olympus, SZX-12, Japan) before and after each subsampling. Experiments were carried out in triplicate, and data from each replicate were the mean of at least 3 growth rates (4 sampling dates).

For enumeration of cells, subsamples were fixed in Lugol's solution (5 % final concentration). The abundances were determined by counting all or >300 cells in 3 1-mL Sedgwick-Rafter chambers (SRCs). The specific growth rate, μ (d^{-1}), was calculated as:

$$\mu = [\mathrm{Ln}\ (C_t/C_0)] / t$$

where C_0 and C_t = the concentrations of *A. poporum* in exponential growth at the previous and last subsampling date, respectively; t = time elapse during the subsampling interval. The dilution produced after subsampling was considered in the measurements of growth rates.

Irradiance was measured initially during the setting of the experiments using a LI-COR LI-1400 radiation sensor equipped with a LI-COR Quantum flat probe (model Q 39265). The temperature was monitored daily. The salinity was measured at the beginning and every second day during subsampling. The temperature was measured with a standard thermometer and the salinity was measured using a YSI pH-meter (model 63-10FT).

5.4.5 Occurrence

Data on the occurrence of *A. poporum* were obtained from Shiwha bay, Korea (from 2009 to 2011) by qPCR as in Potvin *et al*. (2013).

5.5 Results

5.5.1 Field

Through the three years survey of Shiwha bay, some parameters such as the temperature, the salinity, the phosphate, and to some extent the nitrite and nitrate, the silicate, and the chlorophyll a showed similarity in there seasonal variability (Fig. 5.1). An increased in the input of nitrite and nitrate as well as silicate in the bay was observed through the years (Fig. 5.1). These increases of input were also associated with an increase of chlorophyll a (Fig. 5.1). No clear tendency was observed for the pH, the dissolved oxygen, the Secchi depth, and the ammonium concentration (Fig. 5.1).

Many parameters were significantly correlated to each other in Shiwha bay (Table 5.1). The chlorophyll a which is a proxy for phytoplankton biomass showed a strong correlation with the salinity (r=0.606), the nitrite and nitrate concentration (r=0.650), as well as the silicate concentration (r=0.448). The phytoplankton biomass appears to decrease with the increase of salinity, while it appears to increase with the increase of the nutrients mentioned above.

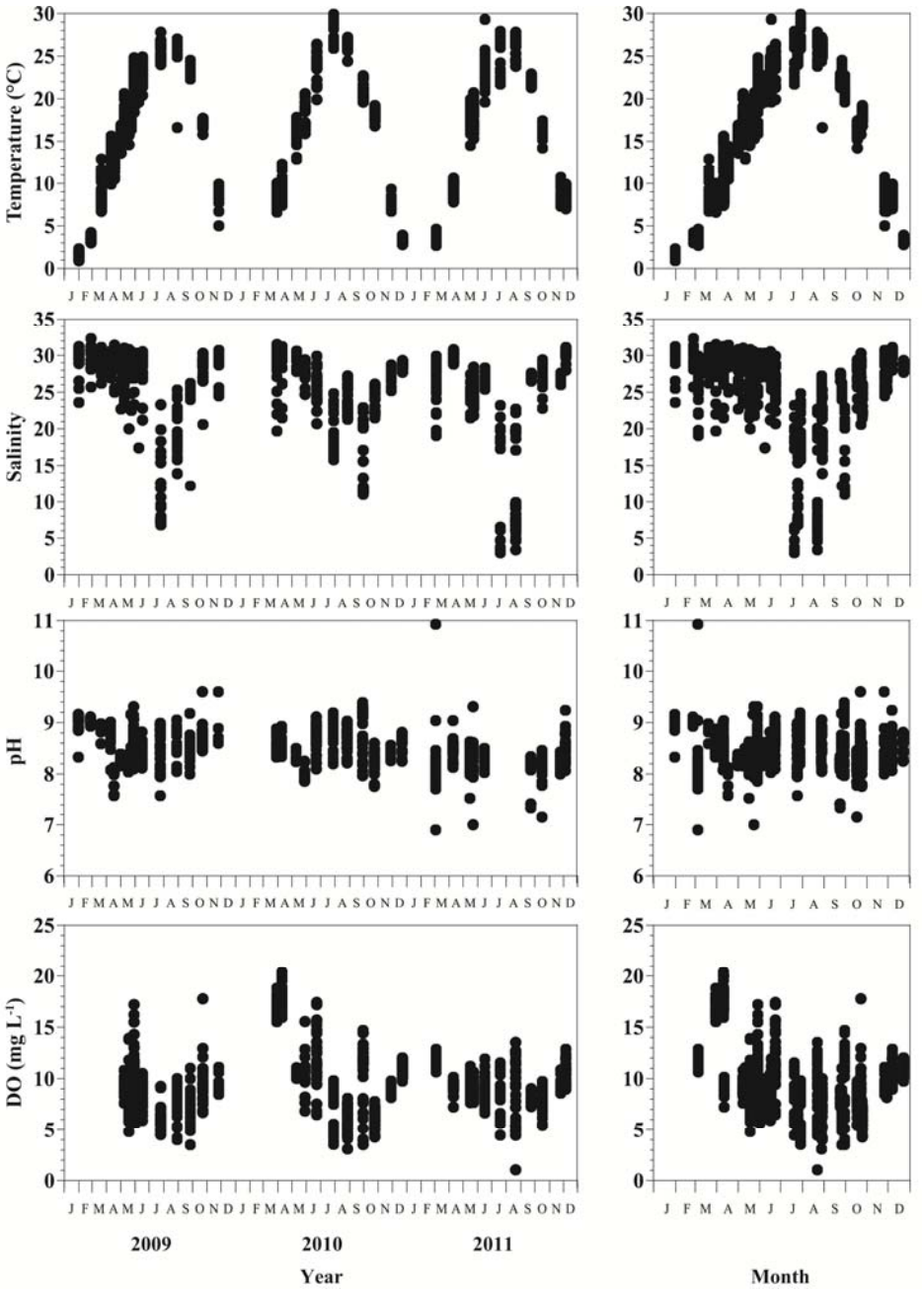

Fig. 5.1 Variation of physical and chemical parameters in Shiwha bay, Korea, from 2009 to 2011 (left) and integrated values through the year (right). The presence of ice prevented sampling in some months. DO: dissolved oxygen, SD: Secchi depth, NH_4^+: ammonium, NO_2^-+NO_3^-: nitrite and nitrate, PO_4^{3-}: phosphate, SiO_3^{2-}: silicate, Chl-a: chlorophyll a

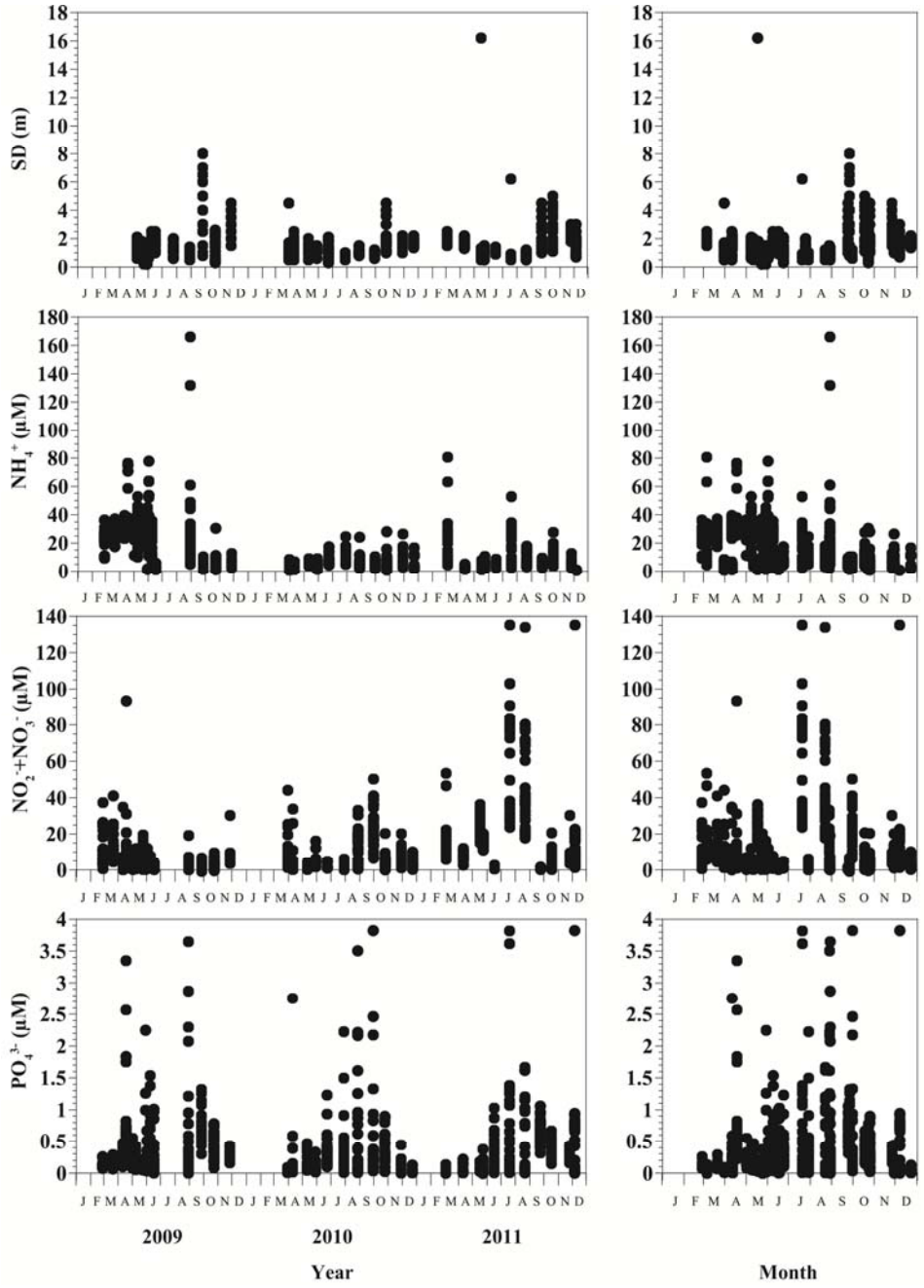

Fig. 5.1 (continued)

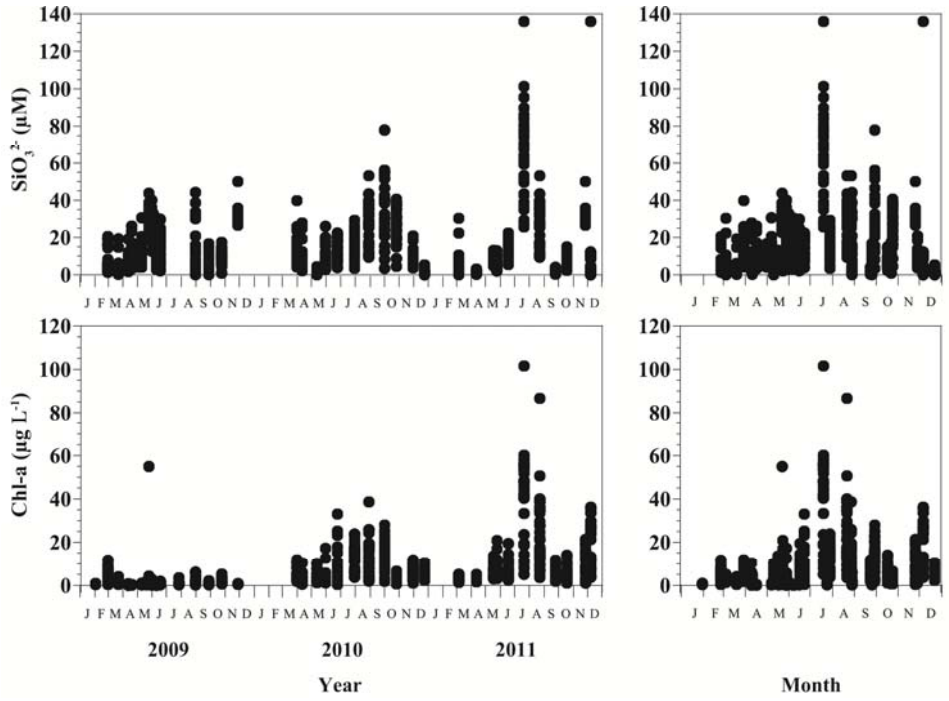

Fig. 5.1 (continued)

Table 5.1 Pearson correlation coefficient matrix (absolute value) between physical and chemical properties of Shiwha bay, Korea, from January 2009 to December 2011

T: temperature, S: salinity, DO: dissolved oxygen, SD: Secchi depth, NH_4^+: ammonium, NO_2^-+NO_3^-: nitrite and nitrate, PO_4^{3-}: phosphate, SiO_3^{2-}: silicate, Chl-a: chlorophyll a

Component	T	S	pH	DO	SD	NH_4^+	NO_2^-+NO_3^-	PO_4^{3-}	SiO_3^{2-}	Chl-a
T	-	0.572**	0.038	0.442**	0.269**	0.017	0.232**	0.239**	0.339**	0.240**
S		-	0.106**	0.163**	0.307**	0.150**	0.689**	0.152**	0.537**	0.606**
pH			-	0.114**	0.085*	0.035	0.019	0.090**	0.035	0.080**
DO				-	0.134**	0.178**	0.008	0.351**	0.146**	0.128**
SD					-	0.114**	0.222**	0.155**	0.119**	0.225**
NH_4^+						-	0.072*	0.091**	0.052	0.244**
NO_2^-+NO_3^-							-	0.153**	0.634**	0.650**
PO_4^{3-}								-	0.281**	0.001
SiO_3^{2-}									-	0.448**
Chl-a										-

Significance level: *p<0.05, **p<0.01

5.5.2 Effect of temperature, salinity, and light on growth

A. poporum was able to grow from 11 °C to 30 °C (Fig. 5.2), but died at 10 °C and 31 °C. The growth increased linearly from 11 °C until it reached its optimum at 25 °C and decreased thereafter. The maximum growth obtained was 0.635 d^{-1}.

A. poporum was able to grow from a salinity of 10 to 50 (Fig. 5.2), but died at 9 and 51. The growth increased in general logarithmically from a salinity of 10 until it reached its optimum at 35 (Fig. 5.2) and decreased thereafter, but at a quicker rate than the increase. The maximum growth obtained was 0.461 d^{-1}.

A. poporum did not grow in darkness. The growth rate of *A. poporum* rapidly increased between 5 and 50 μE m^{-2} s^{-1}, but became saturated at higher intensities (Fig. 5.3). When the data were fitted to the modified formula from Lenderman and Tett, the maximum growth rate of *A. poporum* was 0.53 d^{-1}, the K_s (the irradiance sustaining half the maximum growth rate) was 4.0 μE m^{-2} s^{-1}, and the compensation irradiance (when net growth = 0) was 0.38 μE m^{-2} s^{-1}.

5.5.3 Occurrence

A. poporum occurred in various conditions in regards of the temperature, salinity, pH, dissolved oxygen, Secchi deph, ammonium concentration, nitrite and nitrate concentration, phosphate concentration, silicate concentration, and chlorophyll a concentration (Fig. 5.4). The abundance based on qPCR was strongly correlated with nitrite and nitrate concentration (r=0.530) as well as phosphate concentration (r=0.541), while it was only moderately correlated with the Secchi

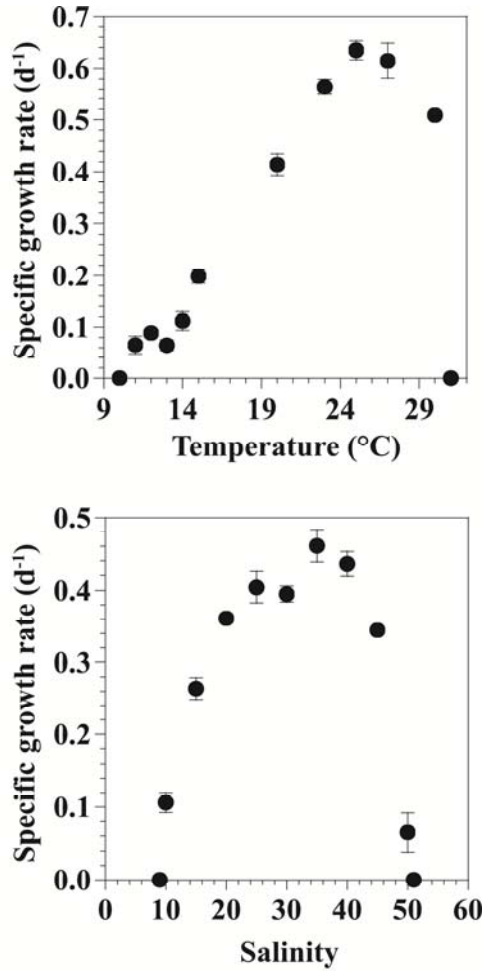

Fig. 5.2 *Azadinium* cf. *poporum*. Specific growth rates (d^{-1}) obtained when the species was adapted to various temperatures and salinities. Symbols represent treatment means ± 1 SE (n=3). No growth was observed at the extreme values of temperature and salinity. The conditions providing no growth were determined twice with the same strain.

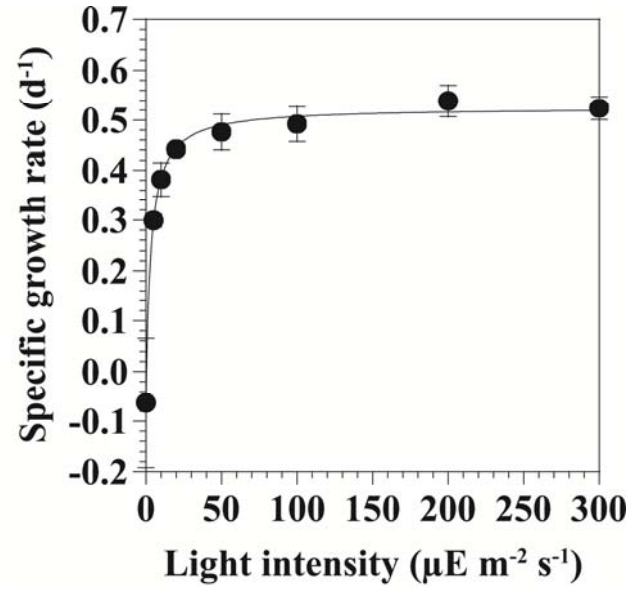

Fig. 5.3 Specific growth rates (GR) of *Azadinium poporum* at 8 different light intensities. Symbols represent treatment means ± 1 SE (n=3). The curve was fitted to the modified formula of Lenderman and Tett using all treatments in the experiment. GR (d^{-1}) = (0.53*(x-0.38)) / ((4.0-0.38) + (x-0.38)), r^2 = 1.00

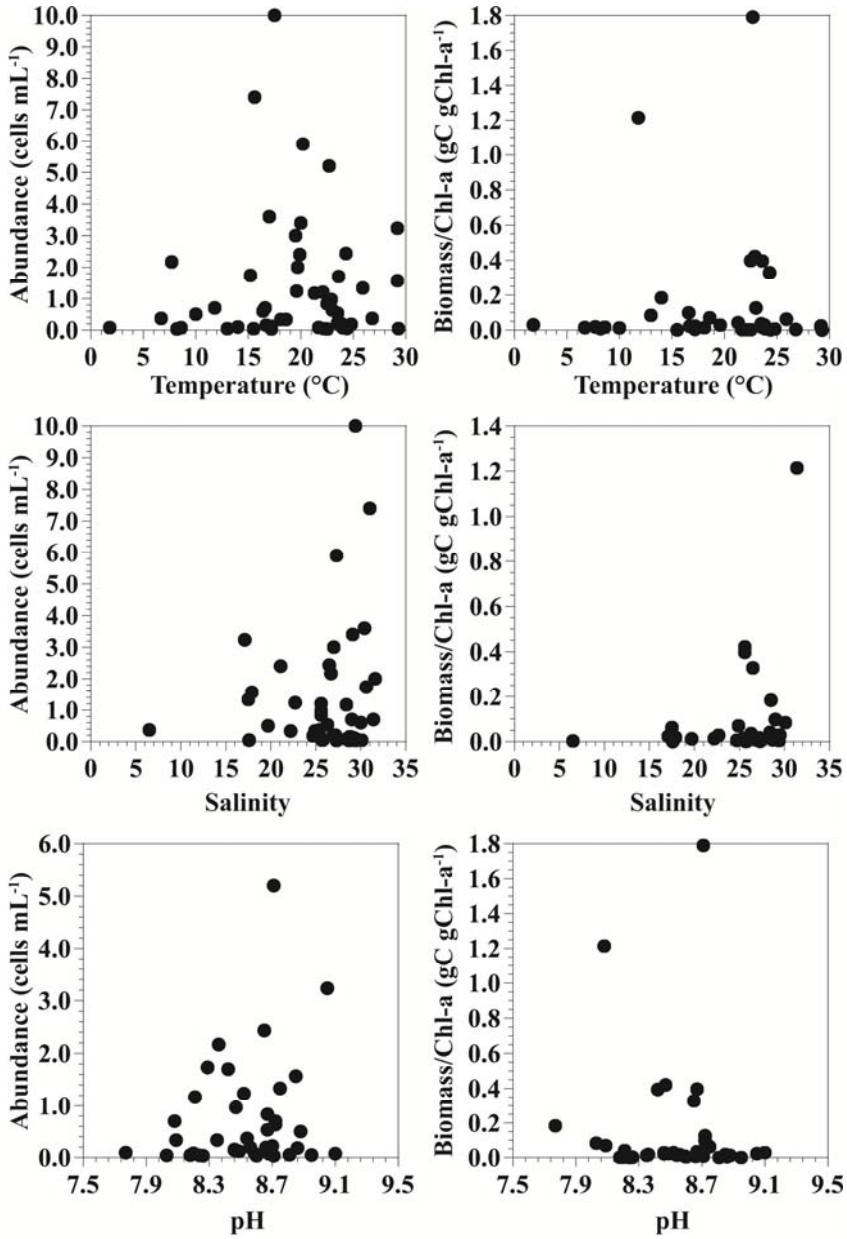

Fig. 5.4 Physical and chemical parameters in relation with the abundance of *Azadinium poporum* based on qPCR and the ratio of biomass of *A. poporum* to Chl-a. Data were obtained from Shiwha bay, Korea (from 2009 to 2011), and the West coast of Korea (from 2007-2012). The linear regression present in some graphs are significant ($p<0.05$). DO: dissolved oxygen, SD: Secchi depth, NH_4^+: ammonium, NO_2^-+NO_3^-: nitrite and nitrate, PO_4^{3-}: phosphate, SiO_3^{2-}: silicate, Chl-a: chlorophyll a.

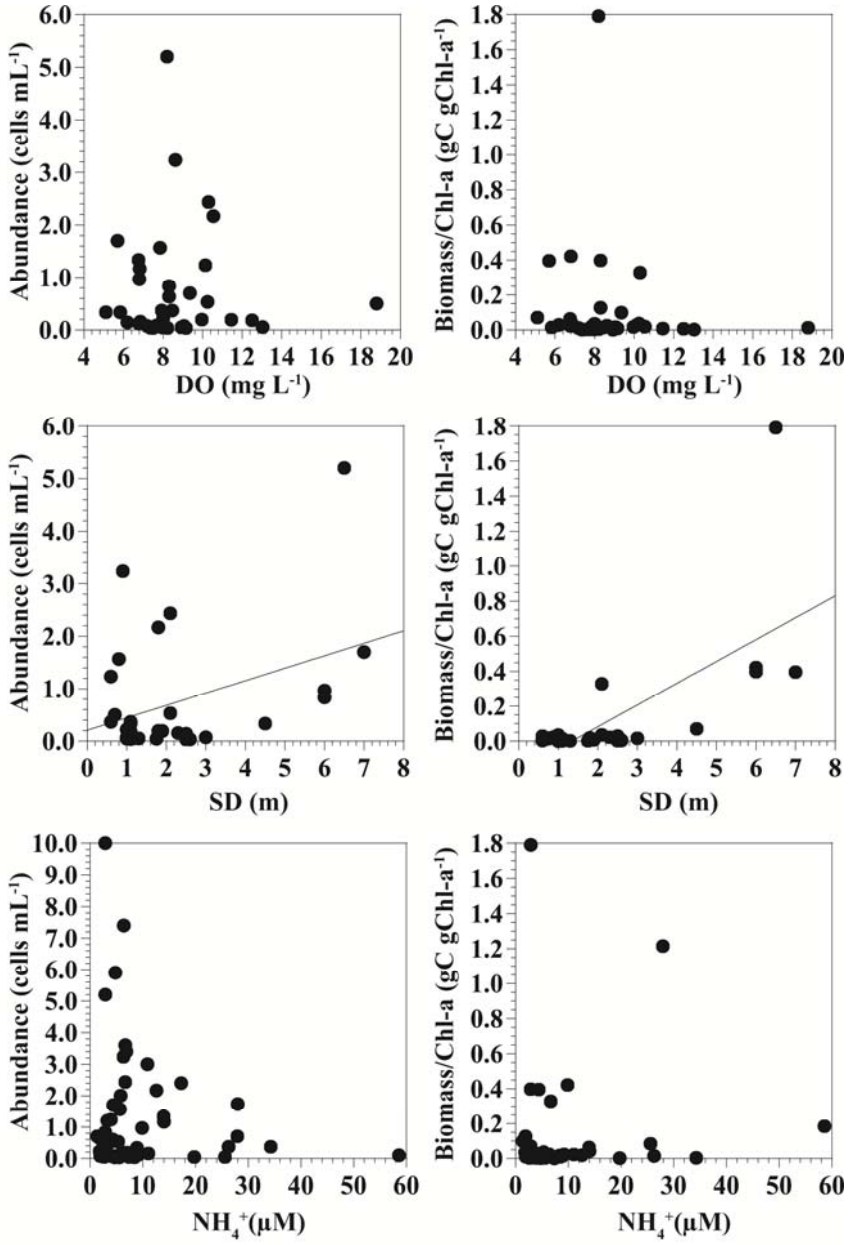

Fig. 5.4 (continued)

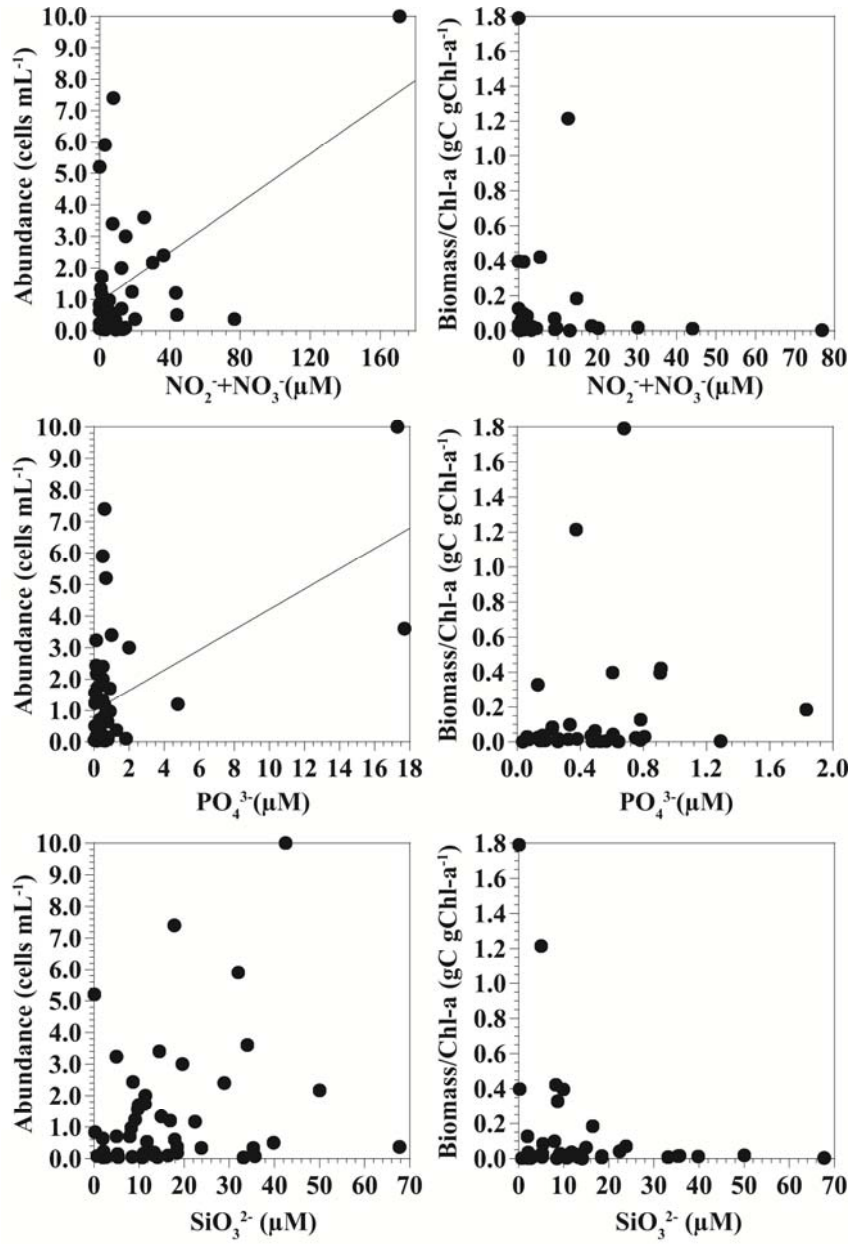

Fig. 5.4 (continued)

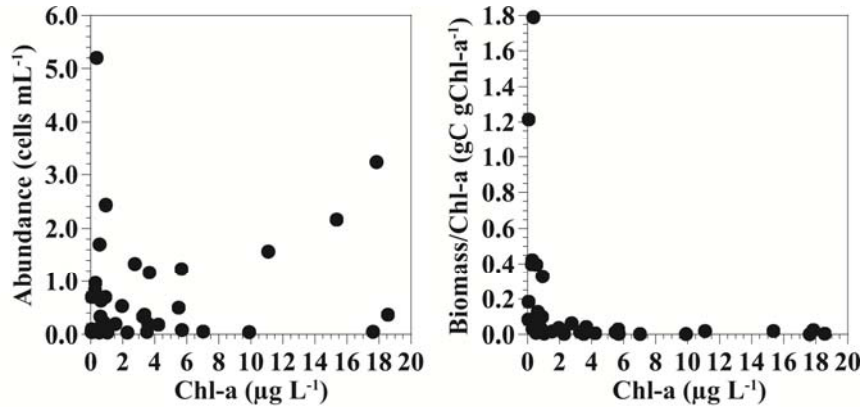

Fig. 5.4 (continued)

depth (r=0.370; Table 5.2). Extreme values of nitrite and nitrate as well as phosphate concentrations might have bring bias to the relationships found.

The representation of *A. poporum* within the community, here defined as the ratio of the biomass in carbon of *A. poporum* to the measure of chlorophyll a in the field, is only strongly correlated to the Secchi deph (r=0.673; Table 5.2). The highest values of representation of *A. poporum* were in general in the lowest values of ammonium concentration, nitrite and nitrate concentration, silicate concentration, and chlorophyll a concentration as well as the highest values of Secchi depth.

5.6 Discussion

In order to determine the causes explaining the dynamics of *A. poporum* in Shiwha bay, the tendencies through time of some parameters such as the temperature, the salinity, the pH, the dissolved oxygen, the Secchi depth, the concentration of nutrients, and the concentration of chlorophyll a were assessed. The effects of temperature, salinity, and light on the growth of *A. poporum* in laboratory as well as the relationships between environmental parameters and *A. poporum* in the field were assessed.

The species revealed to grow on a wide range of temperature characterizing the species as eurytherm. Therefore, the species was generally well adapted to the high variability observed in Shiwha bay. However, *A. poporum* was not able to grow below 10 °C implying that the vegetative cells of *A. poporum* cannot overwinter in Shiwha bay. This is corroborated by the low occurrence of *A. poporum* below 10 °C. Gu *et al*. (2013) observed cysts in cultures of *A. poporum*.

Table 5.2 Pearson correlation coefficients (absolute value) between *Azadinium poporum* (concentration and representation) and physical/chemical properties of Shiwha bay, Korea, from January 2009 to December 2011

T: temperature, S: salinity, DO: dissolved oxygen, SD: Secchi depth, NH_4^+: ammonium, NO_2^-+NO_3^-: nitrite and nitrate, PO_4^{3-}: phosphate, SiO_3^{2-}: silicate, Chl-a: chlorophyll a

Component	*Azadinium poporum*	Representation
		Ratio of *A. poporum* carbon content to Chl-a
T	0.036	0.009
S	0.141	0.247
pH	0.195	0.096
DO	0.017	0.100
SD	0.370*	0.673**
NH_4^+	0.159	0.068
NO_2^-+NO_3^-	0.530**	0.146
PO_4^{3-}	0.541**	0.152
SiO_3^{2-}	0.236	0.271
Chl-a	0.178	0.258

Significance level: *p<0.05, **p<0.01

Thus, it is likely that the species resist to low temperature in the form of cyst.

A. poporum possessed a relatively wide salinity tolerance indicating that that the species is euryhaline and able to adapt to broad fluctuations of salinity particularly occurring during wet season.

The requirements for irradiance are different among phytoplankton (Table 5.3). The compensation irradiance (I_0) and the half-saturation light intensity (K_s) of *A. poporum* are among the lowest suggesting that the species is acclimated to low light. The intermediate competition coefficient (α) of *A. poporum* suggests that the species is also fairly competitive in regards of light.

Despite the high tolerance of *A. poporum* in regards of the temperature and salinity, the relatively high growth obtained in laboratory studies when compared to other photosynthetic or mixotrophic dinoflagellates (Kondo *et al*. 1990, Hansen & Nielsen 1997, Yamaguchi *et al*. 1997, Yamamoto & Tarutani 1997, Hansen 2002, Jeong *et al*. 2005d, Nagasoe *et al*. 2006, Navarro *et al*. 2006, Richardson *et al*. 2006, Hansen *et al*. 2007, Matsubara *et al*. 2007, Baek *et al*. 2008, Jeong *et al*. 2010b; Fig. 5.5), and the competitive advantage of *A. poporum* in regards of light, the abundances of *A. poporum* from the field are low. Furthermore, *A. poporum* appears to behave at the opposite of the general phytoplankton biomass of Shiwha bay by being more represented in the field in low concentration of nitrite and nitrate as well as silicate. In addition, *A. poporum* revealed to be more represented in the field when the phytoplankton biomass was low and the transparency was high. These parameters correspond to a reduced trophic state. This suggests that *A. poporum* use these reduced trophic states as windows of opportunity to thrive and survive in eutrophic environment.

Table 5.3 Compensation irradiance (I_0, μE m^{-2} s^{-1}), half-saturation light intensity (K_s, μE m^{-2} s^{-1}) and competition coefficient (α) reported for phytoplankton

Species	I_0	K_s	α (μ_m/K_s)	Reference
Azadinium poporum	0.38	4.0	0.13	This study
Karenia mikimotoi	0.7	110	-	Yamaguchi & Honjo (1989)
Chattonella antiqua	10.3	110	-	Yamaguchi *et al*. (1991)
Chattonella marina	10.5	110	-	Yamaguchi *et al*. (1991)
Alexandrium tamarense	76	90	-	Yamamoto & Tarutani (1997)
Cochlodinium polykrikoides	10.38	90	0.01	Kim *et al*. (2004a)
Gyrodinium instriatum	10.61	70	0.01	Nagasoe *et al*. (2006)
Akashiwo sanguinea	14.4	114	0.01	Matsubara *et al*. (2007)
Prorocentrum donghaiense	0.1	30	0.26	Xu *et al*. (2010)
Phaeocystis globosa	0.5	60	0.10	Xu *et al*. (2010)
Pseudo-nitzschia pungens	0.1	90	0.35	Xu *et al*. (2010)

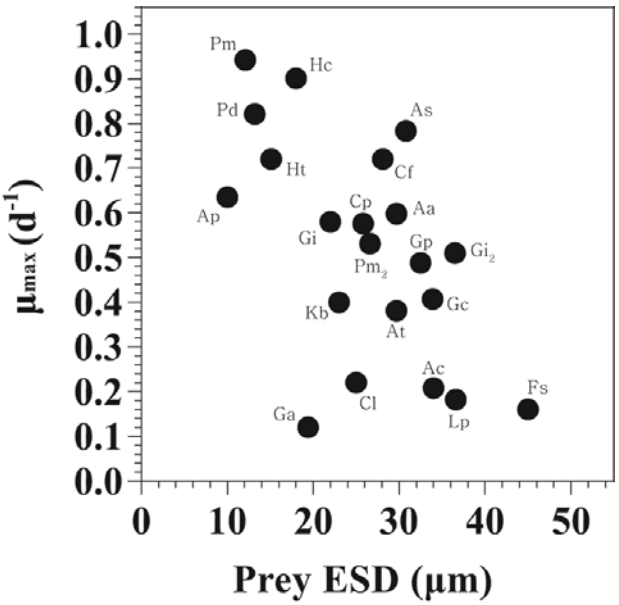

Fig. 5.5 Maximum growth rate of photosynthetic or mixotrophic dinoflagellate species when growing photosynthetically. ESD: Equivalent spherical diameter (μm), μ_{max}: maximum growth rate (d^{-1}). Temperature effect was not considered because optimal temperature for each dinoflagellate species is different from the other. Pm: *Prorocentrum minimum*, Pd: *Prorocentrum donghaiense*, Ht: *Heterocapsa triquetra*, Hc: *Heterocapsa circularisquama*, Ga: *Gymnodinium aureolum*, Gi: *Gymnodinium impudicum*, Kb: *Karenia brevis*, Cl: *Ceratium lineatum*, Cp: *Cochlodinium polykrikoides*, Pm_2: *Prorocentrum micans*, Cf: *Ceratium furca*, Aa: *Alexandrium affine*, At: *Alexandrium tamarense*, As: *Akashiwo sanguinea*, Gp: *Gonyaulax polygramma*, Gc: *Gymnodinium catenatum*, Ac: *Alexandrium catenella*, Gi_2: *Gyrodinium instriatum*, Lp: *Lingulodinium polyedrum*, Fs: *Fragilidium subglobosum*.

The apparent increased of nitrite and nitrate as well as silicate inputs were associated with an increase of phytoplankton biomass in Shiwha bay from 2009 to 2011. The operation of the Shiwha bay tidal power plant beginning in 2011 will enhance the exchange between Shiwha bay and the Yellow Sea and is likely to change the dynamics of Shiwha bay. Further monitoring is required to determine how these changes will affect the dynamics of *A. poporum*.

.

Conclusion

Shiwha bay, Korea, is a eutrophic bay with frequent blooms occurring through the year. While the bay is generally considered eutrophic, its state varies through the year. The azaspiracid producer *Azadinium poporum* was found in Shiwha bay. The species generally occurs in low concentrations in the field. These concentrations are usually too low to alter the dynamics of predators and predation itself is unlikely to be the main factor responsible of the dynamics of *A. poporum*. The higher representation of *A. poporum* in a reduced trophic state, particularly when the biomass of phytoplankton and the concentration of nutrients such as nitrite and nitrate in the field is low, suggests that *A. poporum* might be outcompeted by other phytoplankton species when the biomass is important. Therefore, a deeper understanding of factors affecting the competition between species such as allelopathy and cell contact is desirable. The low nutrients concentrations present in these low trophic states might not be sufficient to enable high growth and further explained the low concentrations obtained in the field. On this aspect, further investigations are required to determine the effect of nutrients on the growth of *A. poporum*. Knowledge on these additional factors is likely to bring a better understanding of the dynamics of the species in the field.

Bibliography

Adachi M, Sako Y, Ishida Y (1996) Analysis of *Alexandrium* (Dinophyceae) species using sequences of the 5.8S ribosomal DNA and internal transcribed spacer regions. J Phycol 32: 424-432

Adachi M, Sako Y, Ishida Y (1997) Analysis of *Gymnodinium catenatum* Dinophyceae using sequences of the 5.8S rDNA-ITS Regions and Random Amplified Polymorphic DNA. Fisheries Sci 63: 701-707

Adolf JE, Krupatkina D, Bachvaroff T, Place AR (2007) Karlotoxin mediates grazing by *Oxyrrhis marina* on strains of *Karlodinium veneficum.* Harmful Algae 6: 400-412

Akselman R, Negri RM (2012) Blooms of *Azadinium* cf. *spinosum* Elbrächter *et* Tillmann (Dinophyceae) in northern shelf waters of Argentina, Southwestern Atlantic. Harmful Algae 19: 30-38

Alfonso A, Vieytes MR, Ofuji K, Satake M, Nicolaou KC, Frederick MO, Botana LM (2006) Azaspiracids modulate intracellular pH levels in human lymphocytes. Biochem Biophys Res Commun 346: 1091-1099

Álvarez G, Uribe E, Ávalos P, Mariño C, Blanco J (2010) First identification of azaspiracid and spirolides in *Mesodesma donacium* and *Mulinia edulis* from northern Chile. Toxicon 55: 638-641

Amzil Z, Sibat M, Royer F, Savar V (2008) First report on azaspiracid and yessotoxin groups detection in French shellfish. Toxicon 52: 39-48

Anderson DM, White AW (1992) Marine biotoxins at the top of the food chain. Oceanus 35: 55-61

APHA (American Public Health Association) (1995) Standard methods for the examination of water and wastewater. 19th ed. APHA, Washington

Baden DG (1983) Marine food-borne dinoflagellate toxins. Int Rev Cytol 82: 99-150

Baek SH, Shimode J, Kikuchi T (2008) Growth of dinoflagellates, *Ceratium furca* and *Ceratium fusus* in Sagami bay, Japan: the role of temperature, light intensity and photoperiod. Harmful algae 7:163-173

Bagnis R, Chanteau S, Chungue E, Hurtel JM, Yasumoto T, Inoue A (1980) Origins of ciguatera fish poisoning: a new dinoflagellate, *Gambierdiscus toxicus* Adachi and Fukuyo, definitively involved as a causal agent. Toxicon 18: 199-208

Berdalet E (1992) Effects of turbulence on the marine dinoflagellate *Gymnodinium nelsonii*. J Phycol 28: 267-272

Berdalet E, Peters F, Koumandou VL, Roldan C, Guadayol O, Estrada M (2007) Species-specific physiological response of dinoflagellates to quantified small-scale turbulence. J Phycol 43: 965-977

Besiktepe S, Dam HG (2002) Coupling of ingestion and defecation as a function of diet in the calanoid copepod *Acartia tonsa.* Mar Ecol Prog Ser 229: 151-164

Blossom H, Daugbjerg N, Hansen PJ (2012) Toxic mucus traps: a novel mechanism that mediates prey uptake in the mixotrophic dinoflagellate *Alexandrium pseudogonyaulax*. Harmful Algae 17: 40-53

Bourdelais AJ, Tomas CR, Naar J, Kubanek J, Baden DG (2002) New fish-killing alga in coastal Delaware produces neurotoxins. Environ Health Pers 110: 465-470

Braña Magdalena A, Lehane M, Krys S, Fernandez ML, Furey A, James KJ (2003) The first identification of azaspiracids in shellfish from France and Spain. Toxicon 42: 105-108

Broglio E, Jónasdóttir SH, Calbet A, Jakobsen HH, Saiz E (2003) Effect of heterotrophic versus autotrophic food on feeding and reproduction of the calanoid copepod *Acartia tonsa*: relationship with prey fatty acid composition. Aquat Microb Ecol 31: 267-278

Brombacher S, Edmonds S, Volmer DA (2002) Studies on azaspiracid biotoxins. II. Mass spetral behavior and structural elucidation of azaspiracid analogs. Rapid Commun. Mass Spectrom 16: 2306-2316

Brownlee DC, Jacobs F (1987) Mesozooplankton and microzooplankton in the Chesapeake bay. In: Majumdar SK, Hall LW Jr, Austin HM (eds) Contaminant problems and management of living Chesapeake bay resources. The Pennsylvania Academy of Science, Easton, PA, pp. 217-269

Burkholder JM, Glasgow HB, Hobbs CW (1995) Fish kills linked to a toxic ambush-predator dinoflagellate: distribution and environmental considerations. Mar Ecol Prog Ser 124: 43-61

Calbet A, Vaqué D, Felipe J, Vila M, Sala MM, Alcaraz M, Estrada M (2003) Relative grazing impact of microzooplankton and mesozooplankton on a bloom of the toxic dinoflagellate *Alexandrium minutum*. Mar Ecol Prog Ser 259: 303-309

Cembella AD, Lewis NI, Quilliam MA (2000) The marine dinoflagellate *Alexandrium ostenfeldii* (Dinophyceae) as the causative organism of spirolide shellfish toxins. Phycologia 39: 67-74

Cembella AD (2003) Chemical ecology of eukaryotic microalgae in marine ecosystems. Phycologia 42: 420-447

Chen B, Liu H, Lau MTS (2010) Grazing and growth responses of a marine oligotrichous ciliate fed with two nanoplankton: does food quality matter for micrograzers? Aquat Ecol 44: 113-119

Choi JK, Shim JH (1986a) The ecological study of phytoplankton in Kyeonggi bay, Yellow Sea I. Environmental characteristics. Journal of the Korean Society of Oceanography 21: 56-71

Choi JK, Shim JH (1986b) The ecological study of phytoplankton in Kyeonggi bay, Yellow Sea. III. Phytoplankton composition, standing crops, tychopelagic plankton. Journal of the Korean Society of Oceanography 21: 156-170

Choi JK, Lee EH, Noh JH, Huh SH (1997) The study on the phytoplankton bloom and primary productivity in lake Shihwa and adjacent coastal areas. The Sea, Journal of the Korean Society of Oceanography 2: 78-86

Cohen JH, Tester PA, Forward RB Jr (2007) Sublethal effects of the toxic dinoflagellate *Karenia brevis* on marine copepod behavior. J Plankton Res 29: 301-315

Coleman AW, Mai JC (1997) Ribosomal DNA ITS-1 and ITS-2 sequence comparisons as a tool for predicting genetic relatedness. J Mol Evol 45: 168-177

Colman JR, Twiner MJ, Hess P, McMahon T, Satake M, Yasumoto T, Doucette GJ, Ramsdell JS (2005) Teratogenic effects of azaspiracid-1 identified by microinjection of Japanese medaka (*Oryzias latipes*) embryos. Toxicon 45: 881-890

Conover D (1980) Practical nonparametric statistics. 2nd ed. John Wiley and Sons, New York, 493 p.

De Schrijver K, Maes I, De Man L, Michelet J (2002) An outbreak of diarrhoeic shellfish poisoning in Antwerp, Belgium. Euro Surveill 7: 138-141

Diaz Sierra M, Furey A, Hamilton B, Lehane M, James KJ (2003) Elucidation of the fragmentation pathways of azaspiracids, using electrospray ionisation, hydrogen/deuterium exchange, and multiple-stage mass spectrometry. J Mass Spectrom 38: 1178-1186

Dickey RW, Borzin SC, Faulkner DJ, Bencsath FA, Andrzejewski D (1990) Identification of okadaic acid from a Caribbean dinoflagellate, *Prorocentrum concavum.* Toxicon 28: 371-377

Doblin MA, Blackburn SI, Hallegraeff GM (1999) Comparative study of selenium requirements of three phytoplankton species: *Gymnodinium catenatum*, *Alexandrium minutum* (Dinophyta) and *Chaetoceros* cf. *tenuissimus* (Bacillariophyta). J Plankton Res 21: 1153-1169

ECOHAB (1995) The ecology and oceanography of harmful algal blooms. A national research agenda. Woods Hole Oceanographic Institute, Woods Hole, MA. pp. 1-66

Elgarch A, Vale P, Rifai S, Fassouane A (2008) Detection of diarrheic shellfish poisoning and azaspiracid toxins in Moroccan mussels: comparison of the LC-MS method with the commercial immunoassay kit. Mar Drugs 6: 587-594

Falkowski PG, Katz ME, Knoll AH, Quigg A, Raven JA, Schofield O, Taylor FJR (2004) The evolution of modern eukaryotic phytoplankton. Science 305: 354-360

FAO (2004) Report of the joint FAO/IOC/WHO *ad hoc* expert consultation on biotoxins in bivalve molluscs, Oslo, Norway, 31 p.

Fenchel T (1987) Ecology of protozoa - the biology of freeliving phagotrophic protists. Springer-Verlag, New York, NY

Flynn KJ, Flynn K, John EH, Reguera B, Reyero MI, Franco JM (1996) Changes in toxins, intracellular and dissolved free amino acids of the toxic dinoflagellate *Gymnodinium catenatum* in response to changes in inorganic nutrients and salinity. J Plankton Res 18: 2093-2111

Frangópulos M, Guisande C, Maneiro I, Riveiro I, Franco J (2000) Short-term and long-term effects of the toxic dinoflagellate *Alexandrium minutum* on the copepod *Acartia clausi*. Mar Ecol Prog Ser 203: 161-169

Frost BW (1972) Effects of size and concentration of food particles on the feeding behavior of the marine planktonic copepod *Calanus pacificus.* Limnol Oceanogr 17: 805-815

Furey A, Moroney C, Braña Magdalena A, Saez MJF, Lehane M, James KJ (2003) Geographical, temporal, and species variation of the polyether toxins, azaspiracids, in shellfish. Environ Sci Technol 37: 3078-3084

Furey A, O'Doherty S, O'Callaghan K, Lehane M, James KJ (2010) Azaspiracid poisoning (AZP) toxins in shellfish: toxicological and health considerations. Toxicon 56: 173-190

Fux E, Biré R, Hess P (2009) Comparative accumulation and composition of lipophilic marine biotoxins in passive samplers and in mussels (*M. edulis*) on the West Coast of Ireland. Harmful Algae 8: 523-537

Gaines G, Elbrächter M (1987) Heterotrophic nutrition. In: Taylor FJR (ed) The biology of dinoflagellates. Bot Monogr 21: 224-268

Garrison DL, Conrad SM, Eilers PP, Waldron EM (1992) Confirmation of domoic acid production by *Pseudonitzschia australis* (Bacillariophyceae) cultures. J Phycol 28: 604-607

Gedaria AI, Luckas B, Reinhardt K, Azanza RV (2007) Growth response and toxin concentration of cultured *Pyrodinium bahamense* var. *compressum* to varying salinity and temperature conditions. Toxicon 50: 518-529

Geraci JR, Anderson DM, Timperi RJ, St Aubin DJ, Early GA, Prescott JH, Mayo CA (1989) Humpback whales (*Megaptera novaeangliae*) fatally poisoned by dinoflagellate toxin. Can J Fish Aquat Sci 46: 1895-1898

Glibert PM, Burkholder JM, Kana TM, Alexander J, Skelton H, Shilling C (2009) Grazing by *Karenia brevis* on *Synechococcus* enhances its growth rate and may help to sustain blooms. Aquat Microb Ecol 55: 17-30

Goldman JC, Dennett MR, Gordin H (1989) Dynamics of herbivorous grazing by the heterotrophic dinoflagellate *Oxyrrhis marina.* J Plankton Res 11: 391-407

Gómez F (2005) A list of dinoflagellates in the world oceans. Acta Bot Croatica 84: 129-212

Granéli E, Hansen PJ (2006) Allelopathy in harmful algae: a mechanism to compete for resources? In: Granéli E, Turner JT (eds) Ecology of harmful algae. Springer, Berlin, pp. 189-201

Granéli E, Turner JT (2006) Ecology of harmful algae. Springer, The Netherlands, 413 p.

Grzebyk D, Séchet V (2003) Toxinogénèse et physiologie cellulaire. In: Frémy, JM, Lassus P (eds) Toxines d'algues dans l'alimentation. Ifremer, Brest, pp. 191-228

Grzebyk D, Bechemin C, Ward CJ, Verite C, Codd GA, Maestrini SY (2003) Effects of salinity and two coastal waters on the growth and toxin content of the dinoflagellate *Alexandrium minutum*. J Plankton Res 25: 1185-1199

Gu H, Luo Z, Krock B, Witt M, Tillmann U (2013) Morphology, phylogeny and azaspiracid profile of *Azadinium poporum* (Dinophyceae) from the China sea. Harmful Algae 21-22: 64-75

Guillard RRL, Ryther JH (1962) Studies of marine planktonic diatoms. I. *Cyclotella nana* Hustedt, and *Detonula confervacea* (Cleve) Gran. Can J Microbiol 8: 229-239

Hall TA (1999) BioEdit: a user-friendly biological sequence alignment editor and analysis program for Windows 95/98/NT. Nucleic Acids Symp Ser 41: 95-98

Han MW, Park YC (1999) The development of anoxia in the artificial lake Shihwa, Korea, as a consequence of intertidal reclamation. Marine Pollution Bulletin 38: 1194-1199

Hansen B, Bjørnsen PK, Hansen PJ (1994) The size ratio between planktonic predators and their prey. Limnol Oceanogr 39: 395-403

Hansen PJ (1989) The red tide dinoflagellate *Alexandrium tamarense*: effects on behaviour and growth of a tintinnid ciliate. Mar Ecol Prog Ser 53: 105-116

Hansen PJ (1995) Growth and grazing response of a ciliate feeding on the red tide dinoflagellate *Gyrodinium aureolum* in monoculture and in mixture with a non-toxic alga. Mar Ecol Prog Ser 121: 65-72

Hansen PJ, Nielsen TG (1997) Mixotrophic feeding of *Fragilidium subglobosum* (Dinophyceae) on three species of *Ceratium*: effects of prey concentration, prey species and light intensity. Mar Ecol Prog Ser 147: 187-196

Hansen PJ, Bjørnsen PK, Hansen BW (1997) Zooplankton grazing and growth: scaling within the 2-2,000-µm body size range. Limnol Oceanogr 42: 687-704

Hansen PJ (2002) Effect of high pH on the growth and survival of marine phytoplankton: implications for species succession. Aquat Microb Ecol 28: 279-288

Hansen PJ, Lundholm N, Rost B (2007) Growth limitation in marine red-tide dinoflagellates: effects of pH versus inorganic carbon availability. Mar Ecol Prog Ser 334: 63-71

Heinbokel JF (1978) Studies on the functional role of tintinnids in the Southern California Bight. I. Grazing and growth rates in laboratory cultures. Mar Biol 47: 177-189

Hernández-Becerril DU, Barón-campis SA, Escobar-Morales S (2012) A new record of *Azadinium spinosum* (Dinoflagellata) from the tropical Mexican Pacific. Rev biol mar oceanogr 47: 553-557

Hess P, Nguyen L, Aasen J, Keogh M, Kilcoyne J, McCarron P, Aune T (2005) Tissue distribution, effects of cooking and parameters affecting the extraction of azaspiracids from mussels, *Mytilus edulis*, prior to analysis by liquid chromatography coupled to mass spectrometry. Toxicon 46: 62-71

Houde SEL, Roman MR (1987) Effects of food quality on the functional ingestion response of the copepod *Acartia tonsa*. Mar Ecol Prog Ser 40: 69-77

Hu HH, Chen WD, Shi YJ, Cong W (2006) Nitrate and phosphate supplementation to increase toxin production by the marine dinoflagellate *Alexandrium tamarense*. Mar Pollut Bull 52: 756-760

Hu T, Curtis JM, Walter JA, Wright JLC (1995) Identification of DTX-4, a new water-soluble phosphatase inhibitor from the toxic dinoflagellate *Prorocentrum lima.* J Chem Soc Chem Commun 5: 597-599

Huelsenbeck JP, Ronquist F (2001) MRBAYES: Bayesian inference of phylogenetic trees. Bioinformatics 17: 754-755

Huntley M, Barthel K-G, Star JL (1983) Particle rejection by *Calanus pacificus*: discrimination between similarly sized particles. Mar Biol 74: 151-160

Huntley M, Sykes P, Rohan S, Marin V (1986) Chemically mediated rejection of dinoflagellate prey by the copepods *Calanus pacificus* and *Paracalanus parvus*: mechanism, occurrence and significance. Mar Ecol Prog Ser 28: 105-120

Hwang DF, Lu YH (2000) Influence of environmental and nutritional factors on growth, toxicity, and toxin profile of dinoflagellate *Alexandrium minutum*. Toxicon 38: 1491-1503

Ito E, Satake M, Ofuji K, Higashi M, Harigaya K, McMahon T, Yasumoto T (2002) Chronic effects in mice caused by oral administration of sublethal doses of azaspiracid, a new marine toxin isolated from mussels. Toxicon 40: 193-203

Jahan R, Choi HC, Park YS, Park YC, Seo JH, Choi JK (2013) Implementation of self-organizing maps (SOM) to analyses of environmental parameters and phytoplankton biomass in a macrotidal estuary and artificial lake. Journal of the Marine Biological Association of the United Kingdom 93: 1-12

James KJ, Furey A, Satake M, Yasumoto T (2000) Azaspiracid poisoning (AZP): a new shellfish toxic syndrome in Europe. In: Hallegraeff GM, Blackburn SI, Bolch CJS, Lewis RJ (eds) Proceedings of the 9 International Conference on

Harmful Algal Blooms in Hobart, Australia. International Oceanogrphic Commission of UNESCO, pp. 250-253

James KJ, Furey A, Lehane M, Ramstad H, Aune T, Hovgaard P, Morris S, Higman W, Satake M, Yasumoto T (2002) First evidence of an extensive northern European distribution of azaspiracid poisoning (AZP) toxins in shellfish. Toxicon 40: 909-915

James KJ, Sierra MD, Lehane M, Magdalena AB, Furey A (2003a) Detection of five new hydroxyl analogues of azaspiracids in shellfish using multiple tandem mass spectrometry. Toxicon 41: 277-283

James KJ, Moroney C, Roden C, Satake M, Yasumoto T, Lehane M, Furey A (2003b) Ubiquitous "benign" alga emerges as the cause of shellfish contamination responsible for the human toxic syndrome, azaspiracid poisoning. Toxicon 41: 145-154

Jauffrais T, Kilcoyne J, Séchet V, Herrenknecht C, Truquet P, Hervé F, Bérard JB, Nulty C, Taylor S, Tillmann U, Miles CO, Hess P (2012) Production and isolation of azaspiracid-1 and -2 from *Azadinium spinosum* culture in pilot scale photobioreactors. Mar Drugs 10: 1360-1382

Jeong HJ (1999) The ecological roles of heterotrophic dinoflagellates in marine planktonic community. J Eukaryot Microbiol 46: 390-396

Jeong HJ, Shim JH, Lee CW, Kim JS, Koh SM (1999) Growth and grazing rates of the marine planktonic ciliate *Strombidinopsis* sp. on red-tide and toxic dinoflagellates. J Eukaryot Microbiol 46: 69-76

Jeong HJ, Kang H, Shim JH, Park JK, Kim JS, Song JY, Choi HJ (2001) Interactions among the toxic dinoflagellate *Amphidinium carterae*, the

heterotrophic dinoflagellate *Oxyrrhis marina*, and the calanoid copepods *Acartia* spp. Mar Ecol Prog Ser 218: 77-86

Jeong HJ, Yoon JY, Kim JS, Yoo YD, Seong KA (2002) Growth and grazing rates of the prostomatid ciliate *Tiarina fusus* on red-tide and toxic algae. Aquat Microb Ecol 28: 289-297

Jeong HJ, Park KH, Kim JS, Kang H, Kim CH, Choi H-J, Kim YS, Park JY, Park MG (2003a) Reduction in the toxicity of the dinoflagellate *Gymnodinium catenatum* when fed on by the heterotrophic dinoflagellate *Polykrikos kofoidii.* Aquat Microb Ecol 31: 307-312

Jeong HJ, Kim JS, Yoo YD, Kim ST, Kim TH, Park MG, Lee CH, Seong KA, Kang NS, Shim JH (2003b) Feeding by the heterotrophic dinoflagellate *Oxyrrhis marina* on the red-tide raphidophyte *Heterosigma akashiwo*: a potential biological method to control red tides using mass-cultured grazers. J Eukaryot Microbiol 50: 274-282

Jeong HJ, Park JY, Nho JH, Park MO, Ha JH, Seong KA, Jeng C, Seong CN, Lee KY, Yih WH (2005a) Feeding by the red-tide dinoflagellates on the cyanobacterium *Synechococcus*. Aquat Microb Ecol 41: 131-143

Jeong HJ, Yoo YD, Park JY, Song JY, Kim ST, Lee SH, Kim KY, Yih WH (2005b) Feeding by the phototrophic red-tide dinoflagellates: five species newly revealed and six species previously known to be mixotrophic. Aquat Microb Ecol 40: 133-155

Jeong HJ, Kim JS, Park JY, Kim JH, Kim S, Lee I, Lee SH, Ha JH, Yih WH (2005c) *Stoeckeria algicida* n. gen., n. sp. (Dinophyceae) from the coastal waters off Southern Korea: morphology and small subunit ribosomal DNA gene sequence. J Eukaryot Microbiol 52: 382-390

Jeong HJ, Kim JS, Kim JH, Kim ST, Seong KA, Kim TH, Song JY, Kim SK (2005d) Feeding and grazing impact of the newly described heterotrophic dinoflagellate *Stoeckeria algicida* on the harmful alga *Heterosigma akashiwo.* Mar Ecol Prog Ser 295: 69-78

Jeong HJ, Ha JH, Park JY, Kim JH, Kang NS, Kim S, Kim JS, Yoo YD, Yih WH (2006) Distribution of the heterotrophic dinoflagellate *Pfiesteria piscicida* in Korean waters and its consumption of mixotrophic dinoflagellates, raphidophytes and fish blood cells. Aquat Microb Ecol 44: 263-278

Jeong HJ, Yoo YD, Kim JS, Seong KA, Kang NS, Kim TH (2010a) Growth, feeding and ecological roles of the mixotrophic and heterotrophic dinoflagellates in marine planktonic food webs. Ocean Sci J 45: 65-91

Jeong HJ, Yoo YD, Kang NS, Rho JR, Seong KA, Park JW, Nam GS, Yih WH (2010b) Ecology of *Gymnodinium aureolum*. I. Feeding in western Korean water. Aquat Microb Ecol 59: 239-255

Jeong HJ, Kim TH, Yoo YD, Yoon EY, Kim JS, Seong KA, Kim KY, Park JY (2011a) Grazing impact of heterotrophic dinoflagellates and ciliates on common red-tide euglenophyte *Eutreptiella gymnastica* in Masan bay, Korea. Harmful Algae 10: 576-588

Jeong HJ, Lee KH, Yoo YD, Kang NS, Lee K (2011b) Feeding by the newly described, nematocyst-bearing heterotrophic dinoflagellate *Gyrodiniellum shiwhaense.* J Eukaryot Microbiol 58: 511-524

John U, Fensome RA, Medlin LK (2003) The application of a molecular clock based on molecular sequences and the fossil record to explain biogeographic distributions within the *Alexandrium tamarense* "species complex" (Dinophyceae). Mol Biol Evol 20: 1015-1027

Kalaitzis JA, Chau R, Kohli GS, Murray SA, Neilan BA (2010) Biosynthesis of naturally-occurring seafood conataminats. Toxicon 56: 244-258

Kamiyama T, Arima S (2001) Feeding characteristics of two tintinnid ciliate species on phytoplankton including harmful species: effects of prey size on ingestion rates and selectivity. J Exp Mar Biol Ecol 257: 281-296

Kamiyama T, Tsujino M, Matsuyama Y, Uchida T (2005) Growth and grazing rates of the tintinnid ciliate *Favella taraikaensis* on the toxic dinoflagellate *Alexandrium tamarense*. Mar Biol 147: 989-997

Kamiyama T, Nagai S, Suzuki T, Miyamura K (2010) Effect of temperature on production of okadaic acid, dinophysistoxin-1, and pectenotoxin-2 by *Dinophysis acuminata* in culture experiments. Aquat Microb Ecol 60: 193-202

Kang NS, Jeong HJ, Moestrup Ø, Park TG (2011) *Gyrodiniellum shiwhaense* n. gen., n. sp., a new planktonic heterotrophic dinoflagellate from the coastal waters of western Korea: morphology and ribosomal DNA gene sequence. J Eukaryot Microbiol 58: 284-309

Karp-Boss L, Boss E, Jumars PA (2000) Motion of dinoflagellates in a simple shear flow. Limnol Oceanogr 45: 1594-1602

Khan S, Ahmed MS, Arakawa O, Onoue Y (1995a) Properties of neurotoxins separated from a harmful redtide organism *Chattonella marina*. The Israeli Journal of Aquaculture – Bamidgeh 47: 137-141

Khan S, Haque M, Arakawa O, Onoue Y (1995b) Toxin profiles and ichthyotoxicity of three phytoflagellates. Bangladesh Fish 15: 73-81

Kibbe WA (2007) OligoCalc: an online oligonucleotide properties calculator. Nucleic Acids Res 35: W43-W46

Kilcoyne J, Keogh A, Clancy G, Leblanc P, Burton I, Quilliam MA, Hess P, Miles CO (2012) Improved isolation procedure for azaspiracids from shellfish, structural elucidation of azaspiracid-6, and stability studies. J Agric Food Chem 60: 2447-2455

Kim JS, Jeong HJ (2004) Feeding by the heterotrophic dinoflagellates *Gyrodinium dominans* and *G. spirale* on the red-tide dinoflagellate *Prorocentrum minimum.* Mar Ecol Prog Ser 280: 85-94

Kim DI, Matsuyama Y, Nagasoe S, Yamaguchi M, Yoon YH, Oshima Y, Imada N, Honjo T (2004a) Effects of temperature, salinity and irradiance on the growth of the harmful red tide dinoflagellate *Cochlodinium polykrikoides* Margalef (Dinophyceae). J Plankton Res 26: 61-66

Kim T, Park Y, Lee H, Kim D (2004b) The environmental impacts of seasonal variation on characteristics of geochemical parameters in lake Shihwa, Korea. Journal of Environmental Science 13: 1089-1102

Kimura M (1980) A simple method for estimating evolutionary rate of base substitution through comparative studies of nucleotide sequences. J Mol Evol 16: 111-120

Kivi K, Setälä O (1995) Simultaneous measurement of food particle selection and clearance rates of planktonic oligotrich ciliates (Ciliophora: Oligotrichina). Mar Ecol Prog Ser 119: 125-137

Klontz KC, Abraham A, Plakas SM, Dickey RW (2009) Mussel-associated azaspiracid intoxication in the United States. Ann Intern Med 150: 361

KMA (Korea Meterological Administration) (2010) Available at http://web.kma.go.kr

Koch BP, Dittmar T (2006) From mass to structure: an aromaticity index for high-resolution mass data of natural organic matter. Rapid Commun Mass Spectrom 20: 926-932

Kofoid CA (1909) On *Peridinium steinii* Jörgensen, with a note on the nomenclature of the skeleton of the Peridinidae. Arch Protistenk 16: 25-47

Kondo K, Seike Y, Date Y (1990) Red tides in the brackish lake Nakanoumi. (II). Relationships between the occurrence of *Prorocentrum minimum* red tide and environmental conditions. Bull Plankt Soc Japan Hiroshima 37: 19-34

Krock B, Tillmann U, John U, Cembella A (2008) LC-MS-MS aboard ship: tandem mass spectrometry in the search for phycotoxins and novel toxigenic plankton from the North Sea. Anal Bioanal Chem 392: 797-803

Krock B, Tillmann U, John U, Cembella AD (2009) Characterization of azaspiracids in plankton size-fractions and isolation of an azaspiracid-producing dinoflagellate from the North Sea. Harmful Algae 8: 254-263

Krock B, Tillmann U, Voß D, Koch BP, Salas R, Witt M, Potvin É, Jeong HJ (2012) New azaspiracids in Amphidomataceae (Dinophyceae). Toxicon 60: 830-839

Kulagina NV, Twiner MJ, Hess P, McMahon T, Satake M, Yasumoto T, Ramsdell JS, Doucette GJ, Ma W, O'Shaughnessy TJ (2006) Azaspiracid-1 inhibits bioelectrical activity of spinal cord neuronal networks. Toxicon 47: 766-773

Laabir M, Jauzein C, Genovesi B, Masseret E, Grzebyk D, Cecchi P, Vaquer A, Perrin Y, Collos Y (2011) Influence of temperature, salinity and irradiance on the growth and cell yield of the harmful red tide dinoflagellate *Alexandrium catenella* colonizing Mediterranean waters. J Plankton Res 33: 1550-1563

LaJeunesse TC (2001) Investigating the biodiversity, ecology, and phylogeny of endosymbiotic dinoflagellates in the genus *Symbiodinium* using the ITS region: in search of a "species" level marker. J Phycol 37: 866-880

Larkin MA, Blackshields G, Brown NP, Chenna R, McGettigan PA, McWilliam H, Valentin F, Wallace IM, Wilm A, Lopez R, Thompson JD, Gibson TJ, Higgins DG (2007) Clustal W and Clustal X version 2.0. Bioinformatics 23: 2947-2948

Lartigue J, Jester ELE, Dickey RW, Villareal TA (2009) Nitrogen source effects on the growth and toxicity of two strains of the ciguatera-causing dinoflagellate *Gambierdiscus toxicus*. Harmful Algae 8: 781-791

Laycock MV, De Freitas ASW, Wright JLC (1989) Glutamate agonists from marine algae. J Appl Phycol 1: 113-122

Lefèvre M (1932) Monographie des espèces d'eau douce du genre *Peridinium*. Arch Bot 2: 1-208

Legrand AM, Cruchet P, Bagnis R, Murata M, Ishibashi Y, Yasumoto T (1990) Chromatographic and spectral evidence for the presence of multiple ciguatera toxins. In: Granéli E, Anderson DM, Edler L, Sundström BG (eds) Toxic marin phytoplankton. Elsevier, New York, pp. 374-378

Legrand C, Rengefors K, Fistarol GO, Granéli E (2003) Allelopathy in phytoplankton - biochemical, ecological and evolutionary aspects. Phycologia 42: 406-419

Lehane M, Braña-Magdalena A, Moroney C, Furey A, James KJ (2002) Liquid chromatography with electrospray ion trap mass spectrometry for the determination of five azaspiracids in shellfish. J Chromatogr A 950: 139-147

Lenderman TC, Tett P (1981) Problems in modeling the photosynthesis-light relationship for phytoplankton. Bot Mar 24: 125-134

Lessard EJ (1991) The trophic role of heterotrophic dinoflagellates in diverse marine environments. Mar Microb Food Webs 5: 49-58

Lin S, Zhang H, Spencer DF, Norman JE, Gray MW (2002) Widespread and extensive editing of mitochondrial mRNAs in dinoflagellates. J Mol Biol 320: 727-739

Lin YY, Risk M, Ray SM, Van Engen D, Clardy J, Golik J, James JC, Nakanishi K (1981) Isolation and structure of brevetoxin B from the "red tide" dinoflagellate *Ptychodiscus brevis* (*Gymnodinium breve*). J Am Chem Soc 103: 6773-6775

Litaker RW, Vandersea MW, Kibler SR, Reece KS, Stokes NA, Steidinger KA, Millie DF, Bendis BJ, Pigg RJ, Tester PA (2003) Identification of *Pfiesteria piscicida* (Dinophyceae) and *Pfiesteria*-like organisms using Internal Transcribed Spacer-specific PCR assays. J Phycol 39: 754-761

López-Rivera A, O'callaghan K, Moriarty M, O'driscoll D, Hamilton B, Lehane M, James KJ, Furey A (2010) First evidence of azaspiracids (AZAs): a family of lipophilic polyether marine toxins in scallops (*Argopecten purpuratus*) and mussels (*Mytilus chilensis*) collected in two regions of Chile. Toxicon 55: 692-701

Lu S, Hodgkiss IJ (2004) Harmful algal bloom causative collected from Hong Kong waters. Hydrobiologia 512: 231-238

MacKinnon SL, Cembella AD, Burton IW, Lewis NI, LeBlanc P, Walter JA (2006) Biosynthesis of 13-desmethyl spirolide C by the dinoflagellate *Alexandrium ostenfeldii*. J Org Chem 71: 8724-8731

Maclean C, Cembella AD, Quilliam MA (2003) Effects of light, salinity and inorganic nitrogen on cell growth and spirolide production in the marine dinoflagellate *Alexandrium ostenfeldii* (Paulsen) Balech *et* Tangen. Botanica Marina 46: 466-476

Magdalena AB, Lehane M, Krys S, Fernández ML, Furey A, James KJ (2003) The first identification of azaspiracids in shellfish from France and Spain. Toxicon 42: 105-108

Maneiro I, Frangopulos M, Guisande C, Fernandez M, Reguera B, Riveiro I (2000) Zooplankton as a potential vector of diarrhetic shellfish poisoning toxins through the food web. Mar Ecol Prog Ser 201: 155-163

Maranda L, Wang R, Masuda K, Shimizu Y (1989) Investigation of the source of domoic acid in mussels. In: Granéli E, Sundström S, Edler L, Anderson DM (eds) Toxic marine phytoplankton. Elsevier, New York, pp. 300-304:

Matsubara T, Nagasoe S, Yamasaki Y, Shikata T, Shimasaki Y, Oshima Y, Honjo T (2007) Effects of temperature, salinity, and irradiance on the growth of the dinoflagellate *Akashiwo sanguinea*. J Exp Mar Biol Ecol 342: 226-230

Matsuoka K, Cho HJ, Jacobson DM (2000) Observations of the feeding behavior and growth rates of the heterotrophic dinoflagellate *Polykrikos kofoidii* (Polykrikaceae, Dinophyceae). Phycologia 39: 82-86

McCarron P, Kilcoyne J, Miles CO, Hess P (2009) Formation of azaspiracids-3,-4,-6, and- 9 via decarboxylation of carboxyazaspiracid metabolites from shellfish. J Agric Food Chem 57: 160-169

McClintock JB, Baker BJ (2001) Marine chemical ecology. CRC Press, Boca Raton, Florida, 610 p.

McMahon T, Silke J (1996) West coast of Ireland; winter toxicity of unknown aetiology in mussels. Harmful Algae News 14: 2

Medlin L, Elwood HJ, Stickel S, Sogin ML (1988) The characterization of enzymatically amplified eukaryotic 16S-like rRNA-coding regions. Gene 71: 491-499

Menden-Deuer S, Lessard EJ (2000) Carbon to volume relationships for dinoflagellates, diatoms, and other protist plankton. Limnol Oceanogr 45: 569-579

Michaelis L, Menten ML (1913) Die kinetik der invertinwirkung. Biochem Z 49: 333-369

Miles CO, Wilkins AL, Stirling DJ, Mackenzie L (2000) New analogue of gymnodimine from a *Gymnodinium* species. J Agric Food Chem 48: 1373-1376

Miles CO, Wilkins AL, Munday R, Dines MH, Hawkes AD, Briggs LR, Sandvik M, Jensen DJ, Cooney JM, Holland PT, Quilliam MA, MacKenzie AL, Beuzenberg V, Towers NR (2004a) Isolation of pectenotoxin-2 from *Dinophysis acuta* and its conversion to pectenotoxin-2 seco acid, and preliminary assessment of their acute toxicities. Toxicon 43: 1-9

Miles CO, Wilkins AL, Samdal IA, Sandvik M, Petersen D, Quilliam MA, Naustvoll LJ, Rundberget T, Torgersen T, Hovgaard P, Jensen DJ, Cooney JM (2004b) A novel pectenotoxin, PTX-12, in *Dinophysis* spp. and shellfish from Norway. Chem Res Toxicol 17: 1423-1433

Mitrovic SM, Amandi MF, McKenzie L, Furey A, James KJ (2004) Effects of selenium, iron and cobalt addition to growth and yessotoxin production of

the toxic marine dinoflagellate *Protoceratium reticulatum* in culture. J Exp Mar Biol Ecol 313: 337-351

MOMAF (Ministry of Maritime Affairs and Fisheries) (2006) PEMSEA parallel site for integrated coastal management in Republic of Korea: Shihwa lake. Seoul, Korea: MOMAF

Montagnes DJS (1996) Growth responses of planktonic ciliates in the genera *Strobilidium* and *Strombidium.* Mar Ecol Prog Ser 130: 241-254

Montresor M, Sgrosso S, Procaccini G, Kooistra WHCF (2003) Intraspecific diversity in *Scrippsiella trochoidea* (Dinophyceae): evidence for cryptic species. Phycologia 42: 56-70

Morrill LC, Loeblich III AR (1981) A survey for body scales in dinoflagellates and a revision of *Cachonina* and *Heterocapsa* (Pyrrhophyta). J Plankton Res 3: 53-65

Murakami Y, Oshima Y, Yasumoto T (1982) Identification of okadaic acid as a toxic component of a marine dinoflagellate *Prorocentrum lima.* Nippon Suisan Gakkaishi 48: 69-72

Murata M, Legrand AM, Ishibashi Y, Fukui M, Yasumoto T (1990) Structures and configurations of ciguatoxin from the moray eel *Gymnothorax javanicus* and its likely precursor from the dinoflagellate *Gambierdiscus toxicus*. J Am Chem Soc 112: 4380-4386

Nagasoe S, Kim DI, Shimasaki Y, Oshima Y, Yamaguchi M, Honjo T (2006) Effects of temperature, salinity and irradiance on the growth of the red tide dinoflagellate *Gyrodinium instriatum* Freudenthal *et* Lee. Harmful Algae 5: 20-25

Navarro JM, Munoz MG, Contreras AM (2006) Temperature as a factor regulating growth and toxin content in the dinoflagellate *Alexandrium catenella*. Harmful Algae 5: 762-769

Nézan É, Tillmann U, Bilien G, Boulben S, Chèze K, Zentz F, Salas R, Chomérat N (2012) Taxonomic revision of the dinoflagellate *Amphidoma Caudata*: transfer to the genus *Azadinium* (Dinophyceae) and proposal of two varieties, based on morphological and molecular phylogenetic analyses. J Phycol 48: 925-939

NFRDI (National Fisheries Research and Development Institute) (2008) Available at http://portal.nfrdi.re.kr/

Nicolaou KC, Frederick MO, Petrovic G, Cole KP, Loizidou EZ (2006) Total synthesis and confirmation of the revised structures of azaspiracid- 2 and azaspiracid-3. Angew Chem Int Ed 45: 2609-2615

Nielsen MV (1996) Growth and chemical composition of the toxic dinoflagellate *Gymnodinium galatheanum* in relation to irradiance, temperature and salinity. Mar Ecol Prog Ser 136: 205-211

Ofuji K, Satake M, McMahon T, Silke J, James KJ, Naoki H, Oshima Y, Yasumoto T (1999) Two analogs of azaspiracid isolated from mussels, *Mytilus edulis*, involved in human intoxication in Ireland. Nat Toxins 7: 99-102

Ofuji K, Satake M, McMahon T, James KJ, Naoki H, Oshima Y, Yasumoto T (2001) Structures of azaspiracid analogs, azaspiracid-4 and azaspiracid-5, causative toxins of azaspiracid poisoning in Europe. Biosci Biotech Biochem 65: 740-742

Oh S, Kim MK, Yi SM, Zoh KD (2010) Distributions of total mercury and methylmercury in surface sediments and fishes in lake Shihwa, Korea. Science of the Total Environment 408: 1059-1068

Paerl HW (1998) Coastal eutrophication and harmful algal blooms: importance of atmospheric deposition and groundwater as 'new' nitrogen and other nutrient sources. Limnol Oceanogr 42: 1154-1165

Painting SJ, Lucas MI, Peterson WT, Brown PC, Hutchings L, Mitchell-Innes BA (1993) Dynamics of bacterioplankton, phytoplankton and mesozooplankton communities during the development of an upwelling plume in the Southern Benguela. Mar Ecol Prog Ser 100: 35-53

Park GS, Park SY (2000) Long-term trends and temporal heterogeneity of water quality in tidally mixed estuarine waters. Marine Pollution Bulletin 40: 1201-1209

Park JK, Kim ES, Cho SP, Kim KT, Park YC (2003) Annual variation of water quality in the Shihwa lake. Ocean and Polar Research 25: 459-468

Parkhill JP, Cembella AD (1999) Effects of salinity, light and inorganic nitrogen on growth and toxigenicity of the marine dinoflagellate *Alexandrium tamarense* from northeastern Canada. J Plankton Res 21: 939-955

Paz B, Vazquez JA, Riobo P, Franco JM (2006) Study of the effect of temperature, irradiance and salinity on growth and yessotoxin production by the dinoflagellate *Protoceratium reticulatum* in culture by using a kinetic and factorial approach. Mar Environ Res 62: 286-300

Pelin M, Zanette C, De Bortoli M, Sosa S, Loggia RD, Tubaro A, Florio C (2011) Effects of the marine toxin palytoxin on human skin keratinocytes: role of ionic imbalance. Toxicology 282: 30-38

Phlips EJ, Badylak S, Christman M, Wolny J, Brame J, Garland J, Hall L, Hart J, Landsberg J, Lasi M, Lockwood J, Paperno R, Scheidt D, Staples A, Steidinger K (2011) Scales of temporal and spatial variability in the distribution of harmful algae species in the Indian River Lagoon, Florida, USA. Harmful Algae 10: 277-290

Pollingher U, Zemel E (1981) *In situ* and experimental evidence of the influence of turbulence on cell division processes of *Peridinium cinctum* forma westii (Lemm.) Lefèvre. Br Phycological J 16: 281-287

Posada D, Crandall KA (1998) MODELTEST: testing the model of DNA substitution. Bioinformatics 14: 817-818

Posada D, Buckley TR (2004) Model selection and model averaging in phylogenetics: advantages of akaike information criterion and bayesian approaches over likelihood ratio tests. Syst Biol 53: 793-808

Potvin É, Jeong HJ, Kang NS, Tillmann U, Krock B (2012) First report of the photosynthetic dinoflagellate genus *Azadinium* in the Pacific Ocean: morphology and molecular characterization of *Azadinium* cf. *poporum*. J Eukaryot Microbiol 59: 145-156

Potvin É, Hwang YJ, Yoo YD, Kim JS, Jeong HJ (2013) Feeding by heterotrophic protists and copepods on the photosynthetic dinoflagellate *Azadinium* cf. *poporum* from western Korean waters. Aquat Microb Ecol 68: 143-158

Prasad AVK, Shimizu Y (1989) The structure of hemibrevetoxin-B: a new type of toxin in the Gulf of Mexico red tide organism. J Am Chem Soc 111: 6476-6477

Prince EK, Myers TL, Kubanek J (2008) Effects of harmful algal blooms on competitors: allelopathic mechanisms of the red tide dinoflagellate *Karenia brevis*. Limnol Oceanogr 53: 531-541

Qiu XC, Yamasaki Y, Shimasaki Y, Gunjikake H, Honda M, Kawagushi M, Matsubara T, Nagasoe S, Etoh T, Matsui S, Honjo T, Oshima Y (2012) Allelopathy of the raphidophyte *Heterosigma akashiwo* against the dinoflagellate *Akashiwo sanguinea* is mediated via allelochemicals and cell contact. Mar Ecol Prog Ser 446: 107-118

RASFF (2008) The rapid alert system for food and feed (RASFF) annual report 2008, 51 p.

Rehmann N, Hess P, Quilliam MA (2008) Discovery of new analogs of the marine biotoxin azaspiracid in blue mussels *Mytilus edulis* by ultra-performance liquid chromatography/tandem mass spectrometry. Rapid Commun Mass Spectrom 22: 549-558

Rhodes L, McNabb P, De Salas M, Briggs L, Beuzenberg V, Gladstone M (2006) Yessotoxin production by *Gonyaulax spinifera*. Harmful Algae 5: 148-155

Rhodes L, Smith K, Selwood A, McNabb P, Munday R, Suda S, Molenaar S, Hallegraeff G (2011) Dinoflagellate *Vulcanodinium rugosum* identified as the causative organism of pinnatoxins in Australia, New Zealand and Japan. Phycologia 50: 624-628

Richardson TL, Pinckney JL, Walker EA, Marshalonis DM (2006) Photopigment radiolabelling as a tool for determining in situ growth rates of the toxic dinoflagellate *Karenia brevis* (Dinophyceae) Eur J Phycol 41: 415-423

Román Y, Alfonso A, Louzao MC, De la Rosa LA, Leira F, Vieites JM, Vieytes MR, Ofuji K, Satake M, Yasumoto T, Botana LM (2002) Azaspiracid-1, a

potent, nonapoptotic new phycotoxin with several cell targets. Cell Signalling 14: 703-716

Rozen S, Skaletsky HJ (2000) Primer3 on the WWW for general users and for biologist programmers. In: Krawetz S, Misener S (eds) Bioinformatics methods and protocols: methods in molecular biology. Humana Press, Totowa, NJ, pp. 365-386

Rundberget T, Gustad E, Samdal IA, Sandvik M, Miles CO (2009) A convenient and cost-effective method for monitoring marine algal toxins with passive samplers. Toxicon 53: 543-550

Sakka A, Legendre L, Gosselin M, LeBlanc B, Delesalle B, Price NM (1999) Nitrate, phosphate, and iron limitation of the phytoplankton assemblage in the lagoon of Takapoto Atoll (Tuamotu Archipelago, French Polynesia). Aquat Microb Ecol 19: 149-161

Salas R, Tillmann U, John U, Kilcoyne J, Burson A, Cantwell C, Hess P, Jauffrais T, Silke J (2011) The role of *Azadinium spinosum* (Dinophyceae) in the production of azaspiracid shellfish poisoning in mussels. Harmful Algae 10: 774-783

Satake M, MacKenzie L, Yasumoto T (1997) Identification of *Protoceratium reticulatum* as the biogenetic origin of yessotoxin. Nat Toxins 5: 164-167

Satake M, Ofuji K, James KJ, Furey A, Yasumoto T (1998a) New toxic event caused by Irish mussels. In: Reguera B, Blanco J, Fernandez ML, Wyatt T (eds) Harmful Algae, proceedings of the VIII international conference on harmful algae, (June 1999, Vigo, Spain). Santiago de Compostela: Xunta de Galicia and Intergovernmental Oceanographic Commission of UNESCO, pp. 468-469

Satake M, Ofuji K, Naoki H, James KJ, Furey A, McMahon T, Silke J, Yasumoto T (1998b) Azaspiracid, a new marine toxin having unique spiro ring assemblies, isolated from Irish mussels, *Mytilus edulis*. J Am Chem Soc 120: 9967-9968

Schantz EJ, Lynch JM, Vayvada G, Matsumoto K, Ropoport H (1966) The purification and characterization of the poison produced by *Gonyaulax catenella* in axenic culture. Biochemistry 5: 1191-1195

Schnepf E, Elbrächter M (1992) Nutritional strategies in dinoflagellates. A review with emphasis on cell biological aspects. Eur J Protistol 28: 3-24

Seki T, Satake M, Mackenzie L, Kaspar HF, Yasumoto T (1995) Gymnodimine, a new marine toxin of unprecedented structure isolated from New Zealand oysters and the dinoflagellate *Gymnodinium* sp. Tetrahedron Lett 36: 7093-7096

Sherr EB, Sherr BF (2007) Heterotrophic dinoflagellates: a significant component of microzooplankton biomass and major grazers of diatoms in the sea. Mar Ecol Prog Ser 352: 187-197

Shi Y, Hu H, Cong W (2005) Positive effects of continuous low nitrate levels on growth and photosynthesis of *Alexandrium tamarense* (Gonyaulacales, Dinophyceae). Phycol Res 53: 43-48

Shimizu Y (1982) Recent progress in marine toxin research. Pure Appl Chem 54: 1973-1980

Shimizu Y, Gupta S, Masuda K, Maranda L, Walker CR, Wang R (1989) Dinoflagellate and other microalgal toxins: chemistry and biochemistry. Pure Appl Chem 61: 513-516

Shumway SE (1990) A review of the effects of algal blooms on shellfish and aquaculture. J World Aquaculture Soc 21: 65-105

Sleigh MA (1989) Protozoa and other protists. Edward Arnold, New York, 342 p.

Smayda TJ (1997) Harmful algal blooms: their ecophysiology and general relevance to phytoplankton blooms in the sea. Limnol Oceanogr 42: 1137-1153

Soh HY, Suh HL (2000) A new species of *Acartia* (Copepoda, Calanoida) from the Yellow Sea. J Plankton Res 22: 321-337

Sommer H, Meyer KF (1937) Paralytic shellfish poisoning. Arch Pathol 24: 560-598

Stamatakis A (2006) RAxML-VI-HPC: maximum likelihood-based phylogenetic analyses with thousands of taxa and mixed models. Bioinformatics 22: 2688-2690

Steidinger KA (1983) A re-evaluation of toxic dinoflagellate biology and ecology. Prog Phycol Res 2: 147-188

Stoecker DK, Guillard RRL, Kavee RM (1981) Selective predation by *Favella ehrenbergii* (Tintinnida) on and among dinoflagellates. Biol Bull 160: 136-145

Straile D (1997) Gross growth efficiencies of protozoan and metazoan zooplankton and their dependence on food concentration, predator-prey weight ratio, and taxonomic group. Limnol Oceanogr 42: 1375-1385

Strom SL, Buskey EJ (1993) Feeding, growth, and behavior of the thecate heterotrophic dinoflagellate *Oblea rotunda*.Limnol Oceanogr 38: 965-977

Strom SL, Postel JR, Booth BC (1993) Abundance, variability, and potential grazing impact of planktonic ciliates in the open subarctic Pacific Ocean. Prog Oceanogr 32: 185-203

Sullivan JM, Swift E, Donaghay PL, Rines JEB (2003) Small-scale turbulence affects the division rate and morphology of two red-tide dinoflagellates. Harmful Algae 2: 183-199

Swofford DL (2002) PAUP*. Phylogenetic analysis using parsimony (*and other methods). Version 4. Sinauer Associates, Sunderland, Massachusetts

Taleb H, Vale P, Amanhir R, Benhadouch A, Sagou R, Chafik A (2006) First detection of azaspiracids in mussels in North West Africa. J Shellfish Res 25: 1067-1070

Tang YZ, Gobler CJ (2010) Allelopathic effects of *Cochlodinium polykrikoides* isolates and blooms from the estuaries of Long Island, New York, on co-occurring phytoplankton. Mar Ecol Prog Ser 406: 19-31

Taylor FJR, Pollingher U (1987) Ecology of dinoflagellate. In: Taylor FJR (ed) The biology of dinoflagellates. Blackwell scientific publications, Oxford, pp. 611-648

Taylor FJR (1987) General group characteristics, special features of interest; and a short history of dinoflagellate study. In: Taylor FJR (ed) The biology of dinoflagellates. Blackwell scientific publications, Oxford, pp. 1-23

Taylor FJR, Hoppenrath M, Saldarriaga JF (2008) Dinoflagellate diversity and distribution. Biodivers Conserv 17: 407-418

Terrado R, Vincent WF, Lovejoy C (2009) Mesopelagic protists: diversity and succession in a coastal Arctic ecosystem. Aquat Microb Ecol 56: 25-40

Tillmann U, John U (2002) Toxic effects of *Alexandrium* spp. on heterotrophic dinoflagellates: an allelochemical defence mechanism independent of PSP-toxin content. Mar Ecol Prog Ser 230: 47-58

Tillmann U, Reckermann M (2002) Dinoflagellate grazing on the raphidophyte *Fibrocapsa japonica.* Aquat Microb Ecol 26: 247-257

Tillmann U, Hansen PJ (2009) Allelopathic effects of *Alexandrium tamarense* on other algae: evidence from mixed growth experiments. Aquat Microb Ecol 57: 101-112

Tillmann U, Elbrächter M, Krock B, John U, Cembella A (2009) *Azadinium spinosum* gen. *et* sp. nov. (Dinophyceae) identified as a primary producer of azaspiracid toxins. Eur J Phycol 44: 63-79

Tillmann U, Elbrächter M, John U, Krock B, Cembella A (2010) *Azadinium obesum* (Dinophyceae), a new nontoxic species in the genus that can produce azaspiracid toxins. Phycologia 49: 169-182

Tillmann U, Elbrächter M, John U, Krock B (2011) A new non-toxic species in the dinoflagellate genus *Azadinium*: *A. poporum* sp. nov. Eur J Phycol 46: 74-87

Tillmann U, Soehner S, Nézan E, Krock B (2012a) First record of the genus *Azadinium* (Dinophyceae) from the Shetland Islands, including the description of *Azadinium polongum* sp. nov. Harmful Algae 20: 142-155

Tillmann U, Salas R, Gottschling M, Krock B, O'Driscoll D, Elbrächter M (2012b) *Amphidoma languida* sp. nov. (Dinophyceae) reveals a close relationship between *Amphidoma* and *Azadinium.* Protist 163: 701-719

Torgersen T, Bruun Bremnes N, Rundberget T, Aune T (2008) Structural confirmation and occurrence of azaspiracids in Scandinavian brown crabs (*Cancer pagurus*). Toxicon 51: 93-101

Torigoe K, Murata M, Yasumoto T, Iwashita T (1988) Prorocentrolide, a toxic nitrogenous macrocycle from a marine dinoflagellate, *Prorocentrum lima.* J Am Chem Soc 110: 7876-7877

Tubaro A, Sidari L, Della Loggia R, Yasumoto T (1998) Occurrence of yessotoxin-like toxins in phytoplankton and mussels from northern Adriatic Sea. In: Reguera B, Blanco J, Fernández ML, Wyatt T (eds) Harmful Algae. Xunta de Galicia and Intergovernmental Oceanographic Commission of UNESCO, Santiago de Compostela, pp. 470-472

Turner JT, Anderson DM (1983) Zooplankton grazing during dinoflagellate blooms in a Cape Cod embayment, with observations of predation upon tintinnids by copepods. Mar Ecol 4: 359-374

Turner JT, Borkman DG (2005) Impact of zooplankton grazing on *Alexandrium* blooms in the offshore Gulf of Maine. Deep-Sea Res. II 52: 2801-2816

Turner JT, Doucette GJ, Keafer BA, Anderson DM (2005) Trophic accumulation of PSP toxins in zooplankton during *Alexandrium fundyense* blooms in Casco bay, Gulf of Maine, April-June 1998. II. Zooplankton abundance and size-fractionated community composition. Deep-Sea Res II 52: 2784-2800

Twiner MJ, Hess P, Bottein Dechraoui M-Y, McMahon T, Samons MS, Satake M, Yasumoto T, Ramsdell JS, Doucette GJ (2005) Cytotoxic and cytoskeletal effects of azaspiracid-1 on mammalian cell lines. Toxicon 45: 891-900

Twiner MJ, Rehmann N, Hess P, Doucette GJ (2008) Azaspiracid shellfish poisoning: a review on the chemistry, ecology, and toxicology with an emphasis on human health impacts. Mar Drugs 6: 39-72

Uchida T (2001) The role of cell contact in the life cycle of some dinoflagellate species. J Plankton Res 23: 889-891

Ueoka R, Ito A, Izumikawa M, Maeda S, Takagi M, Shin-ya K, Yoshida M, Van Soest RWM, Matsunaga S (2009) Isolation of azaspiracid-2 from a marine sponge *Echinoclathria* sp. as a potent cytotoxin. Toxicon 53: 680-684

Usami M, Satake M, Ishida S, Inoue A, Kan Y, Yasumoto T (1995) Palytoxin analogs from the dinoflagellate *Ostreopsis siamensis*. J Am Chem Soc 117: 5389-5390

Uye SI, Takamatsu K (1990) Feeding interactions between planktonic copepods and red-tide flagellates from Japanese coastal waters. Mar Ecol Prog Ser 59: 97-107

Vale C, Nicolaou KC, Frederick MO, Gómez-Limia B, Alfonso A, Vieytes MR, Botana LM (2007) Effects of azaspiracid-1, a potent cytotoxic agent, on primary neuronal cultures. A structure-activity relationship study. J Med Chem 50: 356-363

Vale P (2004) Is there a risk of human poisoning by azaspiracids from shellfish harvested at the Portuguese coast? Toxicon 44: 943-947

Vale P, Biré R, Hess P (2008) Confirmation by LC-MS/MS of azaspiracids in shellfish from the Portuguese north-western coast. Toxicon 51: 1449-1456

Verity PG (1988) Chemosensory behavior in marine planktonic ciliates. Bull Mar Sci 43: 772-782

Vershinin A, Moruchkov A, Morton SL, Leighfield TA, Quilliam MA, Ramsdell JS (2006) Phytoplankton composition of the Kandalaksha Gulf, Russian White Sea: *Dinophysis* and lipophilic toxins in the blue mussel (*Mytilus edulis*). Harmful Algae 5: 558-564

Watras CJ, Garcon VC, Olson RJ, Chisholm SW, Anderson DM (1985) The effect of zooplankton grazing on estuarine blooms of the toxic dinoflagellate *Gonyaulax tamarensis.* J Plankton Res 7: 891-908

White AW (1976) Growth inhibition caused by turbulence in the toxic marine dinoflagellate *Gonyaulax excavata*. J Fish Res Board Can 33: 2598-2602

Work TM, Barr B, Beale AM, Fritz L, Quilliam MA, Wright JLC (1993) Epidemiology of domoic acid poisoning in brown pelicans (*Pelecanus occidentalis*) and Brandt's cormorants (*Phalacrocorax penicillatus*) in California. Journal of Zoo and Wildlife Medicine 24: 54-62

Xu N, Duan SS, Li AF, Zhang CW, Cai ZP, Hu ZX (2010) Effects of temperature, salinity and irradiance on the growth of the harmful dinoflagellate *Prorocentrum donghaiense* Lu. Harmful Algae 9: 13-17

Yamaguchi M, Honjo T (1989) Effect of temperature, salinity and irradiance on the growth of the noxious red tide flagellate *Gymnodinium nagasakiense* (Dinophyceae). Nippon Suisan Gakkaishi 55: 2029-2036

Yamaguchi M, Imai I, Honjo T (1991) Effect of temperature, salinity and irradiance on the growth of the noxious red tide flagellate *Chattonella antique* and *C. marina* (Rhaphidophyceae). Nippon Suisan Gakkaishi 57: 1277-1284

Yamaguchi M, Shigeru I, Nagasaki K, Matsuyama Y, Uchida T, Imai I (1997) Effects of temperature and salinity on the growth of the red tide flagellates

Heterocapsa circularisquama (Dinophyceae) and *Chattonella verruculosa* (Raphidophyceae). J Plankton Res 19: 1167-1174

Yamamoto T, Tarutani K (1997) Effects of temperature, salinity and irradiance on the growth of toxic dinoflagellate *Alexandrium tamarense* isolated from Hiroshima bay, Japan. Japanese J Phycol 45: 95-101

Yamasaki Y, Zou Y, Go J, Shikata T, Matsuyama Y, Nagai K, Shimasaki Y, Yamaguchi K, Oshima Y, Oda T, Honjo T (2011) Cell-contact-dependent lethal effect of the dinoflagellate *Heterocapsa circularisquama* on phytoplankton-phytoplankton interactions. Journal of Sea Research 65: 76-83

Yasumoto T, Nakajima I, Bagnis R, Adachi R (1977) Finding of a dinoflagellate as a likely culprit of ciguatera. Nippon Suisan Gakkaishi 43: 1021-1026

Yasumoto T, Oshima Y, Sugarawa W, Fukuyo Y, Oguri H, Igarashi K, Fujinita N (1980) Identification of *Dinophysis fortii* as the causative organism of diarrhetic shellfish poisoning. Bull Jpn Soc Sci Fsh 46: 1405-1411

Yoo H, Yamashita N, Taniyasu S, Lee KT, Jones PD, Newsted JL, Khim JS, Giesy JP (2009) Perfluoroalkyl acids in marine organisms from lake Shihwa, Korea. Archives of Environmental Contamination and Toxicology 57: 552-560

Yoo YD, Jeong HJ, Kang NS, Kim JS, Kim TH, Yoon EY (2010) Ecology of *Gymnodinium aureolum*. II. Predation by common heterotrophic dinoflagellates and a ciliate. Aquat Microb Ecol 59: 257-272

Yoo YD, Yoon EY, Jeong HJ, Lee KH, Hwang YJ, Seong KA, Kim JS, Park JY (2013) The newly described heterotrophic dinoflagellate *Gyrodinium*

moestrupii, an effective protistan grazer of toxic dinoflagellates. J Eukaryot Microbiol 60: 13-24

Yoon EY, Kang NS, Jeong HJ (2012) *Gyrodinium moestrupii* n. sp., a new planktonic heterotrophic dinoflagellate from the coastal waters of western Korea: morphology and ribosomal DNA gene sequence. J Eukaryot Microbiol 59: 571-586

Zar JH (1999) Biostatistical Analysis. 4th ed. Prentice Hall, Upper Saddle River, NJ

Zhu X, Sato T (2007) The distinction of underivatized monosaccharides using electrospray ionization ion trap mass spectrometry. Rapid Commun Mass Spectrom 21: 191-198

Zirbel MJ, Veron F, Latz MI (2000) The reversible effect of flow on the morphology of *Ceratocorys horrida* (Peridiniales, Dinophyta). J Phycol 36: 46-58